

https://dspace.org/

Modelling the badminton jump smash for injury prevention and performance enhancement

Chohan, Raees Ghalib

2023

University of the Witwatersrand, Johannesburg

https://hdl.handle.net/10539/46275

Chohan, Raees Ghalib . (2023). Modelling the badminton jump smash for injury prevention and performance enhancement [Master`s dissertation, University of the Witwatersrand, Johannesburg]. WIReDSpace.

Downloaded from a DSpace repository. https://dspace.org/



Modelling the badminton jump smash for injury prevention and performance enhancement

Raees Chohan

(Student number: 1254450)

School of Mechanical, Industrial and Aeronautical Engineering

University of the Witwatersrand

Johannesburg, South Africa.

Supervisor:

Taahirah Mangera

A Research Project **dissertation** submitted to the Faculty of Engineering and the Built Environment, University of the Witwatersrand, in fulfilment of the requirements for the degree of Master of Science in Mechanical Engineering

November 2023

SCHOOL OF MECHANICAL, INDUSTRIAL & AERONAUTICAL ENGINEERING

PLAGIARISM DECLARATION TO BE SIGNED BY ALL HIGHER DEGREE STUDENTS

SENATE PLAGIARISM POLICY: APPENDIX ONE

I Raees Ghalib Chohan (Student number: 1254450) am a student registered for the degree of MSc in Mechanical Engineering (Research) in the academic year 2023.

I hereby declare the following:

- I am aware that plagiarism (the use of someone else's work without their permission and/or without acknowledging the original source) is wrong.
- I confirm that the work submitted for assessment for the above degree is my own unaided work except where I have explicitly indicated otherwise.
- I have followed the required conventions in referencing the thoughts and ideas of others.
- I understand that the University of the Witwatersrand may take disciplinary action against me if there is a belief that this is not my own unaided work or that I have failed to acknowledge the source of the ideas or words in my writing.

Signature: _____ Date: 06/12/2023

Acknowledgements

بِسْمِ اللهِ الرَّحْمٰنِ الرَّحِيْمِ. In the name of Allah, the most Gracious, the Most Merciful. All praise is due to Allah, the Compassionate, the Merciful. I express my deepest gratitude to Allah, who is Al-Nafi (The Benefactor), for granting me the strength, wisdom and guidance throughout this journey. Without His blessings, none of this would have been possible.

I extend my heartfelt appreciation to Taahirah Mangera for her supervision, guidance, support, and insightful feedback throughout the course of this research project. Her expertise and encouragement have been instrumental in shaping this dissertation. I would also like to extend my gratitude to Professor Robert Reid for supporting me to the finish line.

I am indebted to my parents, Sajida and Ghalib, for their unconditional love, encouragement, and sacrifices. Your belief in me has been my driving force.

To my beloved wife, Mahdiyyah, your unwavering love, patience, support and sacrifice has been my constant source of strength. I am deeply grateful for your support and sacrifices throughout this journey.

A special thanks to my siblings Hussain, Ismaeel, and Aadila for their encouragement, support and for all the good times.

I would also like to extend my gratitude to Badminton SA and their athletes for their participation in the study.

Abstract

Badminton is considered the fastest competitive racket sport. To gain a competitive edge, athletes commonly execute a forward jump smash to return the shuttlecock with high speeds and steep angles. Research has shown that common injuries in badminton, resulting from incorrect landing during the execution of the jump smash, include rupture of the Achilles tendon and Anterior Cruciate Ligament (ACL). There is a need to identify safe landing techniques to minimise risk of injury while preserving the performance of the manoeuvre.

This study involved assessing four different landing techniques. The techniques involved varying the initial contact with the ground upon landing. The landing techniques assessed were the Normal Landing Technique (NLT), Toe-First (TF) technique, Flat Foot (FF) technique and the Heel First (HF) technique. Data was obtained using an Xsens motion capture suit which uses inertial sensors placed on body segments to capture kinematic and kinetic data. Sixteen athletes from the South African Badminton team participated, however, only data from ten athletes were considered due to the experimental obstacles identified during the analysis of the data. Kinematic data, Newton-Euler equations and inverse kinematics were used to model the ground reaction forces and moments at the foot, ankle, knee and hip joints. The ground reaction forces were validated alongside data collected from a Bertec Force Plate. By use of the Stretch-Shortening Cycle, the force vs time profile of each landing technique was assessed to classify if a landing technique was "good," "moderate" or "poor." The angular velocity of body segments was also assessed at various phases of the jump smash to determine the effect on performance.

The study found that there are no statistical differences in the ground reaction forces when varying the landing technique. When analysing the force vs time profiles during landing, the Normal Landing Technique (NLT), which typically involves landing on the ball of the foot, and the Toe-First (TF) technique exhibited spring like characteristics and were therefore classified as good landing techniques. The Flat Foot (FF) and Heel First (HF) techniques displayed impact peaks and were therefore considered poor landing techniques.

The Heel First and Flat Foot techniques produced the largest reaction moment at the floor and in all lower limb joints, therefore contributing to a higher risk of injury. There were no statistical differences in segment angular velocity when varying the landing technique. Further analysis on differences in biomechanical responses between male and female athletes is advised.

Table of Contents

Acknowledgements iii
Abstract iv
1 Introduction 1
1.1 Background and Motivation 1
1.2 The Jump Smash Manoeuvre 2
1.3 Common Badminton Injuries 3
1.3.1 Joint range of motion 3
1.3.2 Biomechanical Performance Indicators 6
1.4 Literature Review 7
1.4.1 Biomechanical modelling in jumping sports. 7
1.4.2 Optical system motion capture 9
1.4.3 Inertial sensor systems 9
1.4.4 The Stretch Shortening Cycle 11
1.4.5 Laboratory vs Field Test Settings 12
1.4.6 Filtering Methods and Statistical Analysis 12
1.5 Research Question 13
1.6 Research Objectives 13
2 Research Method 14
2.1 Test Participants 14
2.2 Instrumentation 14
2.2.1 Motion Tracker MTX 14
2.2.2 Body Pack, Access Point and Battery Pack 15
2.2.3 Xsens MVN Lycra Suit 16
2.2.4 Bertec FP4060-05-PT Force Plate 16
2.3 XSENS System Calibration 17
2.4 Xsens Processing Software 18
2.5 Ethical Clearance 18
2.6 Off-Body Recording Procedure 18
2.7 Limitations 19
3 Observations 20
4 Data Processing 21
4.1.1 Reference Angles 21
4.2 Foot Contact Data 22

4.3 Data Filtering 24
4.4 Jump Smash Phase Identification 24
4.5 Ground Reaction Force Model 25
4.5.1 Ground Reaction Forces 25
4.5.2 Ground Reaction Moments 27
4.6 Statistical Analysis 28
4.6.1 Bartlett's Test for Homogeneity of Variances 28
4.6.2 One Way Analysis of Variance (Parametric Test) 29
4.6.3 Kruskal Wallis Test (Non-Parametric Test) 31
5 Results and Discussion 32
5.1 Biomechanical Performance Indicators 32
5.2 Injury Risk Assessment 47
6 Conclusion 51
7 Recommendations 53
8 References 54
Appendices I
Appendix A – Ground Reaction Force and Moment equation derivation p I
Wrists II
Forearm II
Upper Arm III
Head & Neck IV
Upper Trunk V
Hips (Lower Trunk) VI
Thigh VII
Shank VIII
Foot IX
Appendix B – Landing Force Profiles XI
Participant 1 XI
Participant 2 XII
Participant 3 XIII
Participant 4 XIV
Participant 5 XV

Participant 6 XVI
Participant 7 XVII
Participant 8 XVIII
Participant 9 XIX
Participant 10 XX
Appendix C – Ethics Clearance Certificate XXI

Table of Figures

Figure 1:Jump smash manoeuvre illustrating the (1) preparation phase, (2) backswing phase, (3) pre-impact phase, (4) impact phase and (5) follow through phase. 2
Figure 2: (a) Range of knee (b) Range of ankle joint motion. 4
Figure 3: Range of motion of hip joint illustrating the (a) extension-flexion, (b) extension-flexion with pelvic rotation, (c) medial and lateral rotation. (d) abduction-adduction and (e) hip hyperextension. 5
Figure 4: Models of the lower extremities put forward by C.T Farley et al. [12]..... 8
Figure 5: SSC model force profiles [20]. 11
Figure 6: Anatomical positions of motion trackers [26]. 15
Figure 7 : Illustration of Xsens MVN set up. 15
Figure 8: Bertec FP4060-05-PT Force Plate [27]. 16
Figure 9: Calibration and segment kinematic steps conducted by the XSENS software [26]. ... 17
Figure 10: Starting position of participant and server. 19
Figure 11: Toe data misalignment..... 20
Figure 12: Ankle, Knee and Hip reference angles. 22
Figure 13: Height of the right toe from the ground for a given jump smash. 23
Figure 14: Comparison between the Xsens toe contact data and the adjusted data. 23
Figure 15: Comparison between filtered and raw acceleration data for a given body segment.. 24
Figure 16: Centre of Mass vs Time for a given jump smash. 25
Figure 17: F Distribution table at a = 0.05 [32]. 31
Figure 18: VGRF comparison between the Xsens data and the force plate data for a given jump smash..... 32
Figure 19: Box Plots for Vertical Ground Reaction Force for the different landing techniques 34
Figure 20: Force profile during landing for each landing technique for a given participant. 35
Figure 21: Box Plots for Ground Reaction Moments 38
Figure 22: Box Plots of Left Ankle Angle at the moment of ground impact. 39
Figure 23: Box Plot of the left ankle flexion range of motion during landing. 40
Figure 24: Left ankle landing angle vs Left ankle range of motion. 41
Figure 25: Left knee landing angle box plots for the different landing techniques. 42
Figure 26:Knee landing angle vs the Knee flexion during landing..... 42
Figure 27: Angular velocity of left (landing) foot during the Follow Through Phase 44
Figure 28: Lower limb angular velocity box plots during the Forward Swing Phase. 44
Figure 29: Angular velocity box plots for the spinal segments during the forward swing phase 46

List of Tables

Table 1: Summary of the lower limb joints and their associated ranges of motion [8] [9]. 4
Table 2: BPIs measured in previous studies [10]. 6
Table 3: Body Dimensions 14
Table 4: Technical Specifications of Bertec FP4060-05-PT Force Plate [27]. 16
Table 5: Data Summary 21
Table 6: Moment of inertia by segment 27
Table 7: One-way ANOVA table [25]. 30
Table 8: Mean ± SD of VGRF for the different landing strategies. 33
Table 9: Mean ± SD of Normalised Ground Reaction Moments BWBH (Body weight x Body Height) for the different landing strategies. 37
Table 10: Joint angles during landing phase of the ankle and knee joints in the landing leg 39
Table 11: Angular Velocity (rad/s) in the sagittal plane for lower limbs during the Forward Swing Phase 43
Table 12: Spinal segment angular velocity (rad/s) during the Forward Swing Phase 45
Table 13: Risk Table for Vertical Ground Reaction Force 47
Table 14: Risk Table for Ground Reaction Moments 48
Table 15: Risk Table lower limb angular velocity during Forward Swing Phase 48
Table 16: Risk table for joint angle at ground impact 49
Table 17: Risk table for spinal segment angular velocity during Forward Swing Phase 49
Table 18:Summarised injury risk table 50

1 Introduction

1.1 Background and Motivation

Badminton is a racquet sport that has been part of the Summer Olympics since 1992. It holds many similarities to tennis and ping pong (table tennis), but unlike these sports, the projectile, which is referred to as the shuttlecock, does not bounce during the rally. The aerodynamic properties allow the shuttlecock to achieve greater top speeds and deceleration compared to a tennis ball. For these reasons, badminton is considered the fastest racquet sport in the world.

At a professional level, badminton demands excellent motor coordination, sophisticated movements, endurance, agility, timing, strength, and speed. The jump smash is a manoeuvre that uses all of these demands to gain a competitive advantage over the opponent by returning the shuttlecock at immense speeds and at steep angles, thus making it difficult for the opponent to return the shot. Tan Boon Heong, a Malaysian athlete who achieved a shuttlecock top speed of 493 km/h [1], holds the Guinness World Record for the fastest jump smash achieved.

The jump smash's advantages are evident; however, knee and ankle related injuries are prevalent when executing the shot. The rupture of the anterior cruciate ligament (ACL) and the Achilles tendon are common injuries exhibited [2]. Approximately 34% of lower limb injuries are due to shifting weight and change in direction and an additional 7.3% of lower limb injuries are a direct result of incorrect landing technique after a executing a jump [3]. Related research has focussed on upper limb and knee injuries, with little emphasis on ankle injuries.

The aim of this study was to develop a biomechanical model for the badminton jump smash to identify the likelihood of injuries related to the lower limbs when jumping and landing. To achieve this, the study encompassed a full body biomechanical model of the jump and landing. Studies often use optical motion capture systems for full body analysis [4]. While these systems have advantages, there are cases of optical occlusion between the reflective markers and the camera which result in data loss. This requires additional data corrective measures to predict where the occluded target may appear to fill the gaps in the data [5]. Suits with inertial movement sensors eliminate the potential for data loss. The introduction of inertial sensors incorporated into a wearable suit will eliminate the potential for data loss and allow for wireless data recording on-court in a way that is closer to the athlete's natural style of play.

1.2 The Jump Smash Manoeuvre

An effective jump smash is comprised of five phases as illustrated in Figure 1. The manoeuvre is initiated with the preparation phase. The body is positioned sideways so that the feet are parallel to the net, the racquet arm is facing away from the net and the free arm is pointed towards the net. The legs are spread with the knees bent to lower the centre of gravity and to widen the athlete's base of support. This allows the athlete to shift their weight quickly to the rear foot to perform a controlled jump. A high centre of gravity can throw the athlete of balance and will disrupt the accuracy and the power of the shot [6].

The backswing phase begins with the athlete initiating the jump with the rear foot. Whilst the athlete rises, the racquet arm extends at the shoulder and flexes at the elbow. Simultaneously the non-racquet arm extends towards the net. The knees also bend behind the athlete's back [6].

The athlete initiates the forward swing phase as soon as the peak of the jump is reached. As the player swings forward, the knees will begin to extend as the body weight is transferred forward. The impact phase occurs when the racquet contacts the shuttlecock. The elbow straightens at contact and the wrists flex downward to increase the power and to steepen the angle of release. The shuttlecock is returned at this angle. At impact, the abdominal muscles are flexed to generate as much smashing force as possible [6].

The athlete concludes the jump smash with the follow through phase. After impact with the ground, the racquet must continue the swing motion to ensure maximum force is applied to the shuttlecock. The racquet should cross the body and lead to the non-racquet arm at the end of the swing. Landing can occur on both feet or on a single foot, usually the foot opposite to the racquet hand. Upon landing, the athlete must quickly return to the base stance [6].

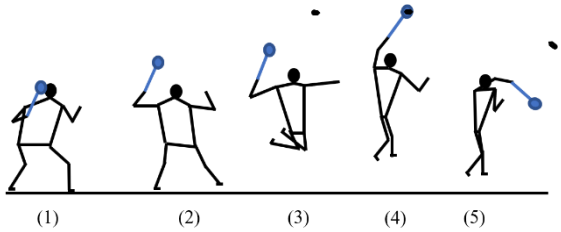


Figure 1:Jump smash manoeuvre illustrating the (1) preparation phase, (2) backswing phase, (3) pre-impact phase, (4) impact phase and (5) follow through phase.

1.3 Common Badminton Injuries

Badminton is a fast-paced game making it a physically demanding sport. A typical match involves abrupt changes in direction, rapid footwork, and repetitive manoeuvres. As a result, the upper and lower limbs experience great stress, which increase the risk for acute or chronic injuries [7].
During the jump smash majority of injuries occur in the ankle or knee joints. An analysis of the jump smash by Rambley et al [4] showed athletes executed a jump smash with the ipsilateral foot (foot on the same side as the racquet) and land with the contralateral foot (foot opposite to the racquet arm). Only 10% of athletes landed with both feet. The study concluded that landing with only a single foot increases the risk of injury in the lower limb joints [4]. The large forces generated during the jump smash are theorised to be contributing factors to ACL injuries and rupture of Achilles tendons [7].

1.3.1 Joint range of motion

The joints of focus for this study are synovial joints. These are joints where the articulating bones are not in direct contact with each other. Instead, they are separated by a cavity filled with synovial fluid, which provides lubrication between the articulating bones. Bones are attached to the joint through ligaments which is connective tissues that provide support to the joint as well as inhibit the range of motion to prevent abnormal joint movements. Tendons are also connective tissue, but unlike ligaments, they attach muscles to bones [8]. Specific joints allow for specific ranges of movement. Common ranges of movement exhibited by joints are flexion/extension, abduction/adduction, rotation, and circumduction. These ranges of motion are further discussed for each joint.

The hip, knee and ankle joints are of key interest in this study. As mentioned previously the rupture of the ACL and Achilles tendon are the most common injuries that are experienced. Flexion and extension in the limbs allow for the change in angle between articulating bones. The hips, knees and ankles experience this motion. Excessive extension or flexion of the joint beyond the normal range of motion can result in injury. This is referred to as hyperextension and hyper-flexion. Injuries related to hyperextension are common at hinge joints like elbows and knees. Abduction and adduction are motion that occurs within the frontal plane. Abduction is the lateral limb movement away from the midline of the body. Adduction is the opposing movement to abduction, allowing for movement towards the midline of the body. This motion is experienced in hip and knee joints. Circumduction is a sequential combination of flexion, extension, abduction and adduction. This is a circular motion of body segments like arms, thighs and hands. Medial and lateral rotation occurs at the hip joint and involves rotating the anterior surface of the limb. The ankle joints experience dorsiflexion and plantar flexion movements. Dorsiflexion is described as lifting the front of the foot so that the toes point upward whereas plantar flexion is described

as lifting the heel of the foot so that the toes point downward [9]. Table 1 summarises the lower limb joints and their range of motion. Figures 2 and 3 illustrate the range of motion.

Table 1: Summary of the lower limb joints and their associated ranges of motion [8] [9].

Joint	Type	Motion	Range (°)
Hip	Ball and Socket	Flexion/Extension	0 – 120
		Hyperextension	0 – 30 or less
		Abduction/Adduction	0 – 40
		Lateral (Outward) rotation	0 – 50
		Medial (Inward) Rotation	0 – 40
Knee	Hinge	Flexion/Extension	0 – 150
Ankle	Hinge	Plantarflexion	0 – 50
		Dorsiflexion	0 – 20
Foot	Plane	Inversion	0 – 35
		Everson	0 – 25

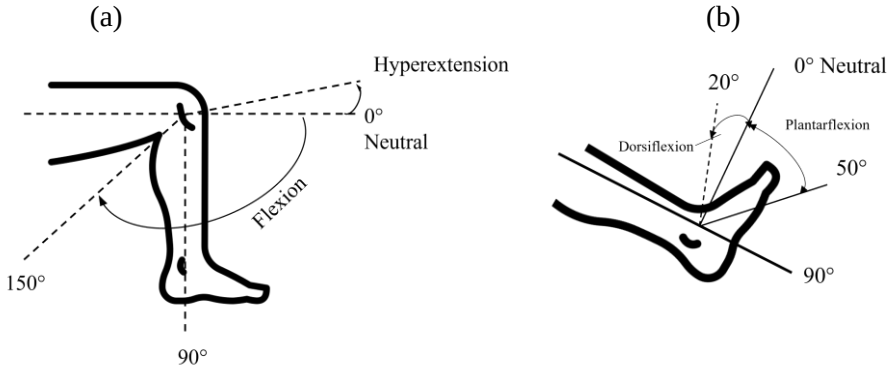


Figure 2: (a) Range of knee (b) Range of ankle joint motion.

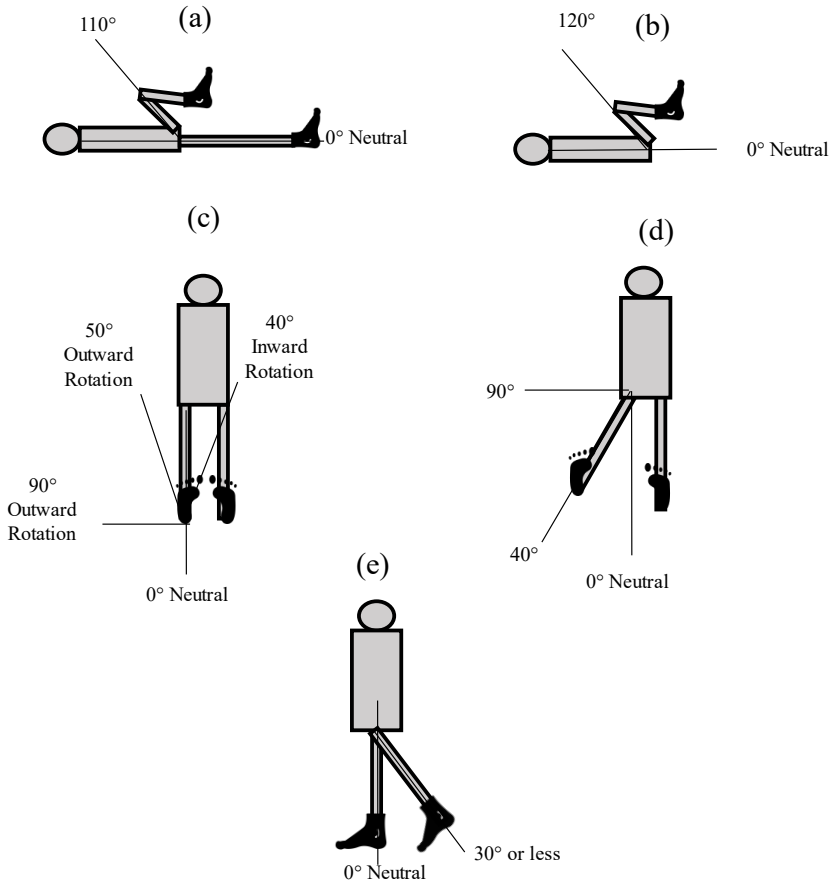


Figure 3: Range of motion of hip joint illustrating the (a) extension-flexion, (b) extension-flexion with pelvic rotation, (c) medial and lateral rotation. (d) abduction-adduction and (e) hip hyperextension.

1.3.2 Biomechanical Performance Indicators

Biomechanical performance indicators are parameters that allow researchers to view biomechanical events from a quantifiable perspective rather than a qualitative one. To quantify the best jump smash manoeuvre to minimise injury risk, improve performance and validate the results, BPIs from previous studies will be considered. The BPIs related to the jump smash are summarised in Table 2.

Table 2: BPIs measured in previous studies [10].

BPI	Description
Centre of mass (m)	Height of the COM is recorded throughout the manoeuvre
Height of jump (m)	Jump height taken as the change in the height of the centre of mass
Knee angle (°)	Measure knee flexion and extension during the distinct phases of the manoeuvre for both racquet and non-racquet legs
Knee angular velocity (°/s)	Angular velocity of knees throughout the manoeuvre for both ipsilateral and contralateral legs
Ankle angle (°)	Measure ankle plantarflexion or dorsiflexion for both ipsilateral and contralateral ankles
Ankle angular velocity (°/s)	Angular velocity of the ankle during take-off and landing for both ipsilateral and contralateral legs
Time (s)	Time taken for centre of mass to move between extreme heights of the jump (max and min heights)
Racquet height (m)	Measured throughout the manoeuvre
Elbow angle (°)	Measure the elbow flexion and extension angle for racquet arm
Elbow angular velocity (°/s)	Angular velocity of the elbow for the racquet arm during the strike of the shuttlecock
Wrist angle (°)	Measure the wrist flexion and extension angles for racquet arm
Wrist angular velocity (°/s)	Angular velocity of the wrist for the racquet arm during the strike of the shuttlecock

1.4 Literature Review

1.4.1 Biomechanical modelling in jumping sports.

In 2005 A.S Rambley investigated the prevalence of the badminton jump smash [4]. The study attempted to use biomechanical modelling to investigate the association of the jump smash technique with injury. Data was collected from 13 male athletes. A total of 84 trials were recorded with an average of 60 frames from the beginning of the preparation phase. Data was collected using 6 cameras (50 Hz shutter) and 25 reflective markers affixed to the participants body segments. The reflective markers were tracked throughout the recording to generate the biomechanical model of the athlete [4].

A.S Rambley analysed the relationship between the athlete's centre of mass and the lower limb angular velocities. The results found that all tests were statistically significant and that 61.9% of landing occurs on the left foot only, 27.4% land with the right foot only and 10.7% land with both feet. [4]. A.S Rambley notes that even though landing with both feet provides a wider base of support, majority of the athletes landed with a single foot only. He suggested that this might be due to the objective of achieving a higher jump and striking the shuttlecock at a higher position. The study also suggests that landing with a single foot could lead to imbalance and thus injury. The study suggested further kinetic analysis to fully quantify the risks.

Y. Ramasamy et al conducted a correlative study to determine the contribution of the upper and lower limbs of badminton players on the shuttlecock velocity [10]. Reflective markers were positioned on the body segments of the athlete and on the racquet. Data was acquired using Qualisys AB 411 05n cameras, which captured footage at 700 frames per second. Kistler force plates were also used to acquire ground reaction forces at 700 Hz. Nineteen Malaysian athletes performed the forehand straight jump smash. Biomechanical parameters such as the centre of gravity (COG), knee angles, leg angles, elbow angles and wrist angles were measured. They also measured the vertical ground reaction force (VGRF). The biomechanical parameters measured were then assessed at a significance level of 0.05 to determine the significance and the contribution towards the results. The study showed that the VGRF, the height of the jump, the angular velocity of the wrist and the racquet head speed contributed to high shuttlecock velocity. The study suggests that by applying the principles of kinetic chain, the force required to execute a high velocity shuttle is transferred through the body to the foot, thus, producing a higher VGRF. This study focuses on upper body kinematics and recommends further investigation on the lower limb kinematics [10].

Another study attempted to investigate the influence of the jump smash on the lower extremity loads by investigating the effects of the forward swing phase on the landing [11]. The torque and

stiffness on the ankle, knee, and hip joints were analysed. The study was conducted on 16 athletes and data was captured using high-speed infrared camera The cameras recorded at 300 Hz. A Kistler Force plate, which sampled at 1500 Hz was used to measure the ground reaction forces that were generated during the landing phase. Reflective markers were affixed to the racquets and shuttlecocks which were tracked through the images to obtain the kinetic and kinematic data of the athlete and the shuttlecock. The kinematic and kinetic parameters of the lower limbs were captured using the Vicon Nexus Version 1.8.5. The athletes performed a lateral jump smash and landed on a single leg [11]. The study found that the main impact points during landing were at the ankle and hip joints. One-legged landing increased the load experienced by the lower extremity joints. The study also showed that after performing a swing, there was a smaller hip joint flexion angle, which resulted in a stiffer landing strategy for the athletes. This study suggests that there is an increasing risk of injury as a result of a stiffer landing strategy that causes higher forces experienced in the joints [11]. This study did not make use of a full body biomechanical model. Instead, it focussed on the lower limbs using the two-dimensional joint stiffness calculation model put forward by C.T Farley et al [12]. This model uses the peak value of the joint torque experienced and the joint angle during landing. The model is illustrated in Figure 4, and the stiffness of the joint was calculated using:

$$k_{joint} = \frac{\Delta M_{joint}}{\Delta \theta_{joint}} \quad (1)$$

where the torsional stiffness of the joint is k_{joint}, the peak value of the torque experienced by the joint is ΔM_{joint} and the joint angle is $\Delta \theta_{joint}$ [12].

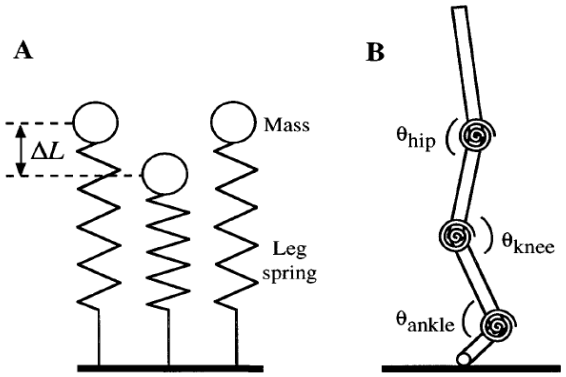


Figure 4: Models of the lower extremities put forward by C.T Farley et al. [12]

The models in Figure 4 were used to assess the stiffness of the lower limbs when hopping on different surfaces. The lower limb is modelled as a linear "leg spring" with a point mass, otherwise known as a simple spring mass system, as indicated in Figure 4A. The stiffness of the entire leg structure during the ground contact phase of landing is represented by the stiffness of the linear spring. C.T Farley et al [12] emphasised that the spring mass model does not represent the actual structure of the musculoskeletal system, but rather the behaviour only. "In reality, the length

change of the leg spring that occurs during the ground-contact phase corresponds to joints flexing and extending. For example, during hopping in place, the ankle, knee, and hip flex during the first half of the ground-contact phase and extend during the second half of the ground contact phase" [12]. Thus, the multi-jointed model shown in Figure 4B, models the leg structure more accurately. This model consists of four segments (head-arms-trunk, thigh, shank, and foot). Each segment is joined by torsional springs, which represent the ankle, knee, and hip joints, as illustrated [12].

In 2014, a study was conducted to determine the effects of different landing techniques on knee kinematics and kinetics [13]. Three-dimensional kinematic and kinetic data for 18 male and 18 female participants were captured for stop-jump and side cutting basketball manoeuvres. Three landing techniques were considered: a natural landing, attempting to land softly and landing with existing knee flexion prior to contact with the ground. The study found that attempting to land softly decreased the peak posterior ground reaction forces (PPGRF) compared to a natural landing. This also led to a decrease in the knee extension moment exhibited. Landing with initial knee flexion at ground contact resulted in higher knee flexion angles compared to the natural landing. Overall, the study showed that ACL loading reduces when landing with greater knee flexion angles and a softer landing, but performance can decrease due to a longer stance time [13].

1.4.2 Optical system motion capture

Previous studies that used 3-D motion capture, such as the study conducted by A.S. Rambley et al [4], C. Hung et al [11], and Y. Ramasamy [10] involved the use of optical systems for data collection. High-speed infrared cameras were used to capture the motion of the athlete with reflective markers fixed at anatomical landmarks. These markers are tracked throughout the footage to obtain a full-body motion capture [11]. The need for a camera set up confines this approach to a laboratory setting. Due to the complexity of manoeuvres, markers are also prone to occlusion, resulting in a loss of potential data [14]. However, there have been advances in wearable technology and can be considered as alternatives for full body motion capture.

1.4.3 Inertial sensor systems

The use of inertial sensors and microelectromechanical sensors (MEMS) allow this modern technology to provide real time feedback and to overcome the limitations of optical motion capture systems. A number of studies utilising inertial sensors have been conducted across different sports to assess the movement of athletes. Systems such as the Spectra Symbol flex sensor uses the change in resistance of a sensor when a force is applied (similar to that of a strain gauge) to track the motion of joints [14]. This flex sensor was previously used in badminton related studies to determine different types of handgrips of the racquet by measuring the flexion angles of the thumb, index and middle fingers [14]. The reliability of inertial systems was found

to be acceptable during a study conducted by Luteberget et al [15]. The study looked at the reliability of inertial systems in the context of Handball manoeuvres. The inertial sensors were assessed in a laboratory setting and during training sessions. The inertial sensors exhibited a CV% range between 3.1% and 6.7% for the laboratory setting. The CV% increased to 5.6% during training sessions [15].

Wearable technology was applied in biomechanical studies for swing sports like tennis, badminton, and golf to classify the different types of swings. By applying wireless inertial sensors to the wrists of the right and left arm, the waist and the right ankle, Z. Wang et al were able to develop a system that can classify different types of badminton strokes using biomechanical data [16]. This study only analysed the motion of the wrists, waist, and ankles. The studies that were mentioned above focussed on performance analysis of specific limbs using wearable technology but do not consider full-body analysis. The sensor fixed to the racquet was mounted just above the handle grip. A video recording system was used to capture and determine the maximum shuttlecock velocity.

T.Jaitner et al utilised wearable inertial sensors to assess the relationship between shuttlecock velocity and the arm kinematics during the execution of a jump smash [17]. Inertial sensors were placed on the racquet, the upper arm and the lower arm. The objectives of the study were to quantify the variables that influence the movement of the arm during the forward swing phase of the jump smash. The study also looked at how these influences were translated to the acceleration of the racquet [17]. The study identified that participant who performed the jump smash with higher acceleration values in the sagittal plane for the arm segments had an extended arm during impact whereas participants with a flexed arm at impact had a higher acceleration in the parallel plane. The shuttlecock velocity was found to have no difference between the two.

The study mentioned above incorporated inertial sensors for assessing performance during the badminton jump smash. They were however limited to single limbs and focus was placed on performance. This study was not expanded to view the effect of full body mechanics on performance or on injury prevention. The use of inertial sensors for full body analysis for injury prevention has been used in areas outside of badminton [17].

Wearable inertial technology was employed by G. Logar et al, to estimate the forces and moments in joints for a take-off in ski jumping [18]. A link-segment model was developed, derived recursive from Newton-Euler inverse dynamics to calculate the ground reaction forces. Data collected from a force platform validated the link-segment model. The link-segment model

allowed for accurate force estimation in the joints as well as the vertical ground reaction force. The equations used for the link-segment model are:

$$\sum_{i}^{n} F_i = m_i a_i \tag{2}$$

$$\sum_{i}^{n} M_i = I_i \dot{\omega}_i \tag{3}$$

where the force of the segment is F_i, the weight of the segment is m_i , the acceleration of the segment is a_i , the moment of the segment is M_i , the moment of Inertia for the segment is I_i , and the angular acceleration of the segment is $\dot{\omega}_i$ [18].

1.4.4 The Stretch Shortening Cycle

The stretch-shortening cycle (SSC) is used to describe the cyclical action of the muscles during jumping techniques. The muscles undergo eccentric contraction before experiencing a period of concentric contraction [19]. The SSC model best describes the behaviour of muscles during activity as having spring like qualities. Pedley et al used the SSC model to characterise different landing profiles in adolescent females [20]. The study assessed the force vs time profiles during the landing phase of middle and high school athletes. Jump profiles were classified as poor if the force vs time profile experienced impact peaks. Jump profiles were classified as good if they exhibited no impact peaks, thus characterising spring like behaviour. Moderate jumps were classified when both impact and spring like behaviour could be identified on the force-time profile [20].

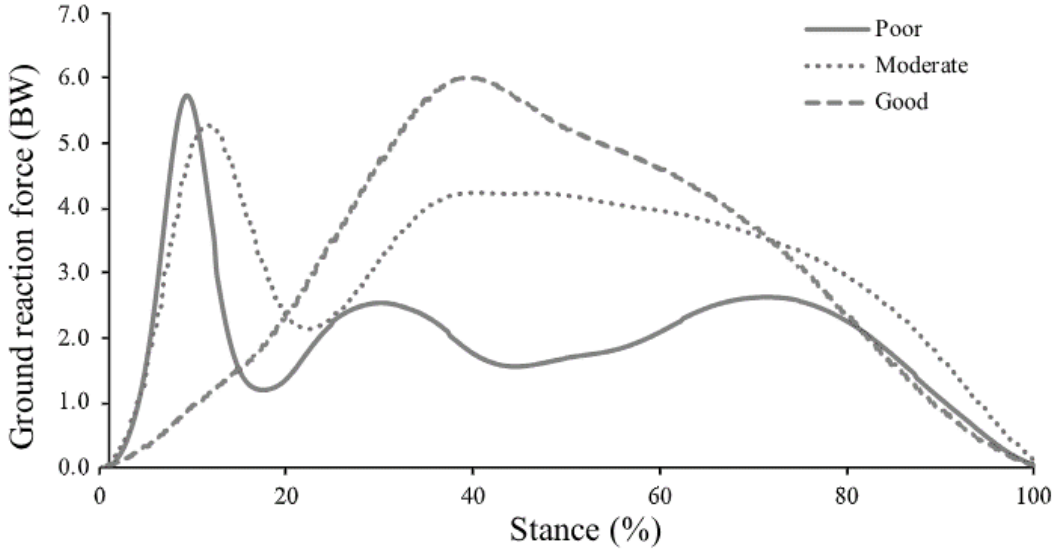


Figure 5: SSC model force profiles [20].

1.4.5 Laboratory vs Field Test Settings

The influence of laboratory vs field testing must always be considered. Traditionally, biomechanical related studies were conducted in a laboratory setting due to limitations in technology required to record data. Laboratory environments are significantly different to the training and on-court environments. While laboratory settings can have tighter controls to reduce the likelihood of error, results must also be valid and applicable in match conditions [21]. Advances in wearable inertial sensor technology allow for improved methods of data capture by allowing researchers to conduct tests in the field setting that is familiar to the athlete rather than in a laboratory setting. Hardey et al [22] investigated the effects of stress on athletes as a result of being in a laboratory setting. The study found that artificial and unfamiliar settings of a laboratory induce heightened anxiety in athletes. This can ultimately have implications on the performance of the athlete and the results of the study thereof [22].

Performance expectations can also be another psychological factor that can affect athletes in a laboratory setting. A. Bandura [23] suggested that under a laboratory setting, athletes experience an increase in pressure to perform as a result of the nature to collect meaningful data. The athlete's beliefs about their capabilities can influence their overall performance [23].

1.4.6 Filtering Methods and Statistical Analysis

Analysis of biomechanical data often involves noisy and complex datasets that require filtering methods and statistical analysis to extract meaningful insights. Butterworth low pass filters are often employed in biomechanics to reduce the effects of noise and to improve signal to noise ratio [24]. The study conducted by C. Hung [8] utilised low pass filters to filter out interference.

Parametric and non-parametric tests are statistical methods that are commonly employed. In the research conducted by C. Hung [8], an analysis of variance test (ANOVA Test) was conducted to compare the means of the different groups that were tested to determine if there are significant differences between the groups [25]

1.5 Research Question

Can modelling the badminton jump-smash manoeuvre provide insights to effectively prevent injury and improve athlete performance?

1.6 Research Objectives

The objectives of this research are to:

1. Determine the BPIs involved with the badminton jump smash. These include but are not limited to the Ground Reaction Forces, joint angle, joint angular velocity, Centre of Mass (COM) height.
2. Assess the effect of several BPIs on the potential for injury. These are including but not limited knee angles, ankle angles, jump height, timing of the shot, forces exerted from the jump and the forces experienced during the follow through phase.
3. Determine the ideal landing position that will minimize the risk of injury while also improving effectiveness of the manoeuvre.

2 Research Method

2.1 Test Participants

The study was conducted on 16 participants from Badminton South Africa (BSA) to capture the variation in jumping styles. Under normal circumstances, an equal amount of both male and female athletes would have been ideal to allow for an opportunity to compare the results between the two genders. However, the COVID-19 pandemic was at its peak during the time of testing. This not only influenced the testing protocols but also the amount of testing sessions that were available. From the 16 athletes tested, 13 were male and 3 were female. The testing took place during the BSA training camps. To calibrate the inertial sensors, the body dimensions in Table 3 were captured for each participant and entered into the motion capture software.

Table 3: Body Dimensions

Parameter	Description
Body Height	Ground to top the head
Shoe Length	Length of foot or shoe
Shoulder Height	Ground to C7 spinal process
Shoulder Width	Right to left distal tip of acromion
Arm Span	Tip of fingers of right hand to the tip of the fingers of the left hand in T- Pose
Hip Height	Ground to greater trochanter
Hip Width	Right to left anterior superior iliac spine
Knee Height	Ground to lateral epicondyle
Ankle Height	Ground to distal tip of lateral malleolus

2.2 Instrumentation

The following items form part of the inertial motion capture system from XSENS MVN Link System that was used to acquire real time three-dimensional biomechanical data of the athletes.

2.2.1 Motion Tracker MTX

The MVN Link system captures the motion of the body segment using a miniaturised inertial sensor called the MTX motion tracker. The motion tracker is equipped with a 3D linear accelerometer, 3D gyroscopes to measure angular velocity and a 3D magnetometer that can measure the magnetic field of the earth. The module also has a barometer that measures the atmospheric pressure. The module also has Velcro allowing it to be easily secured on the athlete. There are 17 motion tracker modules, and they are placed at the indicated positions shown in Figure 6.

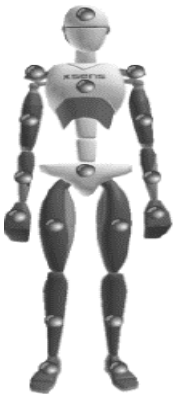


Figure 6: Anatomical positions of motion trackers [26].

2.2.2 Body Pack, Access Point and Battery Pack

The Body Pack (BP) is the data acquisition system. The 17 motion trackers connected to the BP to allow for synchronised data collection. The BP transmitted data to the Access Point along a wireless connection at either 2.4 GHz or 5.0 GHz. The Access Point connected to a PC via Ethernet. Data sampled at 240Hz. A rechargeable Lithium-Ion Battery Pack with an operating life of approximately 9 hours powered the BP and motion trackers [26].

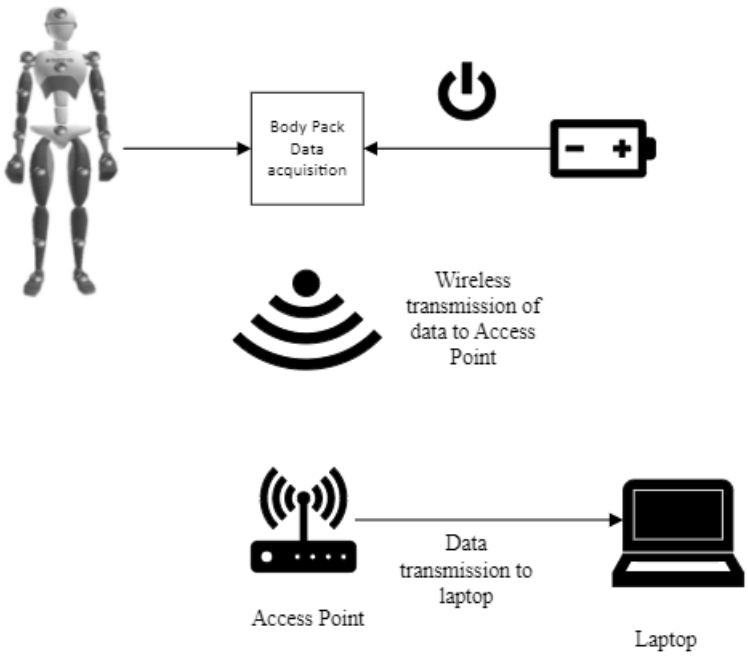


Figure 7 : Illustration of Xsens MVN set up.

2.2.3 Xsens MVN Lycra Suit

The Xsens MVN Lycra Suit allowed the inertial sensors to be secured at specific anatomical points throughout the body. The suit was available in five assorted sizes and allowed for a snug fit on the athletes to ensure the inertial sensors are fixed at the correct anatomical positions. The suit was not too tight, which would have affected the range of motion of the athlete.

The suit also incorporated a headband, gloves and footpads, which allowed the attachment of the inertial sensors to the head, hands and feet.

2.2.4 Bertec FP4060-05-PT Force Plate

The Bertec FP4060-05-PT is a portable force plate that was used to measure the ground reaction forces of the jump. The force plate is capable of measuring the orthogonal forces (F_x, F_y and F_z). The force plate achieved this using strain gauged load transducers. The above-mentioned model is available in standard load ranges of 5000N and 10 000 N [27]. For this research the 10 000N variant was used due to the significant impact forces that were expected during landing. Table 4 summarises the technical specifications of the force plate.



Figure 8: Bertec FP4060-05-PT Force Plate [27].

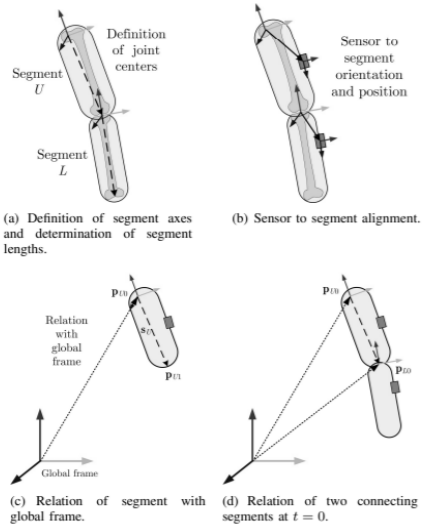
Table 4: Technical Specifications of Bertec FP4060-05-PT Force Plate [27].

Parameters	Value
Dimensions (mm)	400x600x50
Weight (kg)	8
Max Load F_z (N)	10 000
Max Load F_x, F_y (N)	2500
Natural Frequency F_z (Hz)	250
Natural Frequency F_x, F_y (Hz)	150
Static Resolution (N)	±0.05
Resolution (N/LSB)	0.09
Linearity (%FSO)	0.2

2.3 XSENS System Calibration

As intuitive as the XSENS system may be, the instruments required calibration for each individual to align the motion trackers orientation with the orientation of the body segments and to align the relative distances between the joints. Once the body dimensions were loaded on the system and the instruments were secured to the athlete, the N-pose + Walk calibration procedure was completed as follows:

1. The athlete stood in the N-Pose position for 4 seconds. This was an upright position with hands by the side of the athlete and the feet faced forward.
2. Once prompted by the investigator, the athlete walked forward for a few seconds.
3. When prompted by the investigator, the athlete stopped, turned around and walked back to the original starting position.
4. Once the athlete returned to the origin point, the athlete stopped, turned around and assumed the N-pose for a few more seconds until the investigator was satisfied that the Xsens software was no longer recording a calibration.
5. The XSENS software then performed checks to ensure the quality of the calibration. These checks included a measure for standing still and the alignment of the motion trackers on each segment while walking [26].
6. There were four levels of calibration quality. These were “good,” “acceptable,” “poor” and “fail” in descending order of quality. For the sake of consistency between athletes, any quality other than “good” required a recalibration until the required quality was achieved.



(a) Definition of segment axes and determination of segment lengths.
(b) Sensor to segment alignment.
(c) Relation of segment with global frame.
(d) Relation of two connecting segments at $t = 0$.

Figure 9: Calibration and segment kinematic steps conducted by the XSENS software [26].

2.4 Xsens Processing Software

Raw data that is captured in the form of linear acceleration, orientation and positional data of the sensors. The raw data is then processed on the Xsens software using kinematics to produce the linear and angular acceleration, velocity and position of each body segment. Using these calculated variables, the software then animated the model to visually represent the movement that was recorded. The animated visual as well as the pre and post processed data is saved and exported in an "mvnx" file format.

2.5 Ethical Clearance

This study involved collecting biomechanical data from human subjects. As such, ethical clearance was obtained from the human research ethics committee medical (HREC-Medical). The principal investigator Ms Taahirah Mangera requested the ethical clearance. Data was collected following the guidelines set out by the HREC-Medical. Case Number: M200925

2.6 Off-Body Recording Procedure

The testing was conducted during the Badminton South Africa Training Camp. Athletes participated in a match consisting of a set (first team to 21-points). Once the match was completed, the athlete would proceed with the test procedure. All participants were tested after their scheduled match to maintain consistency. This approach was chosen to eliminate participants idly waiting for their turn and would ensure that participants would not require an additional warm-up session prior to the data collection.

Four landing techniques were considered to classify an effective jump smash that would minimise risk of injury. The landing techniques considered were:

1. Normal Landing Technique (The participants land in their usual technique they are comfortable with.)
2. Toe First (Upon landing, the toes of the participant must contact the ground first)
3. Heel First (Upon landing, the heel of the participant must make contact first)
4. Flat Footed (Upon landing, the athlete lands with both the toes and heels simultaneously).

These landing techniques were selected to observe the effect of each landing technique on the resulting indicators for lower limb injuries. Each landing technique was assessed 3 times. Overall, 12 separate jump smashes were executed and recorded per participant.

The testing procedure was as follows:

- Participants would position themselves at the centre and at the edge of their court. On the direct opposite of the court, a volunteer was tasked with serving the shuttlecock to the participant.
- The volunteer served the shuttlecock to the participant high enough for the participant to return the shot with a jump smash.

To minimise variation in the serve, the starting positions of the participant and the position of the server remained constant throughout the testing.

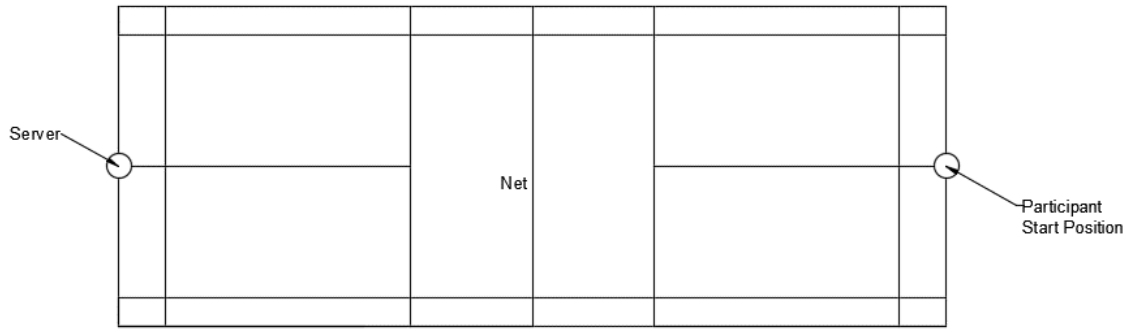


Figure 10: Starting position of participant and server.

After the twelve jump smashes were recorded, three jumps per participant were recorded on the Bertec Force Plate to obtain the vertical ground reaction forces. These jumps were also recorded with the Xsens suits simultaneously. The vertical ground reaction force data obtained from the force plate was used to validate the vertical ground reaction force that was calculated from the Xsens biomechanical data.

2.7 Limitations

The research and methodology focused on the jump smash execution in isolation to develop a strong foundational understanding of the BPIs associated with this manoeuvre. It does not consider the effects of previous manoeuvres leading up to the execution of the jump smash (e.g., athletes recovering from returning a previous shot before executing the jump smash). The research is also unable to provide comparison in the results between male and female participants due to the lack of participation from female badminton athletes.

3 Observations

Once the shuttlecock was served, participants repositioned themselves on the court before taking the preparation phase stance. The jump smash would then be executed. Each time the shuttlecock struck the net, the test would be repeated until the shuttlecock was satisfactorily returned to the opposite court.

Of the 16 athletes that participated, 6 participants did not satisfactorily execute the jump smash with the correct technique described in literature. The model used to assess the jump smash in this study identifies the four phases of the jump smash before proceeding with any additional analysis. This was done to for consistency when referencing the jump smash phases across all participants. Jump smash phases could not be identified for these 6 participants. Upon further inspection it was clear than these participants would execute a small hop off the ground and not fully execute a jump with the knees flexed behind the back. In these cases, where jump smashes were not executed in the correct technique, the data was excluded to avoid skewing the results. The participants that executed the jump smash correctly landed on the foot opposite to the racquet arm (contralateral foot) as per the literature.

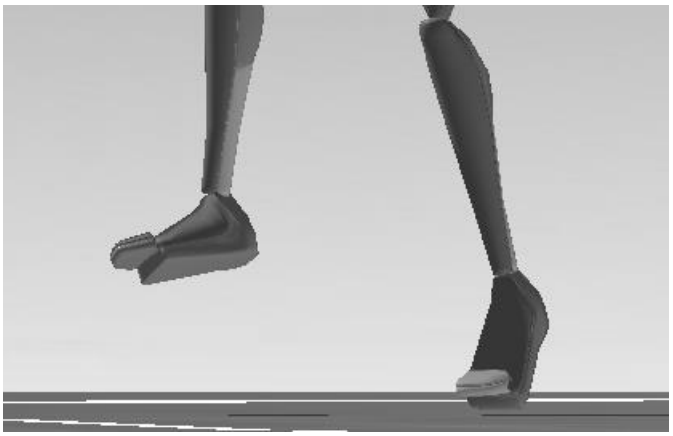


Figure 11: Toe data misalignment

Upon observation of the Xsens avatar model in the Xsens software, it was observed that the toes were not aligned with the rest of the foot for the 7 participants who were assessed in the first testing session. This was resolved for the remaining participants by omitting the sole height measurement in the Xsens model as this is already accounted for in the full body height measurement. The measurement was omitted in the calibration of the remaining 3 participants that were tested in the second session to avoid the error. Due to the toe misalignment, the models indicated that the toes were 10cm above the ground such that the data would suggest that the toes would never contact the ground, even when the athletes landed with their toes first. The toe contact data gathered in the first session required adjustment and correction before data processing could proceed.

4 Data Processing

The original XSENS data files were saved in ".mvn" format. This file format is only readable in the XSENS MVN Studio software; however, the file was exported to an ".mvnx" format, thereby allowing the data to be imported into Matlab as a structured array. The data from the force plate was saved in csv file format, which was also imported into Matlab for further analysis. Each individual jump smash was processed in Matlab, and the results were written to an excel spreadsheet for further statistical analysis. Table 5 summarises the recorded data available for processing and analysis.

Table 5: Data Summary

Field	Data
Segment Data	Orthogonal data for orientation, position, velocity, acceleration, angular velocity and angular acceleration for 23 body segments
Sensor Data	Orthogonal data for sensor acceleration, sensor magnetic field and sensor orientation for all 17 motion trackers
Joint Data	Joint Angle orthogonal data in XYZ and XZY format for 22 joints
Foot Contact Data	Binary data for heel and toe contact for both feet. 1 indicates contact with the ground and 0 for no contact.
Frame Data	Time (s), Time stamp, orthogonal position Centre of Mass (m)

4.1.1 Reference Angles

Reference angles had to be established prior to the development of a biomechanical model and data processing. The ankle, hip and knee joints were analysed during the different phases of the jump smash. More importantly, the joint incident angles were determined (angles of joints during initial ground contact upon landing) to compare the biomechanical response of these joints to the different landing techniques. A reference angle of 0° corresponded to the participant standing as normal.

For the sagittal plane, dorsiflexion of the foot was considered as a positive angular displacement of the ankle. A negative angular displacement was a reference for plantarflexion. Bending the knee and hip joints under flexion were considered the positive displacement and extension of the knee and hip were considered as the negative angular displacement.

For the frontal plane, eversion of the ankle was given a positive displacement whilst inversion was given a negative displacement. For hip and knee joints, abduction was referenced as the positive displacement whilst adduction referenced negative displacement.

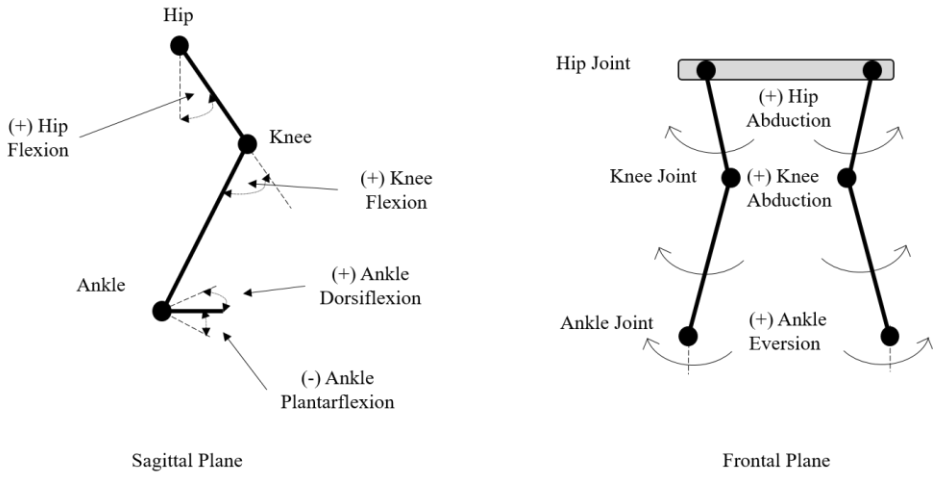


Figure 12: Ankle, Knee and Hip reference angles.

4.2 Foot Contact Data

The foot contact data comprised of four arrays for the different foot contact points. These were the Left Toe, Left Heel, Right Toe and Right Heel. The data is binary, indicating whether the point was in contact with the ground or not. A value of 1 is given if contact with the ground is made, whilst no contact was given a value of zero.

Upon inspection of the data, it was determined that the toe contact data that was created by the XSENS software was unreliable to determine the exact moment that the athlete's toe or heel contacted the ground during the landing phase. At a given moment when the athlete stood completely still with both heels and toes planted firmly on the ground, the toe contact data suggested that the toes were off the ground. Upon closer inspection of the model, it was found that the position of the toes were a few millimetres off the ground at moments when they were in direct contact as illustrated in Figure 13. Due to the unreliability of the foot data, the heel and toe contact data required adjustment. This was achieved by analysing the Preparation Phase whilst the athlete stood still to identify the range that the height of the toe and heel data would fluctuate. This range was set as the height of the ground. Any height that exceeded this limit was referenced as the heel or toe that was not in ground contact. Any height within this range was referenced as the heel or toe in contact with the ground. Figure 14 illustrates a comparison between the unreliable XSENS toe contact data and the Adjusted Toe Contact Data. The original toe contact data fluctuated between 1 and 0 during moments when the athlete is standing still during the execution of the manoeuvre. The adjusted toe contact data eliminated these fluctuations. After adjusting the toe and heel data, the VGRF model was computed.

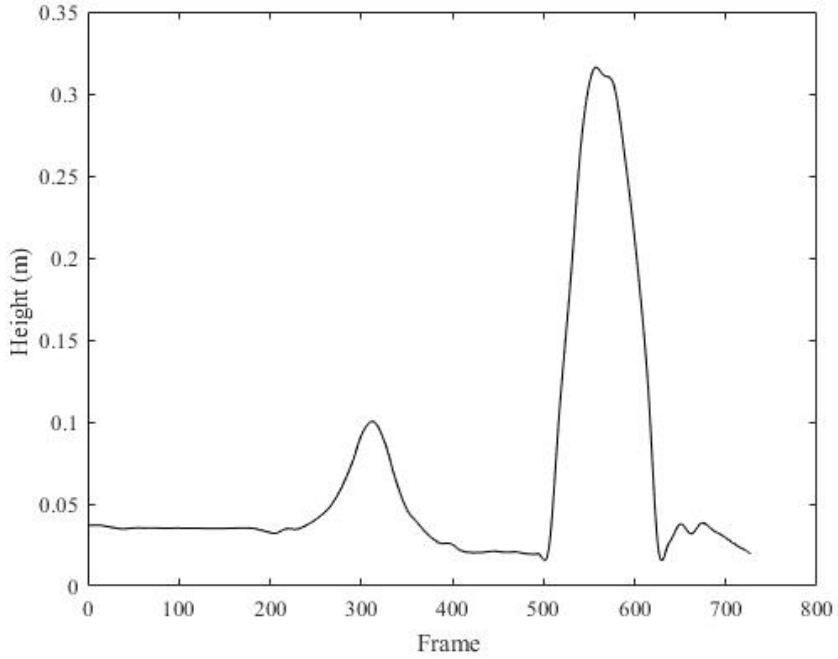


Figure 13: Height of the right toe from the ground for a given jump smash.

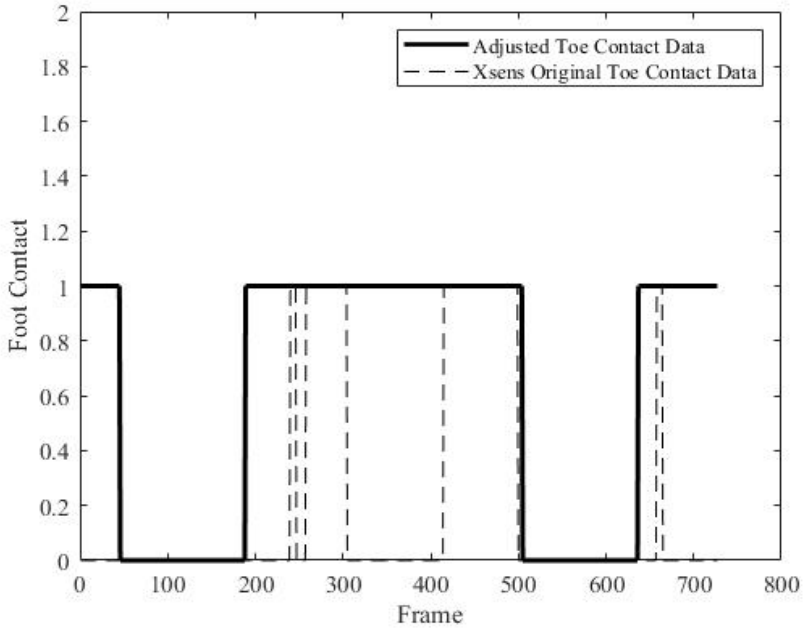


Figure 14: Comparison between the Xsens toe contact data and the adjusted data.

4.3 Data Filtering

The acceleration and velocity data (linear and angular) were susceptible to noise and required filtering to reduce errors in the results. The acceleration, velocity, and angular acceleration and velocity were filtered using a fourth order Butterworth filter with a cut-off frequency of 10 Hz and a sampling frequency of 240 Hz which is the frame rate of the Xsens system. The fourth order was chosen as the optimum filter order which reduced data noise without changing the shape of the data profile.

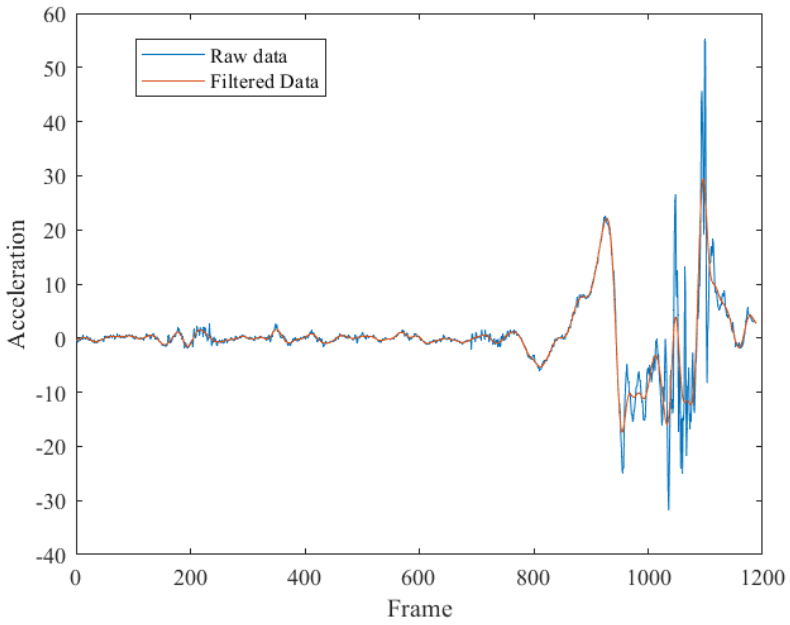


Figure 15: Comparison between filtered and raw acceleration data for a given body segment.

4.4 Jump Smash Phase Identification

Figure 16 illustrates a typical Centre of Mass profile during the execution of the forward jump smash. By observing the centre of mass (COM) data, changes in the COM height proved useful for the identification of the Preparation Phase (PP), Backswing Phase (BSP) and Follow Through Phase (FTP) or Landing Phase. The Forward Swing Phase (FSP), which occurs after the Back Swing Phase until impact with the shuttlecock, cannot be determined using only the COM data. The FSP was identified with the angular velocity data of the racquet hand. The Forward Swing Phase is identified by the sudden change in the angular velocity of the racquet arm after the BSP from positive to negative which coincides with the athlete striking the shuttlecock. The lowest COM position after the execution of the jump is characterised as the end of the Follow Through Phase and hence, the end of the jump smash. The jump smash phases were indexed to allow for the comparison of BPIs between each participant and landing technique.

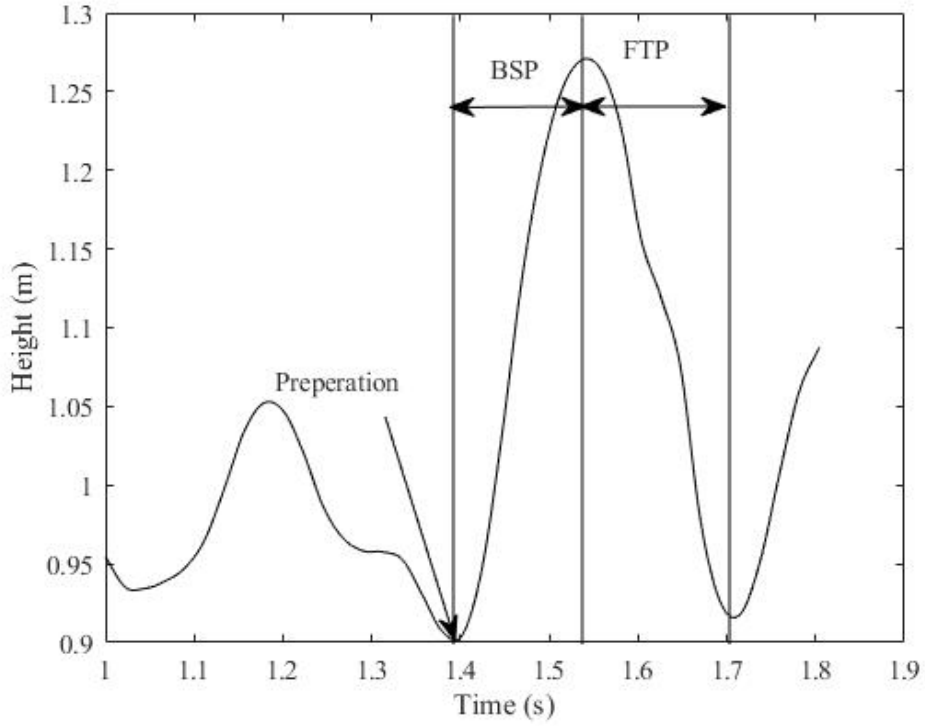


Figure 16: Centre of Mass vs Time for a given jump smash.

4.5 Ground Reaction Force Model

4.5.1 Ground Reaction Forces

The vertical ground reaction force (VGRF) experienced during the PP and FTP was modelled as a multi-segment of rigid bodies. Each body segment was classified as a rigid link with its own mass and connected to other segments (links) at the joints. The Vertical Ground Reaction Force Model was based of the Link-Segment Model [12]. The model began by estimating the contributions of the reaction force of the upper body segments (the hands, forearms, upper arms, head, neck and torso.) The equations for the vertical reaction forces in the upper body segment were derived as:

$$F_{left\ wrist} = m_{left\ hand}\left(9.81 + a_{left\ hand}\right) \quad (4)$$

$$F_{right\ wrist} = m_{right\ hand}\left(9.81 + a_{right\ hand}\right) \quad (5)$$

$$F_{left\ elbow} = m_{forearm}\left(9.81 + a_{left\ forearm}\right) + F_{left\ wrist} \quad (6)$$

$$F_{right\ elbow} = m_{forearm}\left(9.81 + a_{right\ forearm}\right) + F_{right\ wrist} \quad (7)$$

$$F_{left\ shoulder} = m_{upper\ arm}\left(9.81 + a_{left\ upper\ arm}\right) + F_{left\ elbow} \quad (8)$$

$$F_{right\ shoulder} = m_{upper\ arm}\left(9.81 + a_{right\ upper\ arm}\right) + F_{right\ elbow} \quad (9)$$

$$F_{Head\ Neck} = m_{Head\ Neck}\left(9.81 + a_{right\ upper\ arm}\right) \quad (10)$$

$$F_{Upper} = F_{Head\ Neck} + F_{shoulders} + F_{elbows} + F_{wrists} \quad (11)$$

Having determined the contributions of the upper body reaction force, reaction forces were derived for the hip, knee and ankle joints for the different landing scenarios. The considered scenarios were:

1. Left Toe, Left Heel, Right Toe & Right Heel
2. Left Toe & Right Toe
3. Left Heel and Right Heel
4. Left Toe only.
5. Left Heel only.
6. Right Toe only
7. Right Heel only
8. Right Toe & Right Heel

For Scenarios 1, 2 and 3 where components from both feet are in contact with the ground, the reaction force on the hips were derived as:

$$F_{left\ hip} = F_{right\ hip} = \frac{1}{2}\left(m_{torso} \times (9.81 + a_{torso}) + F_{Upper}\right) \quad (12)$$

For the remaining scenarios where only one foot is in contact with the ground at a given time, the reaction force was derived to be equation 13 and 14. For these scenarios, the assumption was made that the hip joint in contact with the ground absorbed the full reaction force of the upper body segments as well as the contributed force of the leg that was not in contact with the ground. In this case, assume the left foot is in contact whilst the right foot is off the ground.

$$F_{right\ hip} = m_{thigh}\left(9.81 + a_{right\ thigh}\right) + m_{shank}\left(9.81 + a_{right\ shank}\right) + m_{foot}\left(9.81 + a_{right\ foot}\right) \quad (13)$$

$$F_{left\ hip} = m_{torso}(9.81 + a_{torso}) + F_{Upper} + F_{right\ hip} \quad (14)$$

Then the reaction forces in the knees were derived as:

$$F_{left/right\ knee} = m_{thigh}\left(9.81 + a_{left/right\ thigh}\right) + F_{left/right\ hip} \quad (15)$$

The reaction forces in the ankles were derived as:

$$F_{left/right\ ankle} = m_{shank}\left(9.81 + a_{left/right\ shank}\right) + F_{left/right\ shank} \quad (16)$$

If the participant had both feet planted on the ground such as scenario one, then the VGRF is derived as:

$$VGRF_{left/right} = F_{left/right\ ankle} + m_{foot}\ (9.81 + a_{left/right\ foot}) \quad (17)$$

If only the toes were in contact with the ground then the VGRF was derived as:

$$F_{toes\ left/right} = F_{left/right\ ankle} + 0.8 \times m_{foot}\ (9.81 + a_{left/right\ toes}) \quad (18)$$

$$VGRF_{left/right} = F_{left/right\ toes} + m_{toes}(9.81 + a_{left/right\ toes}) \quad (19)$$

where, m_{toes} = 0.2 x m_{foot} [28]. For scenarios where the heels were in contact with the ground, then equations 16 was used.

Body segment weight data was obtained from a study conducted by P. de Leva which reported the percentage weight of each body segment [28]. Finally, the ground reaction force was normalised by dividing it by the participant body weight.

The above approach was repeated for the reaction force in the X component, by substituting the acceleration values with the corresponding acceleration in the X direction.

4.5.2 Ground Reaction Moments

Once the ground reaction forces were computed, the ground reaction moments were then calculated using inverse dynamics. The moments of inertia were estimated by modelling each segment as a simplified geometric shape. P. de Leva obtained body segment dimensions for those segments which were not measured on each participant [28].

Table 6: Moment of inertia by segment

Segment	Simplified geometric shape	Moment of Inertia $\boldsymbol{I_s}$
Head & Neck	Sphere	$I_{Head} = \frac{2}{5} m_{Head\ Neck} \times {r_{head}}^2$ (20)
Upper Trunk	Plate	$I_{Upper\ Trunk} = \frac{1}{12} m_{UpperTrunk} \times {l_{UpperTrunk}}^2$ (21)
Middle Trunk	Plate	$I_{\text{MiddleTrunk}} = \frac{1}{12} m_{MiddleTrunk} \times {l_{Middlerunk}}^2$ (22)
Pelvis	Plate	$I_{Pelvis} = \frac{1}{12} m_{Pelvis} \times {l_{Pelvis}}^2$ (23)
Upper Arm	Slender Rod	$I_{Upper\ Arm} = \frac{1}{12} m_{Upper\ Arm} \times {l_{UpperArm}}^2$ (24)
Forearm	Slender Rod	$I_{Forearm} = \frac{1}{12} m_{Forearm} \times {l_{Forearm}}^2$ (25)
Hand	Flat Plate	$I_{Hand} = \frac{1}{12} m_{Hand} \times {l_{Hand}}^2$ (26)
Thigh	Slender Rod	$I_{Thigh} = \frac{1}{12} m_{Thigh} \times {l_{Thigh}}^2$ (27)
Shank	Slender Rod	$I_{Shank} = \frac{1}{12} m_{Shank} \times {l_{Shank}}^2$ (28)
Foot	Flat plate	$I_{Foot} = \frac{1}{12} m_{Foot} \times {l_{Foot}}^2$ (29)

The reaction moment equations were defined as [19]:

$$GRM = \sum_{i=1}^{N}[I_i\dot{\omega}_i + \omega_i \times (I_i\omega_i) - \sum_{i=1}^{N}\sum_{j=1}^{Ki}(r_{ij} \times F_{ij}) \quad (30)$$

where ω_i and $\dot{\omega}_i$ is the angular velocity and angular acceleration of the body segment respectively, GRM is the total external ground reaction moment, I_i is the inertial moment of the body segment, r_{ij} represents the positional vectors of the between the end points and the centre of mass of the segment. Finally, F_{ij} represents the resultant force acting at the end point of a given segment [19]. Once the GRM was calculated, it was normalised by dividing it by the product of the participant body weight, body height and acceleration due to gravity.

4.6 Statistical Analysis

Due to the large dataset, statistical analysis was conducted to determine if the different landing techniques contributed to any significant differences across the sample population. Parametric tests are widely used in medical and biomechanical research. These tests rely on the assumption of normality, which specifies that all data groups in the study have a normal distribution. Parametric tests also rely on the assumption of equal variance. Should the abovementioned assumptions be voided, then non-parametric statistical analysis would be conducted [29].

Although non-parametric analysis can reduce the possibility of drawing incorrect results due to the previously mentioned assumptions, the information from non-parametric analysis is limited in comparison with parametric methods. While parametric analysis emphasises the relationship between means in comparable groups, non-parametric analysis focuses on the relationships between the median values. This is done by categorising the original values into ranks and signs (+ or -) [29].

In this study, the Bartlett's Test for Homogeneity of Variance is used to determine if the data exhibits equal variance across each group. If this was found to be true, the parametric One-Way Analysis of Variance (One Way ANOVA) was implemented to determine if there were any significant differences between the four landing techniques. If the data was found to have non-homogenous variances across the different groups, then the non-parametric Kruskal-Wall test was implemented. All statistical analyses were conducted on MATLAB and the process is further described in the sections below.

4.6.1 Bartlett's Test for Homogeneity of Variances

The Bartlett's Test was used to determine whether there were equal variances across different sample groups. Many statistical tests assume that the data across different groups not only have equal variance but also have normal distribution. Bartlett's Test creates a "null and void"

hypothesis test to confirm homogeneity of the variance between the different groups. Should the variances prove to be homogenous, the analysis can continue with the One Way ANOVA, which requires the homogenous condition [30].

The Bartlett's Test hypothesis is defined as:

$$H_0: \quad {\sigma_1}^2 = {\sigma_2}^2 = \cdots = {\sigma_k}^2 \tag{31}$$

where k is the number of categories. In this analysis, the aim is to evaluate the abovementioned hypothesis against the alternative that at least two variances are unequal:

$$H_a: \quad {\sigma_i}^2 \neq {\sigma_j}^2$$

The test statistic is expressed as follows:

$$B = \frac{(N-k)\left(\frac{\sum_{i=1}^{k}(n_i-1){s_i}^2}{N-k}\right) - \sum_{i=1}^{k}(n_i-1)\ln({s_i}^2)}{1+\frac{1}{3(k-1)}\left[\left(\sum_{i=1}^{k}\frac{1}{n_i-1}\right)-\frac{1}{N-k}\right]} \tag{32}$$

where N is the sum of all sample sizes, ${s_i}^2$ is the variance of the ith group and n_i is the sample size of the i-th group [30].

It is important to note that the test statistic B follows the Chi-Squared distribution with $(k-1)$ degrees of freedom. $p_{Bartlett}$ is the probability on the Chi-Squared distribution that an observed test statistic is larger than the critical test statistic that was computed in equation (32). If $p_{Bartlett} > \alpha$, where α is the significance value set to 0.05, then the null hypothesis cannot be rejected, meaning that the variances are homogenous. Thus, a parametric One-Way ANOVA test could be conducted. If $p_{Bartlett} < \alpha$, then the null hypothesis is false and the variances are not homogenous, then the non-parametric Kruskal Wallis test could be conducted.

4.6.2 One Way Analysis of Variance (Parametric Test)

The one-way analysis of variance (ANOVA) compares if the differences in the separate groups exhibit any statistical significance. Similar to the Bartlett's test, a null hypothesis is created.

$$H_0 = \mu_1 = \mu_1 = \cdots = \mu_k \tag{33}$$

where μ is the data group mean and k is the number of groups [31]. It should be noted that the one-way ANOVA can only determine if test groups are significantly different. It cannot indicate where these differences may occur. The procedure to conduct an ANOVA test is defined below [25].

Calculate the regression sum of squares:

$$SSR = n\sum(\mu_j - \bar{\mu})^2 \tag{34}$$

where n is the size of the group, $\mu_j$is the group mean and $\bar{\mu}$ is the overall mean of the data [25].

Calculate the error sum of squares:

$$SSE = \sum(\mu_{ij} - \bar{\mu}_j)^2 \quad (35)$$

where μ_{ij} is the ith observation in the group j and $\bar{\mu}_j$ is the overall mean of group j [25].

Calculate the total sum of squares:

$$SST = SSR + SSE \quad (36)$$

Once equations 34 – 36 have been computed, Table 7 can be completed:

Table 7: One-way ANOVA table [25].

Source	Sum of Squares (SS)	Degree of Freedom	Mean Squares (MS)	F
Treatment	SSR	$DF1 = k - 1$	$\frac{SST}{DF1}$	$\frac{SST}{SSE} \times \frac{DF2}{DF1}$
Error	SSE	$DF2 = n - k$	$\frac{SSE}{DF2}$	
Total	SST	$n - 1$		

where n is the total observations in the data and k is the number of groups. The abovementioned process demonstrated is to determine the F statistic:

$$F = \frac{SST}{SSE} \times \frac{DF2}{DF1} \quad (37)$$

This statistic needs to be compared to the critical value F_{crit}, which is determined from the F distribution table illustrated in Figure 22. The critical value is determined at a significance value a = 0.05, $DF1$ and $DF2$ [25].

If $F < F_{crit}$, the null hypothesis in equation 33 cannot be rejected. In other words, the data groups do not exhibit any significant differences statistically. If $F > F_{crit}$, the null hypothesis is voided, meaning that statistically, there are significant differences in the data groups.

	DF1	α = 0.05																	
DF2	1	2	3	4	5	6	7	8	9	10	12	15	20	24	30	40	60	120	Inf
1	161.45	199.5	215.71	224.58	230.16	233.99	236.77	238.88	240.54	241.88	243.91	245.95	248.01	249.05	250.1	251.14	252.2	253.25	254.31
2	18.513	19	19.164	19.247	19.296	19.33	19.353	19.371	19.385	19.396	19.413	19.429	19.446	19.454	19.462	19.471	19.479	19.487	19.496
3	10.128	9.5521	9.2766	9.1172	9.0135	8.9406	8.8867	8.8452	8.8123	8.7855	8.7446	8.7029	8.6602	8.6385	8.6166	8.5944	8.572	8.5494	8.5264
4	7.7086	6.9443	6.5914	6.3882	6.2561	6.1631	6.0942	6.041	5.9988	5.9644	5.9117	5.8578	5.8025	5.7744	5.7459	5.717	5.6877	5.6581	5.6281
5	6.6079	5.7861	5.4095	5.1922	5.0503	4.9503	4.8759	4.8183	4.7725	4.7351	4.6777	4.6188	4.5581	4.5272	4.4957	4.4638	4.4314	4.3985	4.365
6	5.9874	5.1433	4.7571	4.5337	4.3874	4.2839	4.2067	4.1468	4.099	4.06	3.9999	3.9381	3.8742	3.8415	3.8082	3.7743	3.7398	3.7047	3.6689
7	5.5914	4.7374	4.3468	4.1203	3.9715	3.866	3.787	3.7257	3.6767	3.6365	3.5747	3.5107	3.4445	3.4105	3.3758	3.3404	3.3043	3.2674	3.2298
8	5.3177	4.459	4.0662	3.8379	3.6875	3.5806	3.5005	3.4381	3.3881	3.3472	3.2839	3.2184	3.1503	3.1152	3.0794	3.0428	3.0053	2.9669	2.9276
9	5.1174	4.2565	3.8625	3.6331	3.4817	3.3738	3.2927	3.2296	3.1789	3.1373	3.0729	3.0061	2.9365	2.9005	2.8637	2.8259	2.7872	2.7475	2.7067
10	4.9646	4.1028	3.7083	3.478	3.3258	3.2172	3.1355	3.0717	3.0204	2.9782	2.913	2.845	2.774	2.7372	2.6996	2.6609	2.6211	2.5801	2.5379
11	4.8443	3.9823	3.5874	3.3567	3.2039	3.0946	3.0123	2.948	2.8962	2.8536	2.7876	2.7186	2.6464	2.609	2.5705	2.5309	2.4901	2.448	2.4045
12	4.7472	3.8853	3.4903	3.2592	3.1059	2.9961	2.9134	2.8486	2.7964	2.7534	2.6866	2.6169	2.5436	2.5055	2.4663	2.4259	2.3842	2.341	2.2962
13	4.6672	3.8056	3.4105	3.1791	3.0254	2.9153	2.8321	2.7669	2.7144	2.671	2.6037	2.5331	2.4589	2.4202	2.3803	2.3392	2.2966	2.2524	2.2064
14	4.6001	3.7389	3.3439	3.1122	2.9582	2.8477	2.7642	2.6987	2.6458	2.6022	2.5342	2.463	2.3879	2.3487	2.3082	2.2664	2.2229	2.1778	2.1307
15	4.5431	3.6823	3.2874	3.0556	2.9013	2.7905	2.7066	2.6408	2.5876	2.5437	2.4753	2.4034	2.3275	2.2878	2.2468	2.2043	2.1601	2.1141	2.0658
16	4.494	3.6337	3.2389	3.0069	2.8524	2.7413	2.6572	2.5911	2.5377	2.4935	2.4247	2.3522	2.2756	2.2354	2.1938	2.1507	2.1058	2.0589	2.0096
17	4.4513	3.5915	3.1968	2.9647	2.81	2.6987	2.6143	2.548	2.4943	2.4499	2.3807	2.3077	2.2304	2.1898	2.1477	2.104	2.0584	2.0107	1.9604
18	4.4139	3.5546	3.1599	2.9277	2.7729	2.6613	2.5767	2.5102	2.4563	2.4117	2.3421	2.2686	2.1906	2.1497	2.1071	2.0629	2.0166	1.9681	1.9168
19	4.3807	3.5219	3.1274	2.8951	2.7401	2.6283	2.5435	2.4768	2.4227	2.3779	2.308	2.2341	2.1555	2.1141	2.0712	2.0264	1.9795	1.9302	1.878
20	4.3512	3.4928	3.0984	2.8661	2.7109	2.599	2.514	2.4471	2.3928	2.3479	2.2776	2.2033	2.1242	2.0825	2.0391	1.9938	1.9464	1.8963	1.8432
21	4.3248	3.4668	3.0725	2.8401	2.6848	2.5727	2.4876	2.4205	2.366	2.321	2.2504	2.1757	2.096	2.054	2.0102	1.9645	1.9165	1.8657	1.8117
22	4.3009	3.4434	3.0491	2.8167	2.6613	2.5491	2.4638	2.3965	2.3419	2.2967	2.2258	2.1508	2.0707	2.0283	1.9842	1.938	1.8894	1.838	1.7831
23	4.2793	3.4221	3.028	2.7955	2.64	2.5277	2.4422	2.3748	2.3201	2.2747	2.2036	2.1282	2.0476	2.005	1.9605	1.9139	1.8648	1.8128	1.757
24	4.2597	3.4028	3.0088	2.7763	2.6207	2.5082	2.4226	2.3551	2.3002	2.2547	2.1834	2.1077	2.0267	1.9838	1.939	1.892	1.8424	1.7896	1.733
25	4.2417	3.3852	2.9912	2.7587	2.603	2.4904	2.4047	2.3371	2.2821	2.2365	2.1649	2.0889	2.0075	1.9643	1.9192	1.8718	1.8217	1.7684	1.711
26	4.2252	3.369	2.9752	2.7426	2.5868	2.4741	2.3883	2.3205	2.2655	2.2197	2.1479	2.0716	1.9898	1.9464	1.901	1.8533	1.8027	1.7488	1.6906
27	4.21	3.3541	2.9604	2.7278	2.5719	2.4591	2.3732	2.3053	2.2501	2.2043	2.1323	2.0558	1.9736	1.9299	1.8842	1.8361	1.7851	1.7306	1.6717
28	4.196	3.3404	2.9467	2.7141	2.5581	2.4453	2.3593	2.2913	2.236	2.19	2.1179	2.0411	1.9586	1.9147	1.8687	1.8203	1.7689	1.7138	1.6541
29	4.183	3.3277	2.934	2.7014	2.5454	2.4324	2.3463	2.2783	2.2229	2.1768	2.1045	2.0275	1.9446	1.9005	1.8543	1.8055	1.7537	1.6981	1.6376
30	4.1709	3.3158	2.9223	2.6896	2.5336	2.4205	2.3343	2.2662	2.2107	2.1646	2.0921	2.0148	1.9317	1.8874	1.8409	1.7918	1.7396	1.6835	1.6223
40	4.0847	3.2317	2.8387	2.606	2.4495	2.3359	2.249	2.1802	2.124	2.0772	2.0035	1.9245	1.8389	1.7929	1.7444	1.6928	1.6373	1.5766	1.5089
60	4.0012	3.1504	2.7581	2.5252	2.3683	2.2541	2.1665	2.097	2.0401	1.9926	1.9174	1.8364	1.748	1.7001	1.6491	1.5943	1.5343	1.4673	1.3893
120	3.9201	3.0718	2.6802	2.4472	2.2899	2.175	2.0868	2.0164	1.9588	1.9105	1.8337	1.7505	1.6587	1.6084	1.5543	1.4952	1.429	1.3519	1.2539
Inf	3.8415	2.9957	2.6049	2.3719	2.2141	2.0986	2.0096	1.9384	1.8799	1.8307	1.7522	1.6664	1.5705	1.5173	1.4591	1.394	1.318	1.2214	1

Figure 17: F Distribution table at a = 0.05 [32].

Figure 17 depicts the F-distribution table that was used to determine the F_{crit} for the ANOVA test.

4.6.3 Kruskal Wallis Test (Non-Parametric Test)

The Kruskal Wallis Test is a non-parametric alternative to the one-way ANOVA test.

Similar to the previous tests, a null hypothesis is stated that the median across the separate groups is equal. Data groups are sorted and ranked in ascending order before calculating the H statistic defined as:

$$H = \left[\frac{12}{n(n+1)}\sum_{j=1}^{k}\frac{{T_j}^2}{n_j}\right] - 3(n+1) \tag{38}$$

where n is the sum of the sample sizes, k is the number of samples, T_j is the sum of the ranks in sample j and n_j is the size of sample j [32].

Once the H statistic is determined, the critical chi-squared χ_{crit} value can be found at c-1 degrees of freedom and at a significance level of 0.05. If p> 0.05, the null hypothesis can be considered true and the medians are equal, (there is no statistically significant difference between the groups). If p < 0.05 the null hypothesis is false, suggesting that there is sufficient evidence statistically to state that the medians are different [33].

5 Results and Discussion

5.1 Biomechanical Performance Indicators

The Ground Reaction Force Model was validated with the data that was collected from the Bertec Force plate by comparing the data from the same jump.

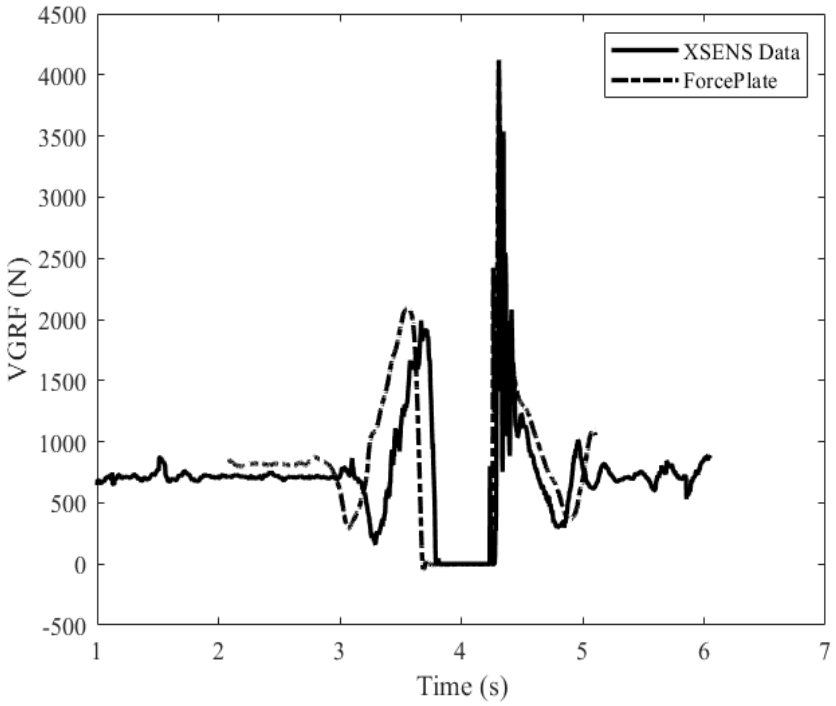


Figure 18: VGRF comparison between the Xsens data and the force plate data for a given jump smash.

Figure 18 illustrates the comparison between the modelled VGRF and the force plate data for a given jump smash. The VGRF model follows the force plate data closely. Certain phases of the jump smash can be identified from Figure 18. For the jump smash that is illustrated, the first 3 seconds coincides with the athlete standing in position while awaiting the serve. The slight decrease in VGRF coincides with the flexion of the knees and hip joints as the centre of mass of the athlete was lowered during the Preparation Phase. The sudden increase in VGRF represents the explosive force that was required to propel the athlete into the air. The Back Swing Phase and Forward Swing Phase of the jump smash takes place when the VGRF is zero. Finally, a sudden spike in the VGRF coincides with the impact on the ground during the Follow Through Phase.
On average, the VGRF model overestimated the measured data by 9.29% (±6.54%) during the Landing Phase.

Table 8 summarises the mean data for the reaction forces in the landing joints. The Box Plots in Figure 19 provide an additional perspective as to how the VGRF data was distributed for each

landing technique. The ground reaction forces were normalised by dividing the VGRF by the participant body weights.

Table 8: Mean ± SD of VGRF for the different landing strategies.

BPI	NLT	TF	FF	HF	P-value	Test
Normalised VGRF (BW)	2.433 (±0.877)	2.395 (±0.687)	2.882 (± 0.786)	2.404 (±0.585)	0.3973	ANOVA
Normalised VGRF Landing Ankle	1.952 (±0.777)	1.946 (±0.479)	2.001 (±0.289)	1.976 (±0.381)	0.9706	Kruskal-Wallis
Normalised VGRF Landing Knee (BW)	1.825 (±0.716)	1.806 (±0.432)	1.876 (±0.292)	1.864 (±0.352)	0.9681	Kruskal-Wallis
Normalised VGRF Landing Hip (BW)	1.385 (±0.464)	1.349 (±0.260)	1.446 (±0.305)	1.466 (±0.263)	0.8526	ANOVA

Table 8 summarises the analysis of how different landing techniques affected the VGRF. The FF technique produced VGRF that is 20% greater than the lowest VGRF produced by the TF strategy. The ANOVA test produced a p-value of 0.3973 for the VGRF. Since this is larger than the critical value of 0.05, it means that there is no significant difference in the VGRF when the landing technique is changed. Looking at the VGRF subplot in Figure 19 shows that the FF and HF techniques had higher median VGRF compared to the NLT and TF techniques. The spread of the VGRF values, as shown by the interquartile, suggests that the FF technique could generate larger VGRF. Additionally, the FF technique is positively skewed towards higher VGRF values, indicating that landing flat footed could result to more instances of higher VGRF.

For the ankle, the mean reaction forces were similar across the different landing techniques as indicated by the large p-value of 0.9706. The FF produced slightly larger VGRF in the ankle compared to the TF technique, the difference of which was only 2.8%. The ankle subplot in Figure 19 shows that the TF technique had a negatively skewed distribution. This suggests that there were more instances of low ankle reaction forces. The NLT technique showed wide distribution for all joint reaction forces. Each participant approached the NLT (Normal Landing Technique)

as per their normal technique, unlike the TF, FF and HF techniques where participants were instructed to land in a particular manner. This variation in the approach of the NLT technique could explain the spread of the data.

For the knee joint, the Kruskal Wallis test found a p-value of 0.9681 for the knee reaction forces indicating that there was no statistical difference in the means across the landing techniques. The FF technique produced the largest mean knee reaction force which was 3.8% larger than the lowest produced by the TF technique. The box plots further illustrate similar trends for knee reaction forces as ankle reaction forces. The TF technique experienced the largest median, followed by the FF, HF and the NLT. The TF and HF had negatively skewed distributions, indicating more instances of low knee reaction forces.

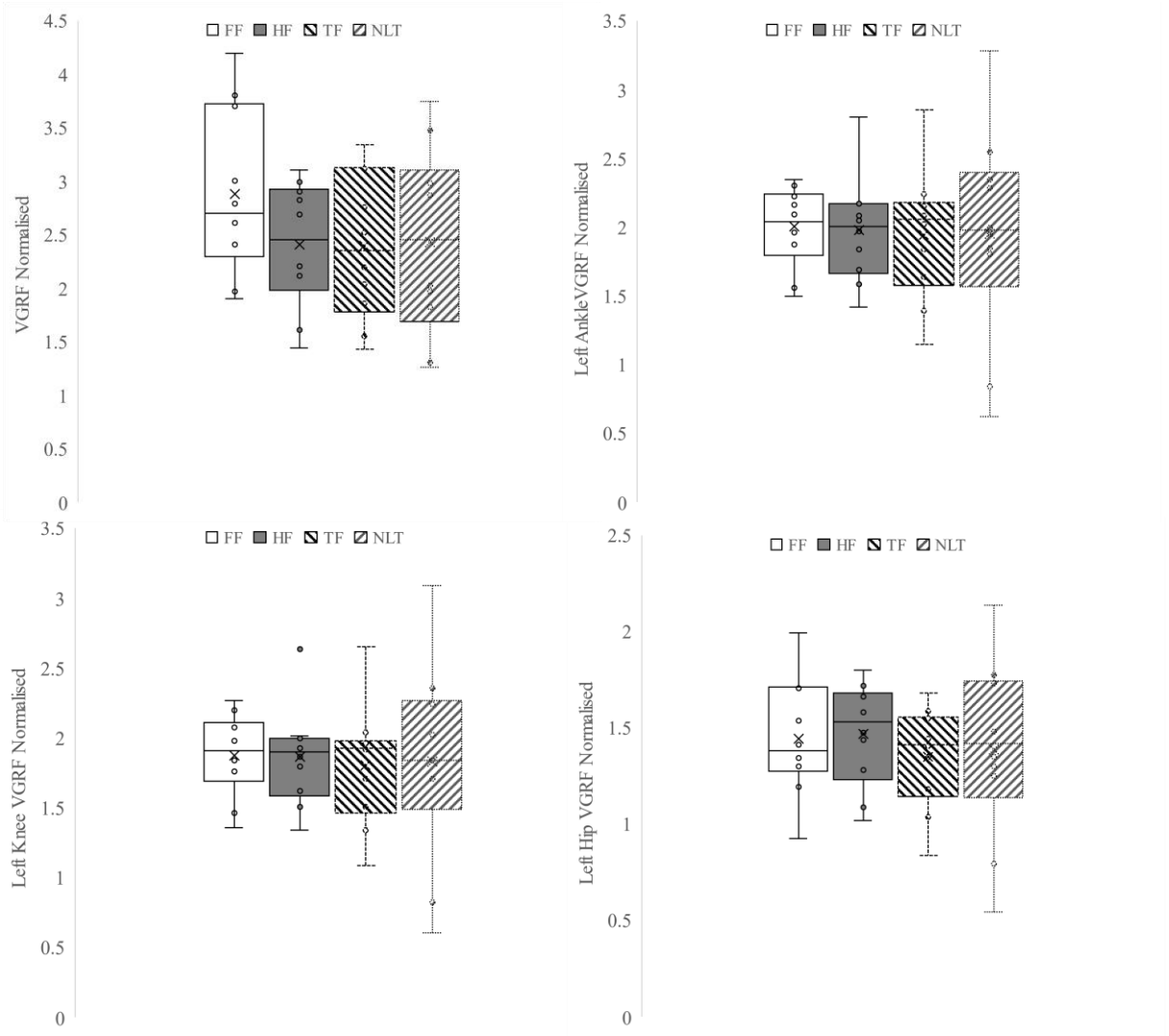


Figure 19: Box Plots for Vertical Ground Reaction Force for the different landing techniques

For the hip joint, the ANOVA test found a p-value to be 0.85. This indicates no statistical difference in the hip reaction forces among the landing techniques. The HF technique generated the largest mean hip reaction force which was 8.7% larger than the smallest produced by the TF strategy. FF technique had a positively skewed distribution, indicating more occurrences of high hip reaction forces. The TF and NLT techniques experienced the similar mean and median hip reaction force values, both of which were lower than other techniques.

Overall, landing with the FF and HF techniques resulted in the largest VGRF and reaction forces at the lower limb joints. Due to the lack of flexion of the ankle during landing, this would result in less energy dissipation at the ankle joint and therefore resulting in a need for greater energy absorption at the knee and hip joints.

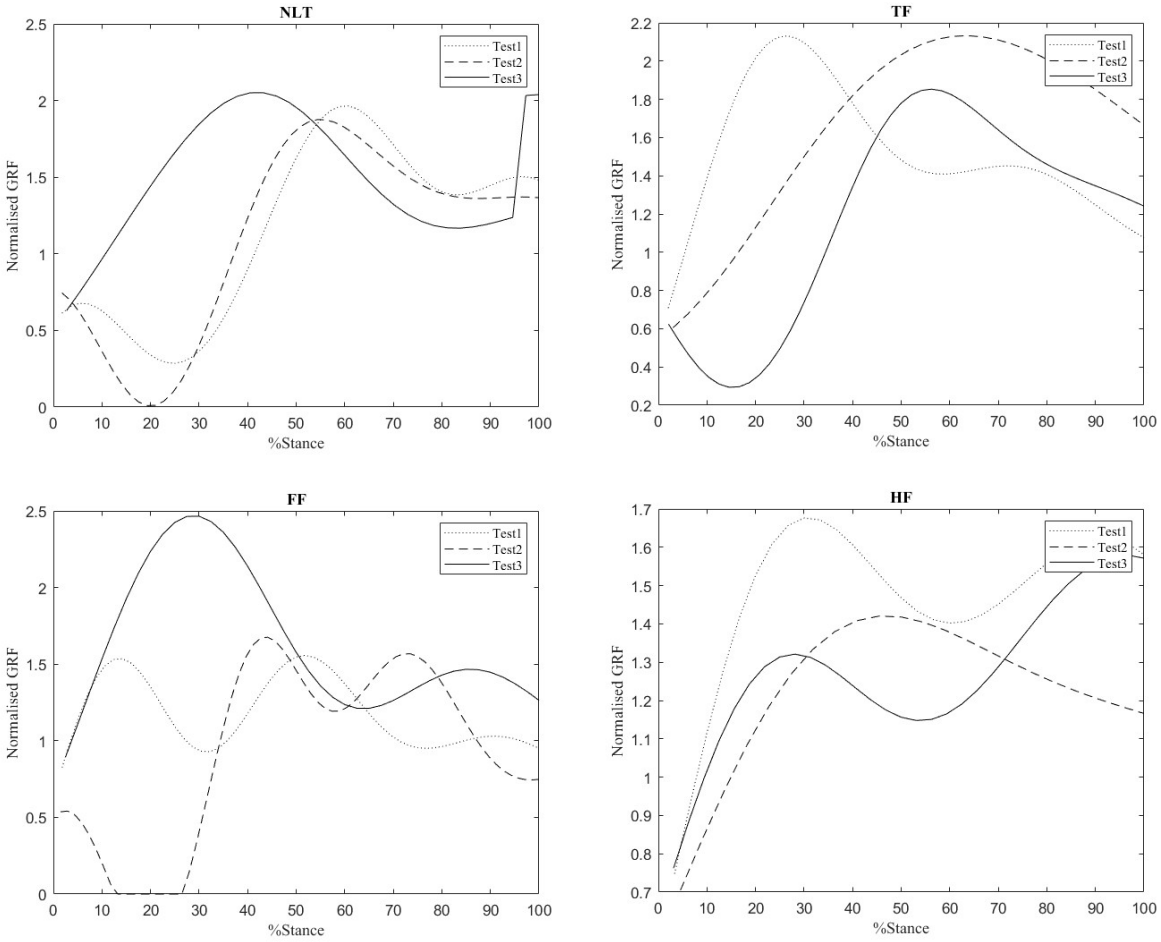


Figure 20: Force profile during landing for each landing technique for a given participant.

Figure 20 depicts the force vs time profile of the VGRF during the landing phase for Participant 1. The figures have been normalised in terms of the participants body weight (BW). Similar plots are available for all participants in the Annexure. The subplot for NLT shows that the peaks in the VGRF occurred at 40-60% into the landing phase with magnitudes between 1.8 and 2.0 BW. The peak then gradually decreased towards a second peak of magnitudes between 1.3 and 1.5 BW. The TF technique showed similar profiles to the NLT technique. The TF technique experienced the first peak between 20-60% with magnitudes between 1.8 and 2.1 BW before it gradually decreased towards a second peak at 1.4 BW. Both NLT and TF techniques were classified as good landing techniques due to the gradual peak behaviour. This is representative of spring like behaviour which is indicative of the Stretch-Shortening Cycle (SSC) principle. For the FF and HF techniques, there appeared to be two impact peaks. The first peak occurred 20% into the landing phase with magnitudes between 1.5 and 1.6. This was followed by a second peak at 50-60% along the landing phase with similar force magnitudes. This was not representative of spring like behaviour and was therefore classified as poor landing techniques.

Table 9 summarises the statistical analysis of the Normalised Ground Reaction Moments and the reaction moment experienced at the lower limb joints. The highest reaction moments were observed with the FF and HF technique at the foot and at each joint. The NLT and TF technique experienced similar mean peak GRM values. The ANOVA test indicates that there were no statistical differences in the mean GRM among the landing technique. However, the p-values for the GRM were not as high as the p-values for the VGRF. This indicates that the GRM was less sensitive to change in the landing technique compared to the VGRF. The box plots for the GRM illustrate that the GRM decreased as the landing strategy was shifted from a heel dominant strategy to toe dominant strategy. The HF strategy produced the highest mean and median reaction moments at the joints.

For the hip reaction moment, the ANOVA found a p-value of 0.0406 which was less than the critical value of 0.05. This indicated that there was a significant difference in the means hip reaction moments across the different landing techniques.

Table 9: Mean ± SD of Normalised Ground Reaction Moments BWBH (Body weight x Body Height) for the different landing strategies.

BPI	NLT	TF	FF	HF	P-value	Test
Normalised GRM (BWBH)	1.347 (±0.495)	1.353 (±0.390)	1.666 (± 0.451)	1.515 (±0.419)	0.3287	ANOVA
Normalised GRM Ankle (BWBH)	0.836 (±0.341)	0.869 (±0.196)	0.904 (±0.184)	0.978 (±0.196)	0.585	ANOVA
Normalised GRM Knee (BWBH)	0.463 (±0.182)	0.491 (±0.092)	0.502 (±0.104)	0.528 (±0.095)	0.585	ANOVA
Normalised GRM Hip (BWBH)	1.385 (±0.464)	1.349 (±0.260)	1.446 (±0.305)	1.466 (±0.263)	0.0406	ANOVA

The FF landing technique produced the largest GRM values which was 23% larger compared to the NLT and FF landing technique. The HF landing technique produced a 12-17% greater GRM compared to the GRM for the NLT and TF technique.

For the ankle, the ANOVA test found that there were no statistical differences in the ankle reaction moment among the different landing techniques. The ankle subplot in Figure 24 illustrates that the NLT technique was positively skewed, indicating a higher occurrence of large ankle reaction moments.

For the knee, the HF technique produced the largest mean knee reaction moment which was 14% larger reaction moments than the NLT technique and 7.5% greater than the TF technique. The knee subplot in Figure 21 further illustrates that the NLT had a positively skewed distribution indicating a higher instance of large knee reaction moments.

The hip experienced the largest reaction moment compared to the knee and ankle joints for all landing techniques. The largest mean reaction moment produced by the HF technique was 8.7 % larger than the lowest mean reaction moment produced by the TF technique. The hip subplot in Figure 21 further illustrates that the reaction moment decreased as the landing technique shifted from a heel dominant to a toe dominant technique.

Overall, the HF landing technique produced the largest reaction moments in each joint and at the ground followed by the FF technique. The NLT and TF techniques produced similar reaction moments at the ground and at the lower joints.

Coaches and athletes can benefit from the study of the ground reaction forces and moments as the data indicates that varying the landing technique did not have a significant effect on the peak reaction force values, however it did affect how the force was experienced by the participants. The NLT and TF landing techniques produced force vs time profiles that exhibited spring like behaviour which suggested that the lower limbs absorbed energy better under these landing strategies as opposed to the impact peaks produced by the HF and FF techniques. Landing with HF and FF techniques will generate large reaction moments at all joints, particularly at the hip joint.

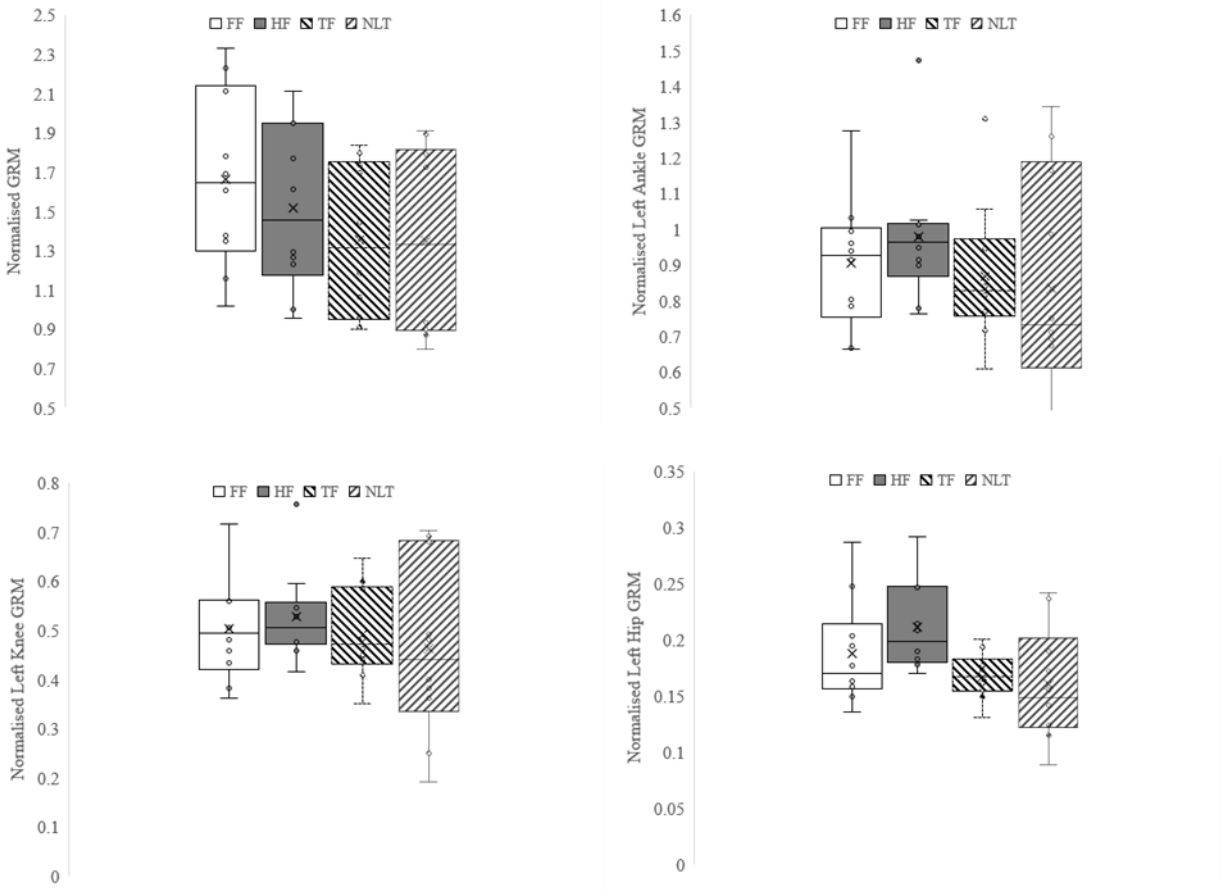


Figure 21: Box Plots for Ground Reaction Moments

Table 10: Joint angles during landing phase of the ankle and knee joints in the landing leg

BPI	NLT	TF	FF	HF	P-value	Test
Left Ankle Landing Angle (°)	-12.204 (±18.787)	-23.917 (±6.671)	-7.108 (±16.786)	9.001 (±8.026)	0.0001	Kruskal-Wallis
Left Ankle Landing Flexion ROM (°)	40.270 (±24.781)	52.163 (±14.387)	41.893 (±16.315)	13.118 (±14.162)	0.002	ANOVA
Left Knee Landing Flexion Angle (°)	35.874 (±21.941)	28.617 (±10.858)	22.988 (±7.568)	22.534 (±7.674)	0.2592	Kruskal-Wallis
Left Knee Landing ROM (°)	30.298 (±14.790)	36.215 (±22.208)	41.370 (±13.969)	35.124 (±15.224)	0.544	ANOVA

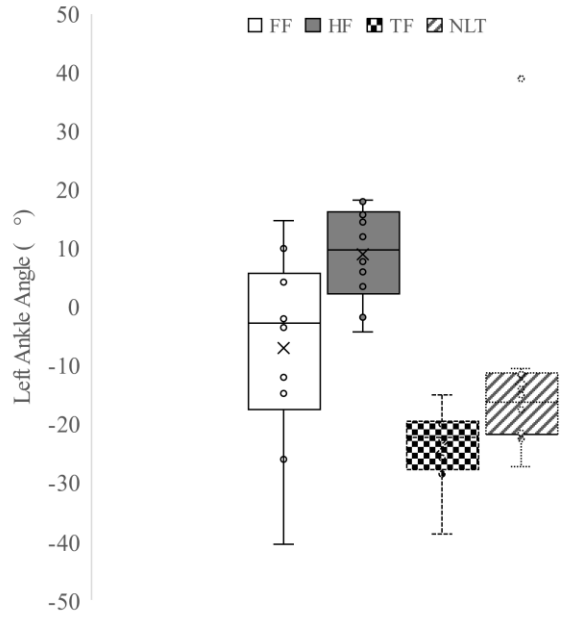


Figure 22: Box Plots of Left Ankle Angle at the moment of ground impact.

The ankle and knee joint flexion angles were analysed in detail during the landing phase of the jump smash. For the ankle angular displacement, the Xsens software defined positive displacement as dorsiflexion and negative displacement as plantarflexion. Extreme positive values indicated landing with the toes first whilst extreme negative values indicated landing with the heel first. For the knee angular displacement, positive was defined as knee flexion whilst negative was defined as knee extension.

Figure 22 depicts that the ankle landing angle shifted from plantarflexion to dorsiflexion as the landing strategy shifted from a toe dominant strategy to a heel dominant strategy. The TF technique had the largest plantarflexion value. The NLT technique also experienced plantarflexion but this was not as extreme as the TF technique. This indicates that the participants were likely landing on the balls of their feet. The HF experienced the greatest dorsiflexion value at the moment of impact with the ground. Figure 22 illustrates that the median ankle angle was almost 0° for the FF technique. For the foot to land completely flat footed, there must be neither dorsiflexion nor plantarflexion. However, Figure 22 indicates that there was a wide distribution of data for the FF landing angle in comparison to the other landing techniques. This indicates that for the FF technique, participants were not always landing completely flat footed. Participants reported difficulty with landing completely flat footed which explains the distribution in the data for this landing technique.

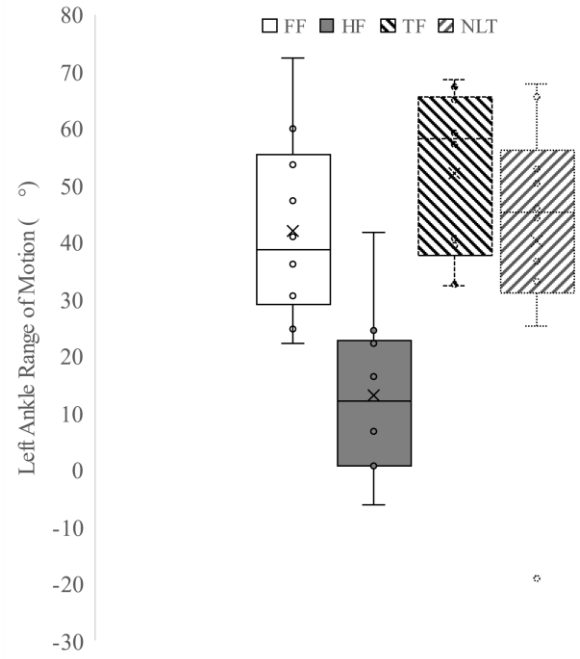


Figure 23: Box Plot of the left ankle flexion range of motion during landing.

For the ankle joint, the flexion range of motion was defined as the total angular displacement of the ankle during the landing phase (from the moment of ground impact until the end of the jump smash). The box plots for the ankle flexion range of motion during the landing phase is shown in Figure 23. The TF technique experienced the largest flexion during the landing phase followed by FF and NLT techniques. The HF technique experienced the lowest the ankle flexion during the landing phase. Figure 24 illustrates that the flexion of the ankle during the landing phase decreased as the landing angle of the ankle changed from plantarflexion to dorsiflexion.

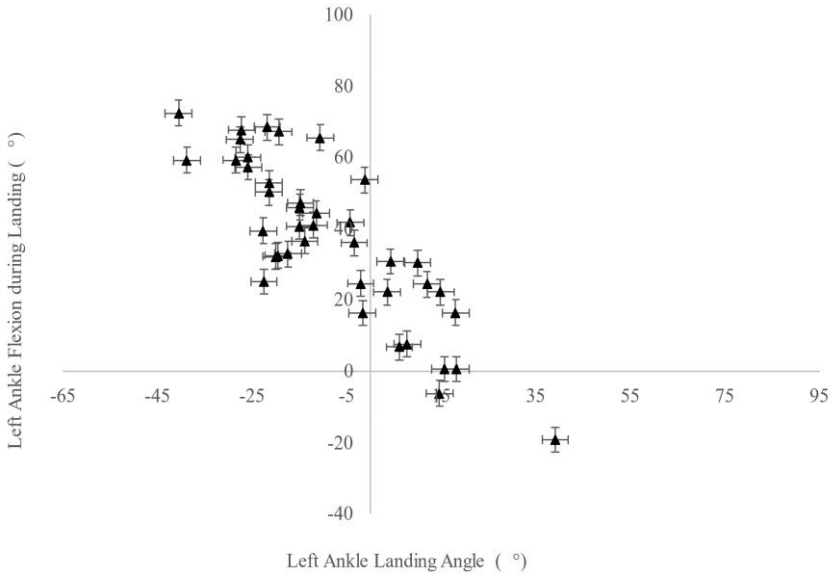


Figure 24: Left ankle landing angle vs Left ankle range of motion.

Table 10 and Figure 25 indicates that the knee experienced a greater flexion angle upon ground impact during the NLT technique. The knee extends further before impact as the landing technique shifted from toe dominant to heel dominant (dorsiflexion to plantarflexion). Figure 26 further illustrates that the knee range of motion decreased as the knee was more flexed at the moment of impact. The lower knee landing angles coincided with ankle dorsiflexion for the FF and HF techniques. Previous literature found that landing with larger knee flexion at ground impact can result in reduced reaction forces and reduced ACL loading [13]. Taking this into consideration, the NLT and TF techniques will produce a “softer landing” as a result of larger knee flexion angles recorded at ground impact. In contrast the HF and FF techniques recorded larger knee extension angles at ground impact, which according to Dai et al would generate greater ACL loading.

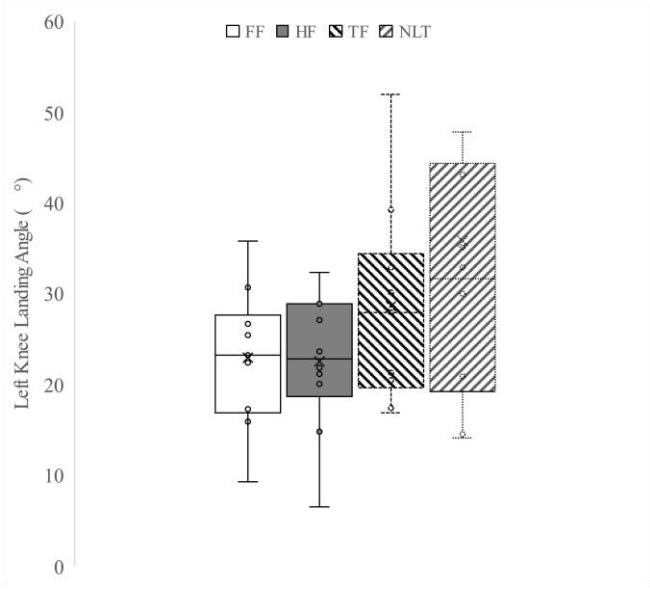


Figure 25: Left knee landing angle box plots for the different landing techniques.

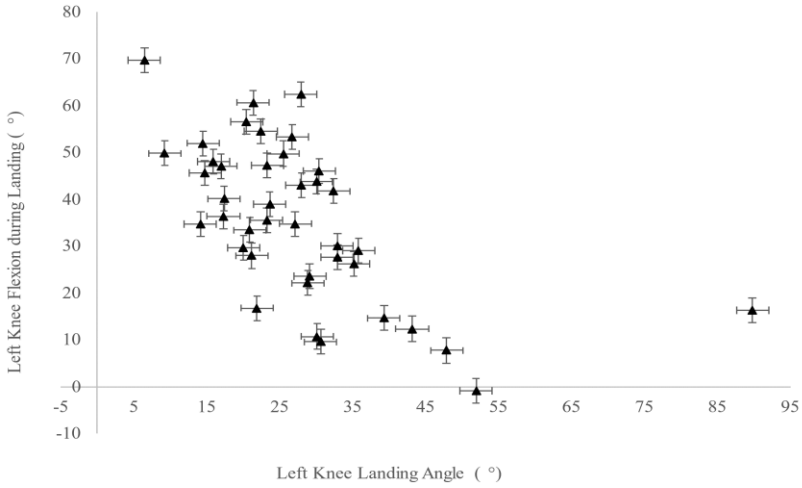


Figure 26:Knee landing angle vs the Knee flexion during landing

Overall, coaches can inform their athletes that the different landing techniques result in different landing angles for the ankle and knee joints. Ankle flexion during landing is greatest for the TF technique, whereas the HF technique experiences the least flexion of the ankle. The NLT technique indicates a softer landing on the knees whereas the HF and FF techniques showcase large knee extension angles at ground impact which could lead to increase ACL loading.

Table 11 summarises the average peak angular velocities achieved for the lower limb segments in the sagittal plane during the Forward Swing Phase. This phase occurs immediately after the peak of the jump was reached. The knees rapidly extended as the body weight was transferred forward to generate additional power to strike the shuttlecock. The greater the speed of the limbs, the more power generated during the Forward Swing Phase. The ANOVA test found large p-

values. This suggests that varying the landing technique did not result in any statistical difference in the angular velocity of the lower limbs during the Follow Through Phase. The landing technique does not influence the power generating effectiveness of the jump smash when viewing only the lower limb angular velocities.

Table 11: Angular Velocity (rad/s) in the sagittal plane for lower limbs during the Forward Swing Phase

BPI	NLT	TF	FF	HF	P-value	Test
Left Shank	6.747 (±3.332)	6.552 (±1.863)	7.318 (±3.760)	7.893 (±3.29)	0.7751	ANOVA
Left Thigh	7.779 (±2.377)	7.440 (±1.505)	7.847 (±3.237)	7.702 (±2.100)	0.982	ANOVA
Right Shank	7.834 (±2.014)	7.117 (±2.603)	7.204 (±2.041)	7.311 (±2.092)	0.8866	ANOVA
Right Thigh	6.151 (±1.757)	7.198 (±2.091)	6.973 (±1.643)	6,882 (±1.195)	0.578	ANOVA

The box plots in Figure 27 review the spread of the angular velocity data. This figure further illustrates the similarity in the means. For the left shank and thigh angular velocity, the FF and HF landing techniques had large interquartile ranges, indicating that there was a larger spread in the data for heal dominated landing strategies. The TF technique has the smallest spread for the left limb segments. The large spread in the box plot data can be attributed to a less precise technique of landing. A box plot with a smaller spread can be attributed to a more precise landing technique. The heal dominated landing techniques can then be described as unrefined techniques to execute the jump smash as these produced varying angular velocities in the left leg segments. This produced inconsistent power generated from the lower limbs when striking the shuttlecock and thus inconsistent performance. The NLT also showcases large spread in the angular velocities for the left limbs. This is likely influenced by the varying techniques that each participant considers normal. The TF technique produced more consistent angular velocities in the left leg segments which results in a more consistent power generation from the lower limbs when striking the shuttlecock. The toe dominated landing techniques will produce more consistent performance of the jump smash.

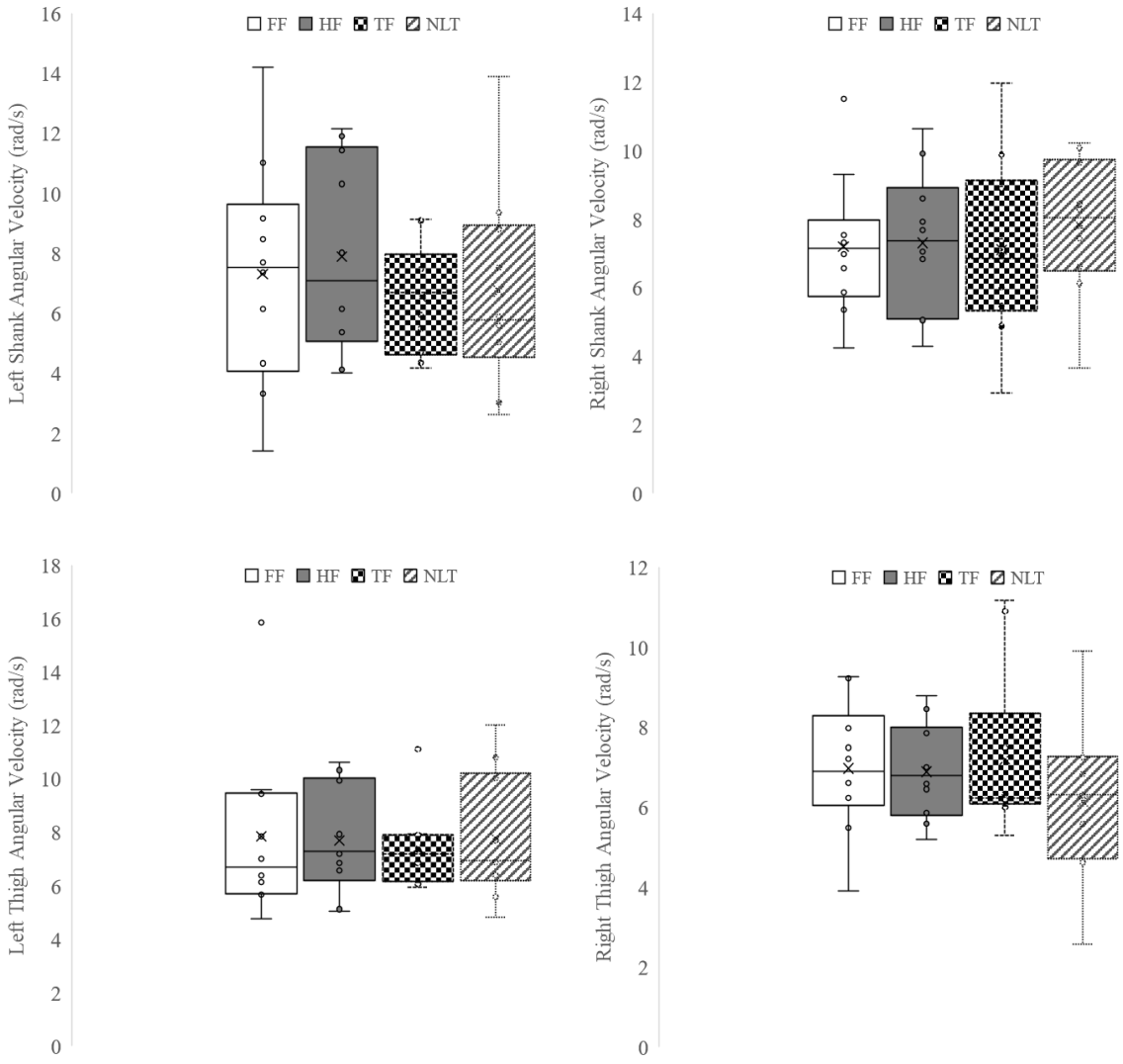


Figure 28: Lower limb angular velocity box plots during the Forward Swing Phase.

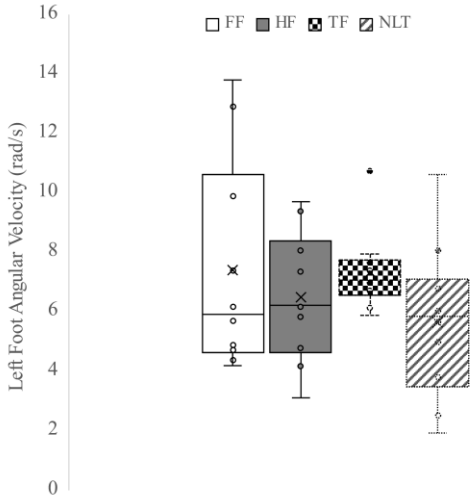


Figure 27: Angular velocity of left (landing) foot during the Follow Through Phase

The large variance in the angular velocities of the lower limbs for the HF and FF technique could be explained by the approach to the execution of the landing. The participants rapidly extended the knee joints to generate power for the shot whilst simultaneously controlling their ankle joints to land in the correct manner. Figure 28 illustrates that the angular velocity of the left foot is also more precise for the TF technique and least precise for the FF technique. The TF landing technique also produced the greatest mean angular velocity during the Forward Swing Phase. The large variance in the angular velocity of the lower limbs for the FF and HF techniques will produce inconsistent performance during the Forward Swing Phase. The inconsistent angular velocity on the landing leg segments may contribute to increased risk of injury during the landing phase of the jump.

Overall, coaches can inform that rapid knee extension is required for generating power to strike the shuttlecock during the forward swing phase. Greater angular velocities of the lower limbs contribute to increased power generation to strike the shuttlecock. The different landing techniques influence the angular velocities of the lower limb segments which would in turn influence the performance of the jump smash. Athletes need to be aware of refining the landing techniques for more consistent power generation.

Table 12: Spinal segment angular velocity (rad/s) during the Forward Swing Phase

BPI	NLT	TF	FF	HF	P-value	Test
Pelvis	5.787 (±1.285)	5.913 (±1.078)	5.058 (±1.057)	5.067 (±1.409)	0.300	ANOVA
L5	6.655 (±1.402)	6.544 (±1.098)	5.902 (±1.041)	5.599 (±1.417)	0.196	ANOVA
T12	7.720 (±1.230)	7.655 (±1.226)	6.981 (±1.127)	6.547 (±1.570)	0.151	ANOVA
T8	8.158 (±1.363)	8.141 (±1.360)	7.425 (±1.194)	6.959 (±1.656)	0.157	ANOVA

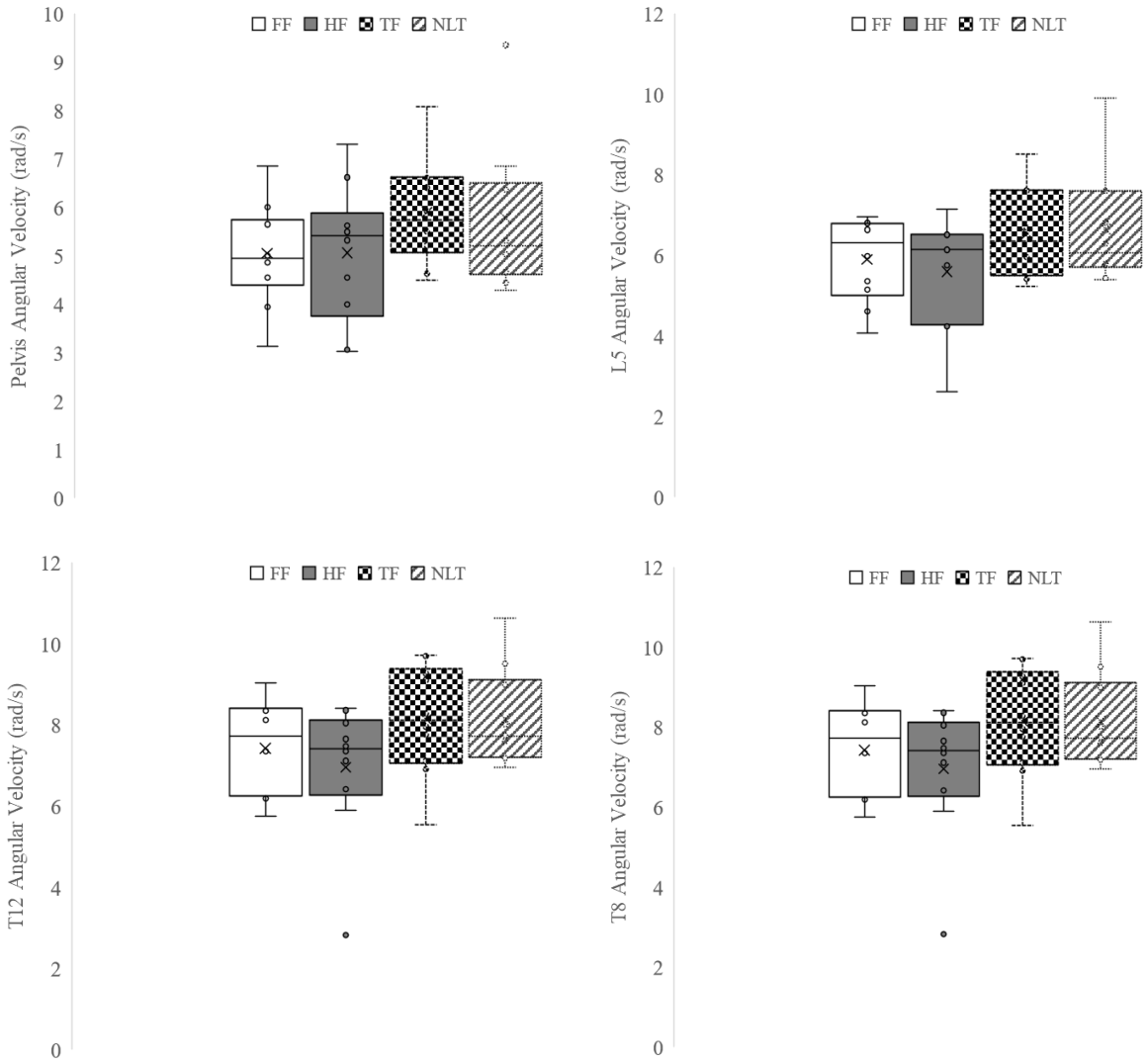


Figure 29: Angular velocity box plots for the spinal segments during the forward swing phase

Similar to the lower limb segments, the spinal segments underwent rotation during the Forward Swing Phase to generate additional power to strike the shuttlecock with force. The ANOVA test found large p-values that were larger than 0.05. Although this would suggest that there are no statistical differences, the p-values are still low. This would suggest that the angular velocities of the spinal segments are sensitive to the landing technique. The NLT and TF landing techniques produced the largest mean angular velocity during this phase of the jump smash. The HF and FF techniques produced the lowest angular velocity during the Forward Swing Phase.

The box plots in Figure 29 illustrate the data spread for the BPIs in Table 12. The HF landing technique produced negatively skewed distributions for the Pelvis and L5 data. This would suggest that the HF technique would likely result in lower pelvis and L5 angular velocities. The box plots for the TF and NLT technique are positively skewed towards higher angular velocities for the Pelvis and L5 indicating that the lower spinal segments (Pelvis and L5) undergo faster rotation.

Overall, different landing techniques impact the angular velocity of the spinal segments during the Forward Swing Phase. This influences power generation and performance of the jump smash. The TF technique correlates with more consistent and higher average angular velocities of the spinal segments. The HF and FF techniques lead to more inconsistent performances. The inconsistent angular velocities generated by the HF and FF techniques may heighten the risk of injury during the landing phase of the jump.

5.2 Injury Risk Assessment

Injury risk was quantified using a ranking system whereby BPIs were allocated on a score from 1 – 4 based on the average results determined. A higher score indicates a higher risk.

Table 13 summarises the risk score for Vertical Ground Reaction Forces. A score of 4 was allocated to the landing technique that produced the largest average ground reaction force. The FF and HF techniques ranked higher than the NLT and TF techniques. Higher reaction forces are generated in the FF and HF technique which will increase the risk of injury.

Table 13: Risk Table for Vertical Ground Reaction Force

Vertical Ground Reaction Forces					
Technique	VGRF	VGRF Ankle	VGRF Knee	VGRF Hip	Risk Score
NLT	2	2	2	2	8
TF	1	1	1	1	4
FF	4	4	4	3	15
HF	3	3	3	4	13

Table 14 summarises the risk score for Ground Reaction Moments. Similarly, to the reaction force risk score, the largest average reaction moment was allocated a score of 4. The HF and FF techniques will generate a higher risk for injury due to the reaction moments.

Table 14: Risk Table for Ground Reaction Moments

Ground Reaction Moments					
Technique	GRM	GRM Ankle	GRM Knee	GRM Hip	Risk Score
NLT	1	1	1	2	5
TF	2	2	2	1	7
FF	4	3	3	3	13
HF	3	4	4	4	15

Table 15 summarises the risk score for the effect of angular velocity of the lower limb segments during the Forward Swing Phase. A score of 4 was attributed to BPIs with the largest angular velocity as this would contribute to increased VGRF upon landing [10]. The HF produced the highest risk score followed by the FF technique. The TF technique produced the lowest risk score.

Table 15: Risk Table lower limb angular velocity during Forward Swing Phase

Angular velocity of lower limbs during Forward Swing Phase					
Technique	Left Shank	Left Thigh	Right Shank	Right Thigh	Risk Score
NLT	2	3	4	1	10
TF	1	1	1	4	7
FF	3	4	2	3	12
HF	4	2	3	2	11

The ankle landing angle was ranked high for injury if there was great dorsiflexion. A larger dorsiflexion upon landing resulted in less flexion of the ankle during the landing phase and thus increased reaction forces. Increased dorsiflexion at the ankle also resulted in decreased flexion of the knee at the landing incident. Greater flexion of the knee upon landing results in lowered VGRF [13]. Therefore, a low landing knee flexion angle was allocated a high-risk score. For the joint range of motion during landing, a high-risk score was allocated for low range of motion. The HF landing technique produced the highest risk score followed by the NLT and FF techniques. The TF technique produced the score with lowest injury risk.

Table 16: Risk table for joint angle at ground impact

Joint angle of lower limbs at ground impact					
Technique	Left Ankle Landing Angle	Left Ankle ROM	Left Knee Landing Angle	Left Knee ROM	Risk Score
NLT	2	3	1	4	10
TF	1	1	2	2	6
FF	3	2	3	1	9
HF	4	4	4	3	15

Table 17 summarises the risk score for the angular velocity of the spinal segments during the Forward Swing Phase. Similar to the angular velocity of the lower limbs, a high-risk score was allocated for high angular velocities. The toe dominant landing techniques produced the highest risk score followed by the FF technique. The HF technique produced the lowest injury risk score in this case.

Table 17: Risk table for spinal segment angular velocity during Forward Swing Phase

Spinal segments angular velocity during Forward Swing Phase					
Technique	Pelvis	L5	T12	T8	
NLT	3	4	4	4	15
TF	4	3	3	3	13
FF	1	2	2	2	7
HF	2	1	1	1	5

Finally, the BPIs were ranked against each other to obtain an overall injury risk score for the landing techniques. For each risk assessment, the risk scores were ranked from 1 – 4 of magnitude. The risk table is summarised in Table 18. The safest landing technique to reduce the risk of injury is the TF landing technique. The current NLT technique is scored as a risker landing than the TF technique. The FF and HF techniques are both ranked as landing techniques with the highest risks.

Table 18:Summarised injury risk table

	Forces	Moments	Lower Limb Angular Velocity	Lower Limb Joint Angles	Spinal segment angular velocity	Risk Score
NLT	2	1	2	3	4	12
TF	1	2	1	1	3	8
FF	4	3	4	2	2	15
HF	3	4	3	4	1	15

6 Conclusion

This study aimed to utilise 3D motion capture from inertial sensors to model the badminton jump smash to prevent injury and enhance performance. Key objectives included determining and quantifying biomechanical performance indicators (BPIs), assessing their impact on injury and identifying the ideal landing technique to minimise the risk of injury.

The results indicated that varying the landing technique affected the BPIs, particularly the VGRF and force vs time profiles. Although the peak VGRF values were similar across the different landing techniques, the force v stime profiles differed. The force vs time profile indicated that more energy was dissipated during the NLT and TF techniques. Additionally, joint angle data showed that there was reduced flexion in the ankle joint for the HF and FF techniques, leading to non-spring like behaviour in the force profiles. Moreover, increasing the dorsiflexion of the ankle at ground impact, resulted in higher reaction moments in the lower limb joints. The HF technique experienced noticeably high hip reaction moments. Variation in the ankle angle at ground impact also influenced the knee angle, particularly in the HF and FF techniques where the knee extended further to allow for landing with dorsiflexion.

During the Forward Swing Phase, varying the landing technique affected the spinal segment angular velocity. Larger spinal angular velocities were recorded for the NLT and TF techniques, indicating that more power was generated when striking the shuttlecock which would suggest that these landing techniques improve the effectiveness of the jump smash. Notably, the NLT and FF techniques produced large variances in the ankle landing angle data. The large variance for the NLT can be explained by the individual landing strategy for each participant. The variance in the FF technique is due to the difficulty experienced by participants to repeatedly land flat footed.

Based on the risk assessments, the TF technique was identified as the most suitable landing technique to minimise injury risk due to the spring-like behaviour, reduced reaction moments and increased joint flexion. NLT was identified to have a higher risk than the TF technique due to the variation in participant landing techniques. The HF and FF techniques posed the highest risk for injury, attributed to the non-spring like behaviour of the joints, the increase in reaction moments and decrease in lower limb flexion.

Coaches can use the findings from this study to refine their teaching and training of the jump smash technique. Coaches can emphasise the importance of the landing technique on desired outcomes. Training drills can be adjusted and tailored to specific athletes for improvements highlighted in this study.

The study was limited in providing comparisons between male and female participants due to the lack of female participation. The study does not take into consideration the effect of previously executed manoeuvres on the jump smash. It only assesses the jump smash in isolation.

7 Recommendations

The following recommendations should be considered for future studies.

1. The study found that to land in a specific manner, the participants would compensate the knee angle to achieve the desired landing technique as indicated by the 14% increase in the knee reaction force for the HF technique. Future work could explore the combined effects of controlling ankle and knee landing position on BPIs.
2. Future studies could increase the number of trials for each landing technique from 3 to 5 to confirm reliability of results.
3. Xsens is capable of utilising additional inertial sensors on external objects which can be incorporated into the biomechanical model. Future studies could use additional inertial sensors on the badminton racquet to record the racquet kinematic data. This data can then be used to validate if changing the landing technique has an effect on the performance of the jump smash by analysing the velocity of the racquet.
4. Only 3 of the 16 participants were female which limited the ability to draw gender-based comparisons from the study. Future studies can consider repeat the study with the aim of exploring the potential differences between male and female by testing with an equal sample size for both genders.
5. The study looks at the jump smash as an isolated manoeuvre. Future studies can investigate the effects of varying the landing technique in a real match setting to compare if the results are comparable with this study.

8 References

[1] Guinness World /Records. Fastest badminton hit in competition (male), 2017. [Online] Available from: https://www.guinnessworldrecords.com/world-records/fastest-badminton-hit-in-competition-(male)#:~:text=The%20fastest%20badminton%20hit%20in,India%2C%20on%2010%20January%202017. [Accessed on 17 July 2020].

[2] M.Phomsoupha and G.Laffaye. Injuries in Badminton: A review. Science & Sports, 2020, 35, p.188-199. [Online]. Available from: https://doi.org/10.1016/j.scispo.2020.01.002 [Accessed on 15 October 2023]

[3] J. Reeves *et al*. A retrospective Review from 2006 to 2011 of Lower Extremity Injuries in Badminton in New Zealand. *Sports*, 2015, 3, p.77-86. [Online]. Available from: https://doi.org/10.3390/sports3020077 [Accessed 17 January 2022].

[4] A.S. Rambley *et al*. The analysis of the jumping smash in the game of badminton. *In Proceedings of the 23rd International Conference of Biomechanics in Sports*. Beijing, China, 2005, p.671– 674.

[5] Y.Zhang et al. Motion Capture and Intelligent Correction Method of Badminton Movement Based on Machine Vision. Mobile Information Systems, 2021, Article ID 3256924, 10 pages. [Online] Available from: https://doi.org/10.1155/2021/3256924. [Accessed 15 October 2023]

[6] Master Badminton. *How to Play the Badminton Jump Smash*, 2010. [Online] Available from: https://www.masterbadminton.com/badminton-jump-smash.html [Accessed 22 July 2020].

[7] D.N. Pardiwala *et al*. Badminton Injuries in Elite Athletes: A Review of Epidemiology and Biomechanics. *Indian Journal of Orthopaedics*, 2020, 54(3), p.237-245.

[8] OpenStax. Anatomy and Physiology. OpenStax CNX, 2016. [Online] Available from: http://cnx.org/contents/14fb4ad7-39a1-4eee-ab6e-3ef2482e3e22@8.24. [Accessed 06 August 2020].

[9] N. Hamilton *et al*. *Kinesiology: Scientific Basis of Human Motion*, 12th edition. New York: McGraw Hill, 2012. [Online] Available from: https://accessphysiotherapy.mhmedical.com/content.aspx?bookid=965&sectionid=53599866 [Accessed 08 August 2020].

[10] Y. Ramasamy et al. Ground Reaction Force and Kinematics of Forehand Jumping Smash Among Elite Malaysian Badminton Players. *In Proceedings of the 37th International Society of Biomechanics in Sport Conference*, Oxford, OH, USA, 21 – 25 July 2019, p.173 – 176

[11] C. Hung *et al*. Influences of Lateral Jump Smash Actions in Different Situations on the Lower Extremity Load of Badminton Players. *Journal of Sports Science & Medicine*, 2020, 19(2), p.264 – 270.

[12] C.T. Farley*et al*. Mechanism of leg stiffness adjustment for hopping on surfaces of different stiffnesses. *Journal of Applied Physiology*, 1998, 85(3), p.1044 – 1055.

[13] B. Dai *et al*. The Effects of 2 Landing Techniques on Knee Kinematics, Kinetics, and Performance During Stop-Jump and Side-Cutting Tasks. *The American Journal of Sports Medicine*, 2015, 43(2), 466 – 474.

[14] Y. Adesida *et al*. Exploring the Role of Wearable Technology in Sport Kinematics and Kinetics: A Systematic Review. *Sensors*, 2019, 19(7), p.1597. [Online] Available from: https://doi.org/10.3390/s19071597. [Accessed 26 August 2020].

[15] L.S Luteberget et al. Reliability of Wearable Inertial Measurement Units to Measure Physical Activity in Team Handball. Int J Sports Physiol Perform, 2018, 13(4) , p.467-473. [Online] Available from: DIO:0.1123/ijspp.2017-0036. [Accessed 15 October 2023]

[16] Z.Wang *et al*. Badminton Strok Recognition Based on Body Sensor Network. IEEE Transactions on Human-Machine Systems, 2016, 46(5), p.769-775

[17] T, Jaitner and W.Gawin. A mobile measure device for the analysis of highly dynamic movement techniques. Procedia Engineering , 2010, 2, p.3005-3010.

[18] G. Logar and M. Munih. Estimation of Joint Forces and Moments for the In-Run and Take-Off in Ski Jumping Based on Measurements with Wearable *Inertial Sensors.* Sensors, 2015, 15, p.11258-11276.

[19] A. Karatsidis et al. Estimation of Ground Reaction Forces and Moments During Gait Using Only Inertial Motion Capture. Sensors, 2017, 17(1) p.75. [Online] Available from: https://doi.org/10.3390/s17010075 [Accessed 20/05/2023]

[20] J. S. Pedley, et al. Maturity alters drop vertical jump landing force-time profiles but not performance outcomes in adolescent females. Scandinavian Journal of Medicine and Science in Sports, 2021, 31(11), 2055–2063. https://doi.org/10.1111/sms.14025 [Accessed 04/06/2023]

[21] B. Elliot *et al*. Field Versus Laboratory Testing in Sports Biomechanics: Systems And Modelling Errors, 2006. [Online] Available from: https://www.researchgate.net/publication/237079374_FIELD_VERSUS_LABORATORY_TESTING_IN_SPORTS_BIOMECHANICS_SYSTEM_AND_MODELLING_ERRORS , [Accessed 17/04/2024]

[22] L. Hardy *et al*. Knowledge and conscious control of motor actions under stress. *British journal of psychology*, 1996, 87, p.621-636 [Online] Available from: https://doi.org/10.1111/j.2044-8295.1996.tb02612.x [Accessed 17/04/2024]

[23] A. Bandura. Self-efficacy: The exercise of control. W H Freeman, 1997.

[24] F. Crenna *et al*. Filtering Biomechanical Signals in Movement Analysis. *Sensors*, 2021, 21 (3), p. 4580 [Online] Available from: https://doi.org/10.3390/s21134580 [Accessed 17/04/2024]

[25] Statology. How to Perform a One-Way ANOVA by Hand, 2020. [Online] Available from: https://www.statology.org/one-way-anova-by-hand/ [Accessed 04/01/2022]

[26] XSENS. *MVN User Manual Revision Z*, 2021. [Online] Available from: https://www.Xsens.com/hubfs/Downloads/usermanual/MVN_User_Manual.pdf [Accessed 26/01/2022]

[27] BERTEC. *Force Plate FP4060-05-PT Product Details and Specifications*. [Online] Available from:https://static1.squarespace.com/static/5b3256317e3c3a8e8e029991/t/5bdb0d63cd8366e93790a8ef/1541082467799/FP4060-05-PT.pdf, [Accessed 30/01/2022]

[28] P. de Leva. Adjustments to Zatsiorsky-Seluanov's segment inertia parameters. *J Biomech*, 1996, 29(9): p.1223-30. doi: 10.1016/0021-9290(95)00178-6. PMID: 8872282.

[29] F. S. Nahm. Nonparametric statistical tests for the continuous data: the basic concept and the practical use. *Korean Journal of Anaesthesiology*, 2016, 69(1), p.8-14 [Online] Available from: [https://doi.org/10.4097/kjae.2016.69.1.8 [Accessed 19/12/2022]

[30] H. Arsham, M. Lovric. Bartlett's Test. *International encyclopaedia of statistical science*, 2011, 1, p.87-88 [Online] Available from: https://www.researchgate.net/profile/Dr-Hossein-Arsham/publication/344731676_BARTLETT'S_TEST/links/5f8ce5cb299bf1b53e324a18/BARTLETTS-TEST.pdf [Accessed 04/01/2023]

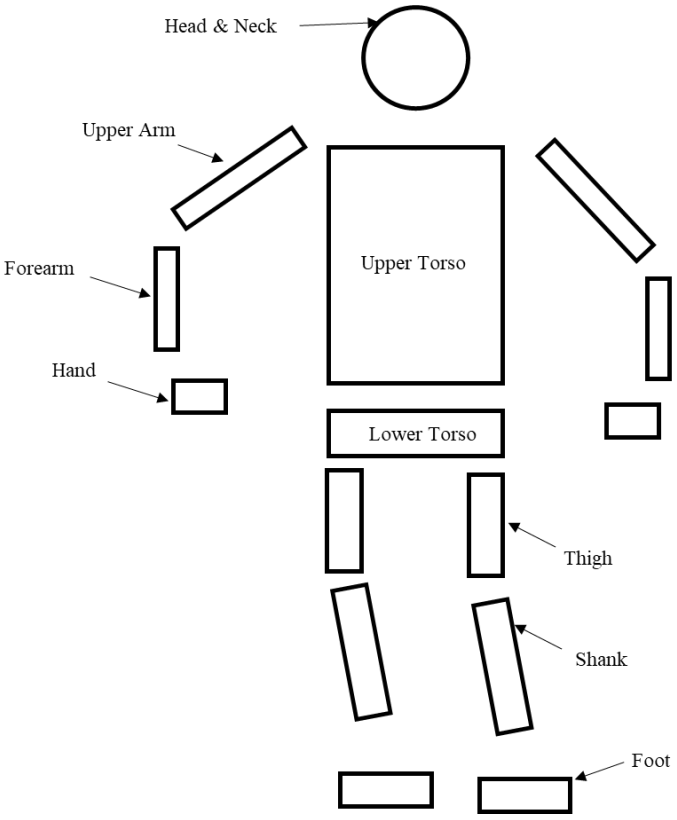
[31] Laerd Statistics. One-Way ANOVA, [no date]. [Online] Available from: https://statistics.laerd.com/statistical-guides/one-way-anova-statistical-guide.php [Accessed 04/01/2023]

[32] Statology. How to Read the F-Distribution Table, [2019] [Online] Available from: https://www.statology.org/how-to-read-the-f-distribution-table/ [Accessed 04/01/2023]

[33] Statistics How to. Kruskal Wallis H Test, [no date] [Online] Available from: https://www.statisticshowto.com/probability-and-statistics/statistics-definitions/kruskal-wallis/ [Accessed 04/01/2023]

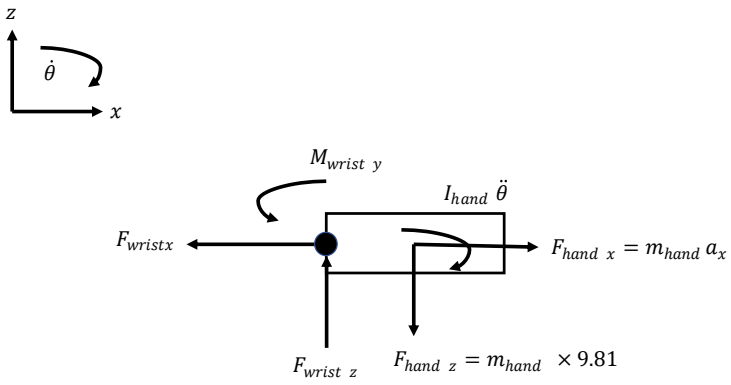
Appendices

Appendix A – Ground Reaction Force and Moment equation derivation p



Body Segments

Wrists



$$\sum F_x = ma_x \quad \rightarrow +$$

$$F_{wrist\ x} = -m_{hand} a_x$$

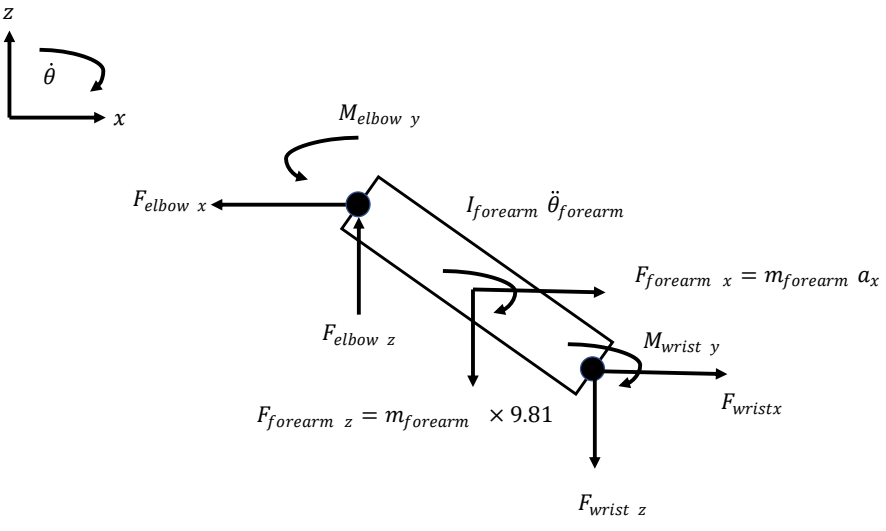
$$\sum F_z = ma_z \uparrow +$$

$$F_{wrist\ z} = m_{hand}(9.81 - a_z)$$

$$\sum M_y = I\ddot{\theta} \ \circlearrowleft +$$

$$M_{wrist} = I_{hand}\ddot{\theta}_{hand} + \dot{\theta} \times \left(I_{hand}\dot{\theta}_{hand}\right)$$

Forearm



$$\sum F_x = ma_x \quad \rightarrow +$$

$$F_{elbow\,x} = F_{wrist\,x} - m_{forearm}a_x$$

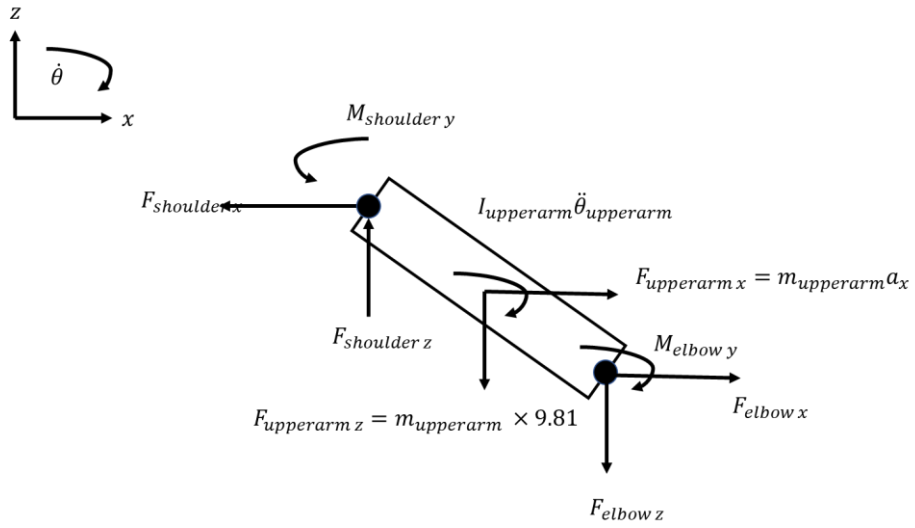
$$\sum F_z = ma_z \uparrow +$$

$$F_{elbow\,z} = F_{wrist\,z} + m_{forearm}(9.81 - a_z)$$

$$\sum M_y = I\ddot{\theta} \circlearrowleft +$$

$$M_{elbow} = I_{forearm}\ddot{\theta}_{forearm} + \dot{\theta} \times \left(I_{forearm}\dot{\theta}_{forearm}\right) - (r_{wrist} \times F_{wrist})$$

Upper Arm



$$\sum F_x = ma_x \quad \rightarrow +$$

$$F_{shoulder\,x} = F_{elbow\,x} - m_{upperarm}a_x$$

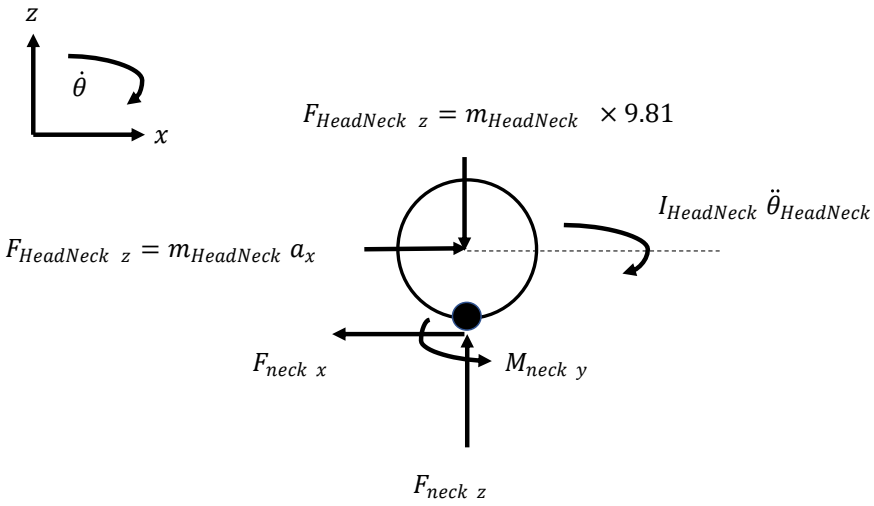
$$\sum F_z = ma_z \uparrow +$$

$$F_{shoulder\,z} = F_{elbow\,z} + m_{upperarm}(9.81 - a_z)$$

$$\sum M_y = I\ddot{\theta} \circlearrowleft +$$

$$M_{shoulder} = I_{upperarm}\ddot{\theta}_{upperarm} + \dot{\theta} \times \left(I_{upperarm}\dot{\theta}_{upperarm}\right) - (r_{elbow} \times F_{elbow})$$

Head & Neck



$$\sum F_x = ma_x \quad \rightarrow +$$

$$F_{neck\,x} = -\,m_{HeadNeck} a_x$$

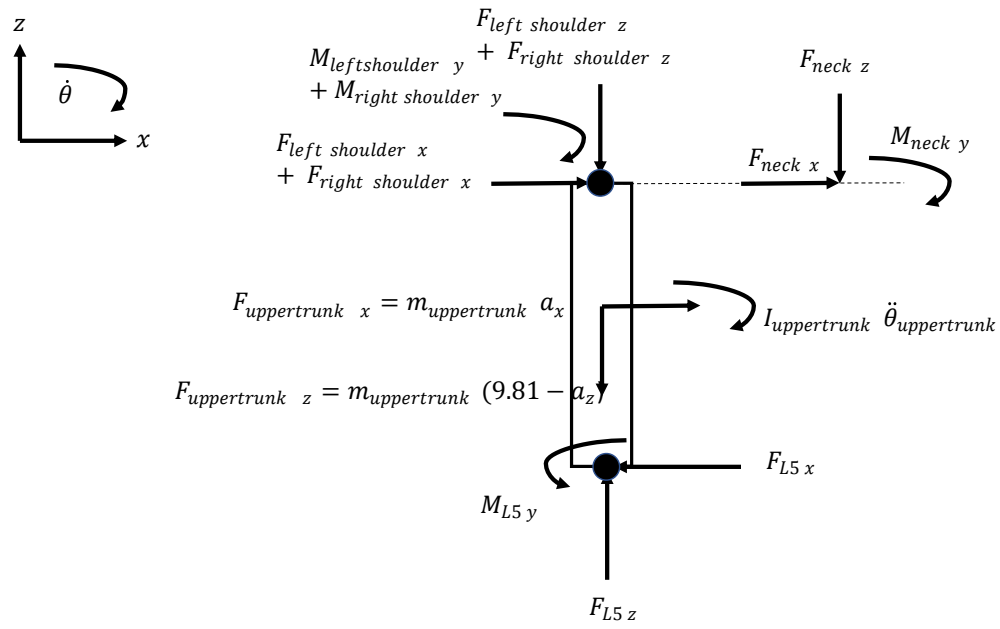
$$\sum F_z = ma_z \uparrow +$$

$$F_{neck\,z} = \ m_{HeadNeck}(9.81 - \ a_z)$$

$$\sum M_y = I\ddot{\theta} \ \circlearrowleft +$$

$$M_{neck} \ = I_{HeadNeck}\ddot{\theta}_{HeadNeck} + \ \dot{\theta} \ \times \left(I_{HeadNeck}\dot{\theta}_{HeadNeck}\right)$$

Upper Trunk



$$\sum F_x = ma_x \quad \rightarrow +$$

$$F_{L5\,x} = F_{leftshoulder\,x} + F_{right\ shoulder\,x} + F_{neck\,x} - m_{upperarm}a_x$$

$$\sum F_z = ma_z \uparrow +$$

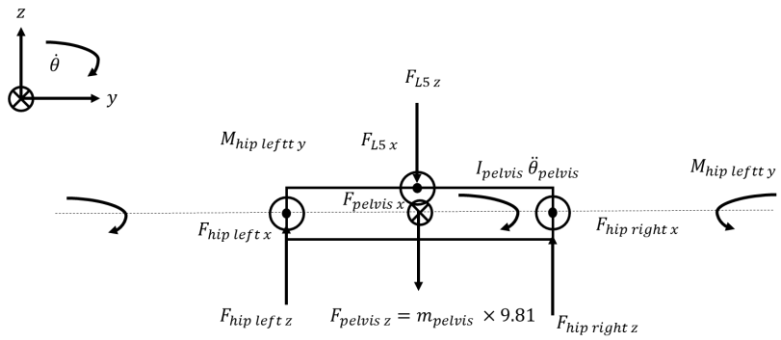
$$F_{L5\,z} = F_{leftshoulder\,z} + F_{rightshoulder\,z} + F_{neck\,z} + m_{upperarm}(9.81 - a_z)$$

$$\sum M_y = I\ddot{\theta}\ \circlearrowleft +$$

$$M_{L5\,y} = I_{UpperTrunk}\ddot{\theta}_{UpperTrunk} + \dot{\theta} \times \left(I_{UpperTrunk}\dot{\theta}_{UpperTrunk}\right)$$

$$-\left(r_{leftshoulder} \times F_{leftshoulder}\right) - \left(r_{rightshoulder} \times F_{rightshoulder}\right) - \left(r_{neck} \times F_{neck}\right)$$

Hips (Lower Trunk)



If both feet are in contact with the ground:

$\sum F_x = ma_x \quad \rightarrow +$

$$F_{hipleft\,x} = F_{hipright\,x} = \frac{1}{2}\left[F_{L5\,x} - m_{hip}(\,a_x\right]$$

$\sum F_z = ma_z \uparrow +$

$$F_{hipleft\,z} = F_{hipright\,z} = \frac{1}{2}\left[F_{L5\,z} + m_{hip}(9.81 - \,a_x\right]$$

$\sum M_y = I\ddot{\theta} \;\circlearrowleft +$

$$M_{L5\,y} = \frac{1}{2}\,I_{Hip}\ddot{\theta}_{Hip} + \,\dot{\theta}\, \times \left(I_{Hip}\dot{\theta}_{Hip}\right) - (r_{L5} \times\, F_{L5})$$

If either foot is in contact with the ground (i.e., left foot on ground and right foot off the ground)

$\sum F_x = ma_x \quad \rightarrow +$

$$F_{hipleft\,x} = F_{hipright\,x} + \,F_{L5r\,x} - m_{hip}(\,a_x)$$

where $F_{hipright\,x}$ is the sum of all X component reaction forces from each segment in the right leg acting as a free weight

$\sum F_z = ma_z \uparrow +$

$$F_{hipleft\,z} = F_{hipright\,z} + \,F_{L5r\,z} + m_{hip}(9.81 - \,a_z)$$

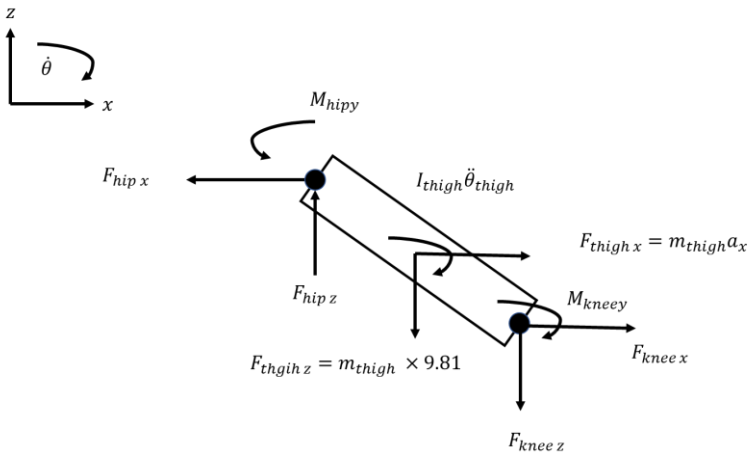
where $F_{hipright\,z}$ is the sum of all Z component reaction forces from each segment in the right leg acting as a free weight

$$\sum M_y = I\ddot{\theta} \ \circlearrowleft +$$

$$M_{hipleft\,y} = I_{Hip}\ddot{\theta}_{Hip} + \dot{\theta} \times \left(I_{Hip}\dot{\theta}_{Hip}\right) - \left(r_{hipright} \times F_{hipright}\right) - (r_{L5} \times F_{L5})$$

where $M_{hipleft\,y}$ is the sum of all reaction moments in each segment in the right leg acting as a free weight

Thigh



Equations below are applicable for both left and right thigh. When foot is in contact with the ground, the forces and moments are derived as:

$$\sum F_x = ma_x \quad \rightarrow +$$

$$F_{knee\,x} = F_{hip\,x} - m_{hip}(a_x)$$

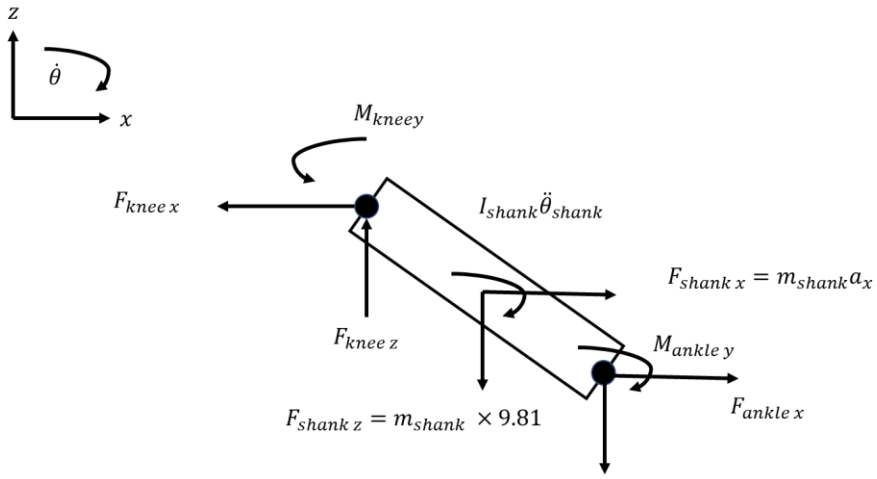
$$\sum F_z = ma_z \uparrow +$$

$$F_{knee\,z} = F_{hip\,z} + m_{hip}(9.81 - a_z)$$

$$\sum M_y = I\ddot{\theta} \ \circlearrowleft +$$

$$M_{knee\,y} = I_{thigh}\ddot{\theta}_{thigh} + \dot{\theta} \times \left(I_{thigh}\dot{\theta}_{thigh}\right) - \left(r_{hip} \times F_{hip}\right)$$

Shank



Equations below are applicable for both left and right shank.

$$\sum F_x = ma_x \quad \rightarrow +$$

$$F_{ankle\,x} = F_{knee\,x} - m_{shank}(a_x)$$

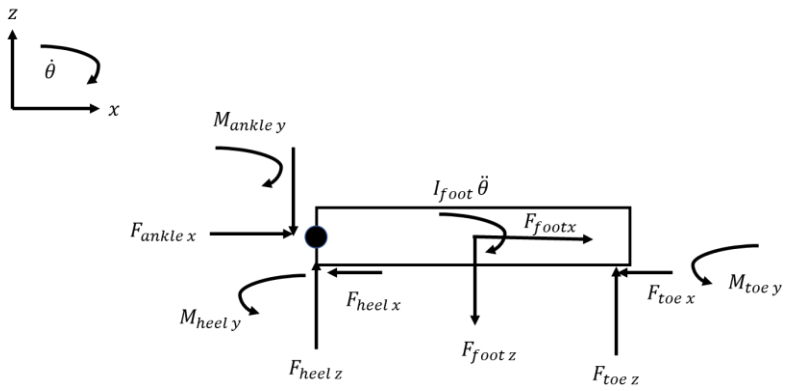
$$\sum F_z = ma_z \uparrow +$$

$$F_{ankle\,z} = F_{knee\,z} + m_{shank}(9.81 - a_z)$$

$$\sum M_y = I\ddot{\theta} \circlearrowleft +$$

$$M_{ankle\,y} = I_{shank}\ddot{\theta}_{shank} + \dot{\theta} \times \left(I_{shank}\dot{\theta}_{shank}\right) - (r_{knee} \times F_{knee})$$

Foot



Equations below are applicable for both left and right feet. If the foot is flat on the ground

$$\sum F_x = ma_x \quad \rightarrow +$$

$$F_{heelx} + F_{toex} = GRF_x$$

$$F_{heelx} = F_{toex} = \frac{1}{2}\,[GRF_x]$$

$$GRF_x = F_{ankle\,x} - m_{foot}(a_x)$$

$$\sum F_z = ma_z \uparrow +$$

$$F_{heel\,z} + F_{toe\,z} = VGRF$$

$$F_{heel\,z} = F_{toe\,z} = \frac{1}{2}\,[VGRF]$$

$$VGRF = F_{ankle\,z} + m_{foot}(9.81 - a_z)$$

$$\sum M_y = I\ddot{\theta} \;\circlearrowleft +$$

$$M_{heel\,y} + M_{toe\,y} = GRM$$

$$M_{heel\,z} = M_{toe\,z} = \frac{1}{2}\,[GRM]$$

$$GRM = I_{foot}\ddot{\theta}_{foot} + \dot{\theta} \times \left(I_{foot}\dot{\theta}_{foot}\right) - (r_{ankle} \times F_{ankle})$$

If the heel is in contact but the toes are not, the reaction forces and moments at the toe were assumed to have no effect:

$$\sum F_x = ma_x \quad \rightarrow +$$

$$F_{heelx} = GRF_x = F_{ankle\,x} - m_{foot}(a_x)$$

$$\sum F_z = ma_z \uparrow +$$

$$F_{heel\,z} = VGRF = F_{ankle\,z} + m_{foot}(9.81 - a_z)$$

$$\sum M_y = I\ddot{\theta} \circlearrowleft +$$

$$M_{heel\,y} = GRM = I_{foot}\ddot{\theta}_{foot} + \dot{\theta} \times \left(I_{foot}\dot{\theta}_{foot}\right) - (r_{ankle} \times F_{ankle})$$

If the toe is in contact but the toes are not, the reaction forces and moments at the heel were assumed to have no effect:

$$\sum F_x = ma_x \quad \rightarrow +$$

$$F_{toex} = GRF_x = F_{ankle\,x} - m_{foot}(a_x)$$

$$\sum F_z = ma_z \uparrow +$$

$$F_{toe\,z} = VGRF = F_{ankle\,z} + m_{foot}(9.81 - a_z)$$

$$\sum M_y = I\ddot{\theta} \circlearrowleft +$$

$$M_{toe\,y} = GRM = I_{foot}\ddot{\theta}_{foot} + \dot{\theta} \times \left(I_{foot}\dot{\theta}_{foot}\right) - (r_{ankle} \times F_{ankle})$$

Finally, the total reaction force and moment experienced is taken as the summation of the reaction forces at the left and right feet.

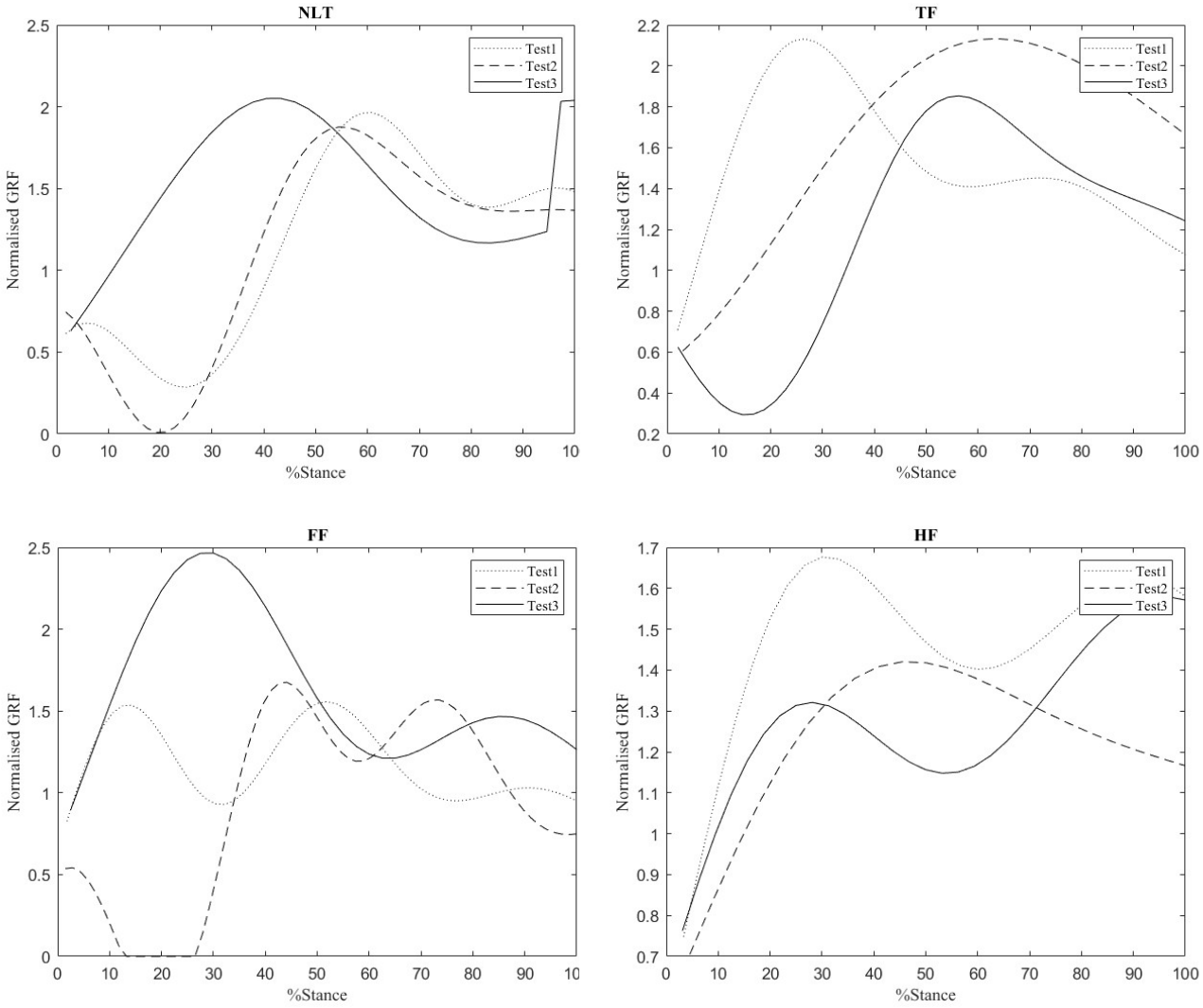
$$VGRF = VGRF_{left} + VGRF_{right}$$

$$GRFx = GRM_{left} + GRM_{right}$$

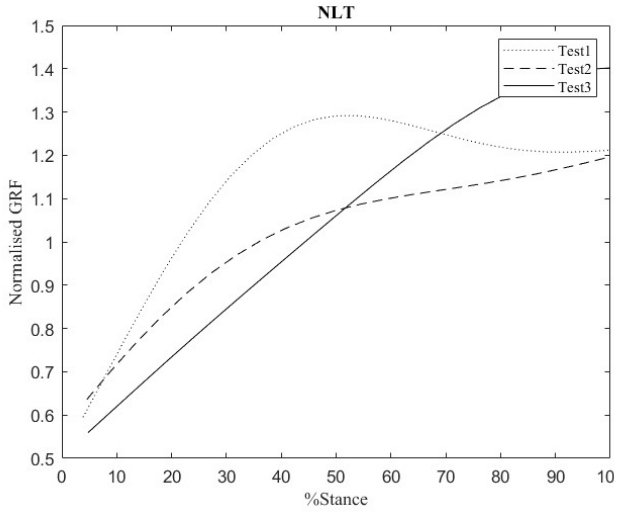
$$GRM = GRM_{left} + GRM_{right}$$

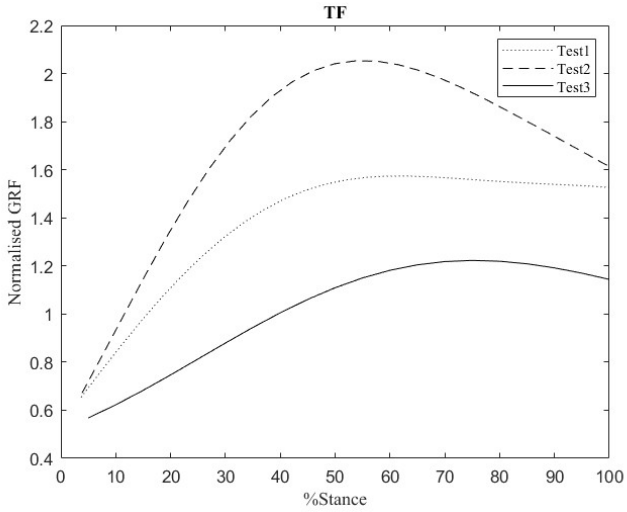
Appendix B – Landing Force Profiles

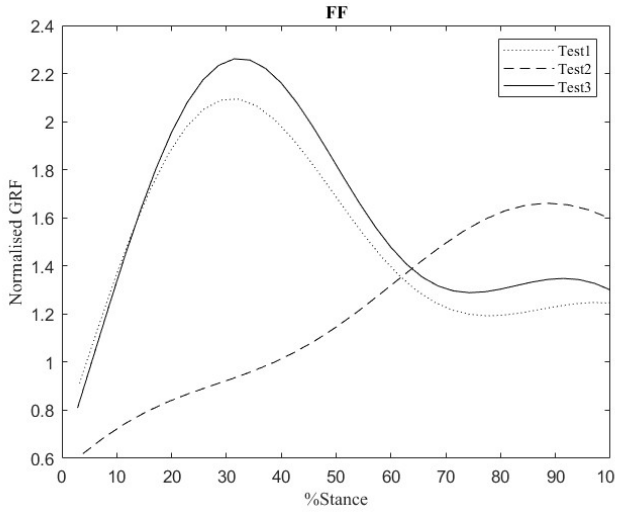
Participant 1

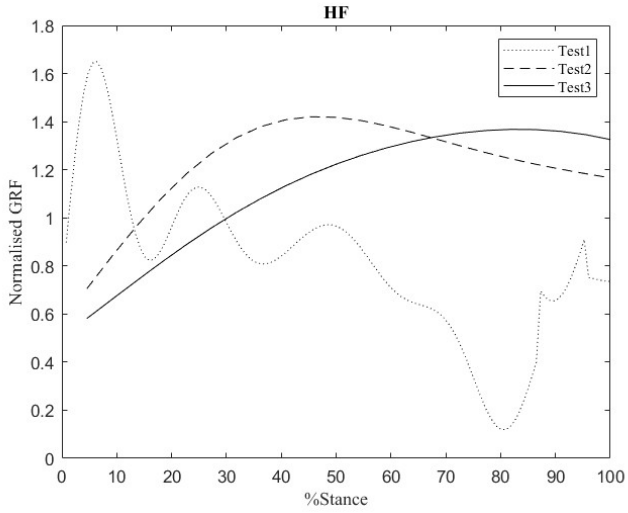


Participant 2

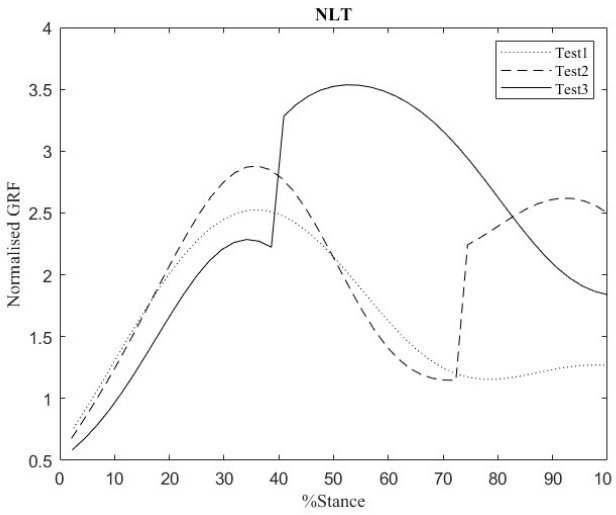


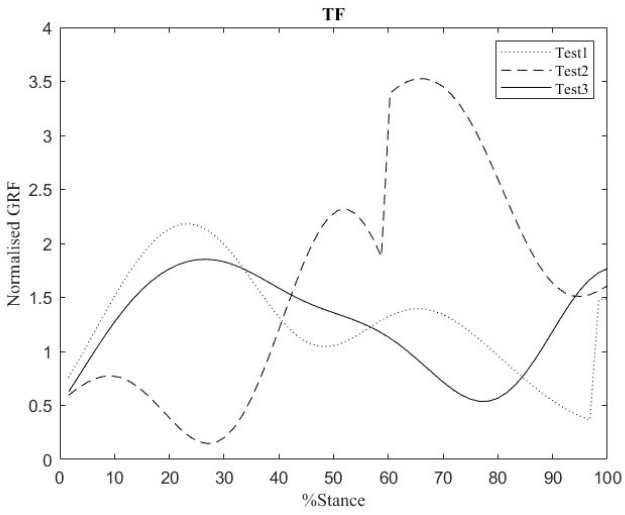


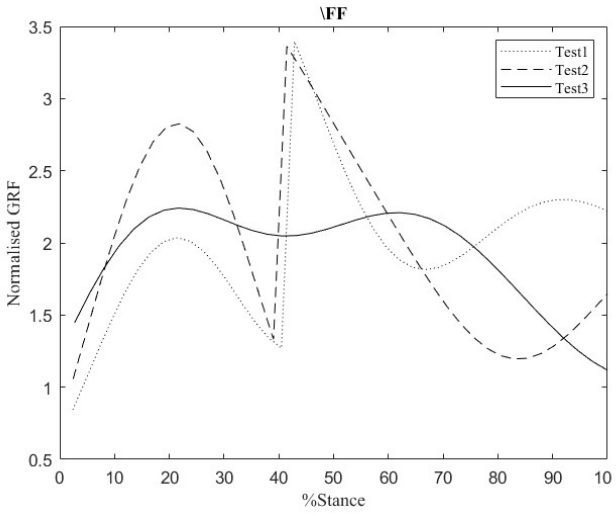


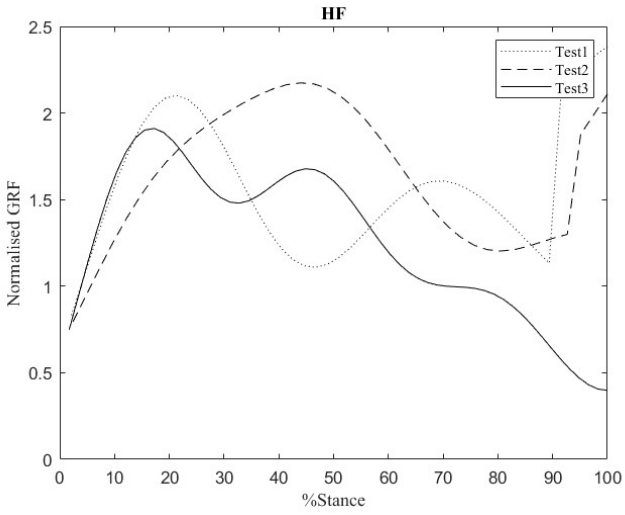


Participant 3

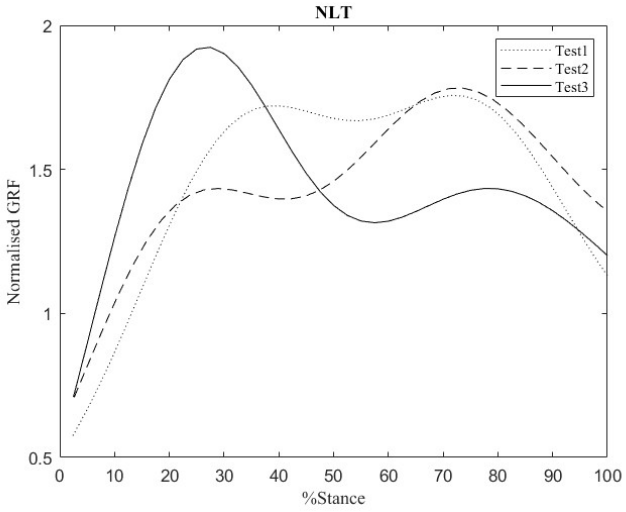


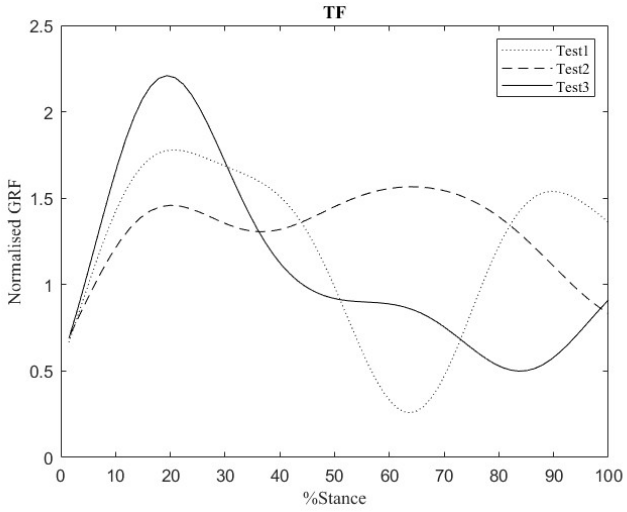


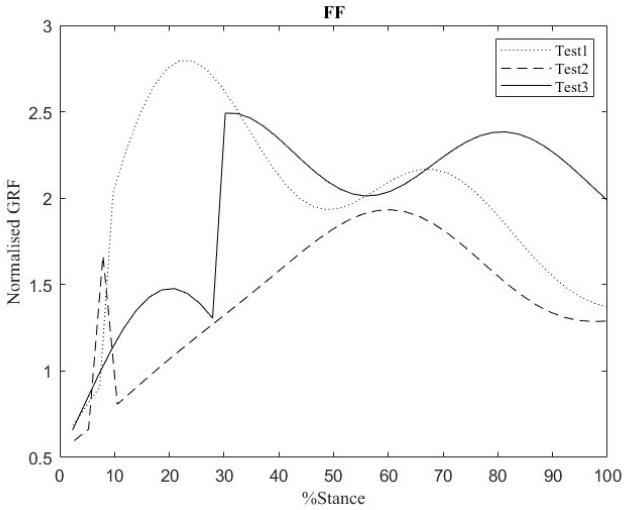


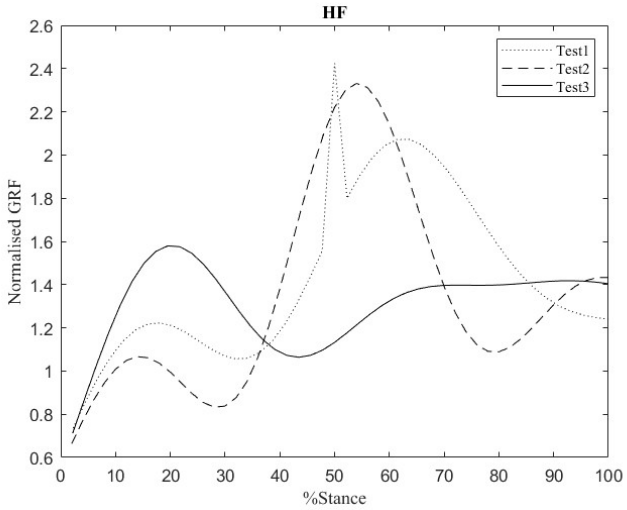


Participant 4

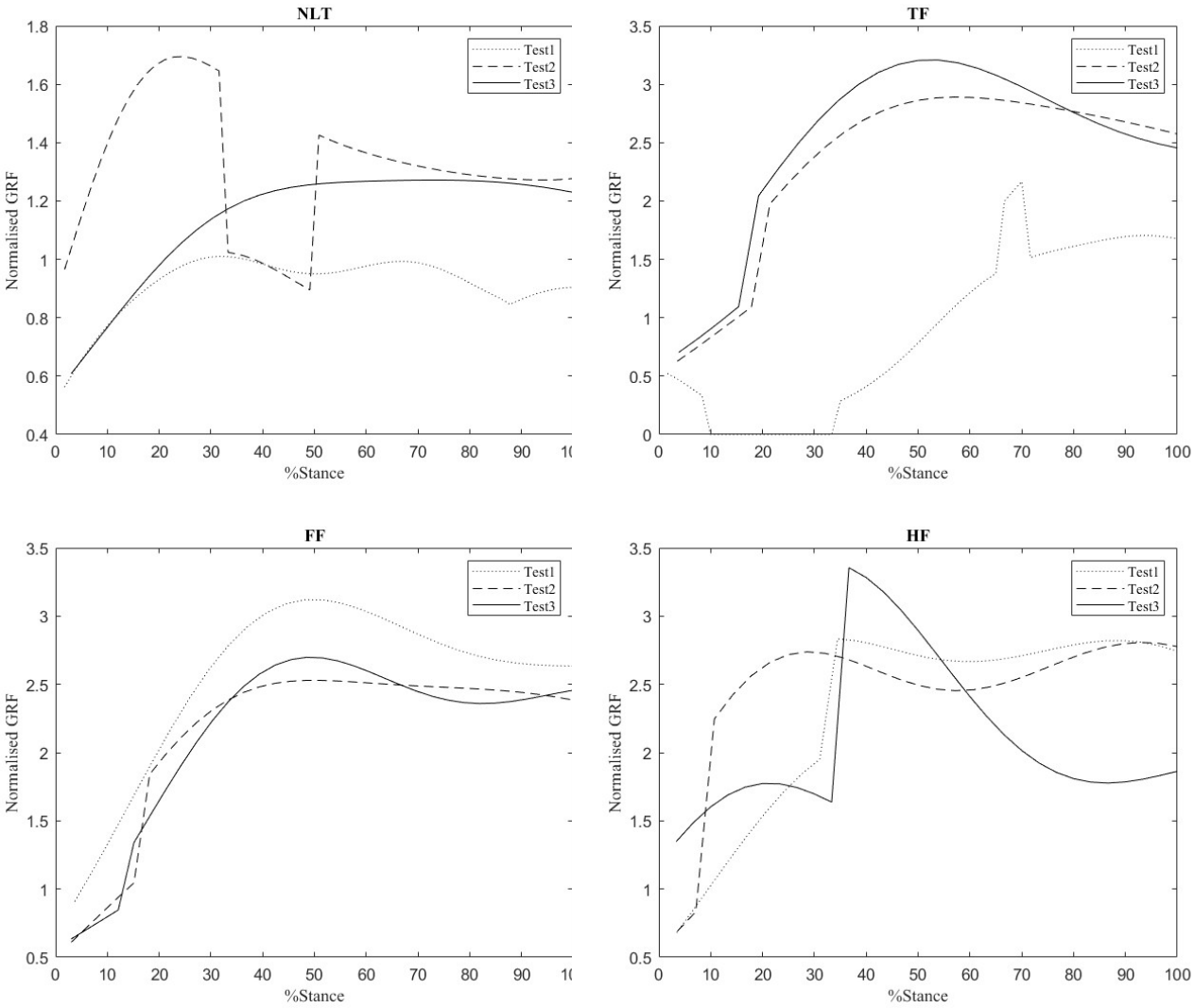




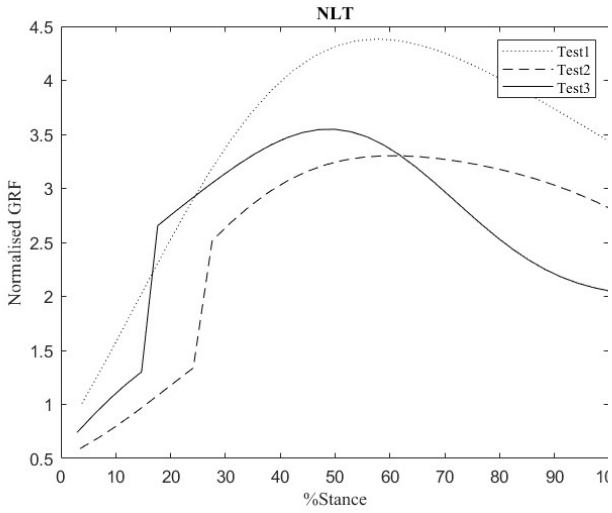


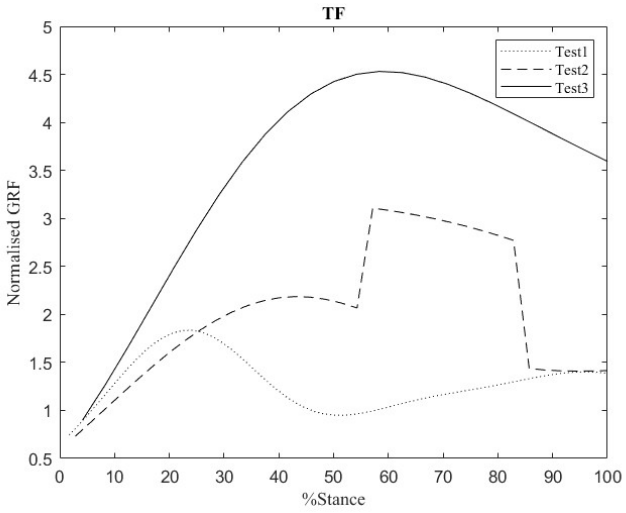


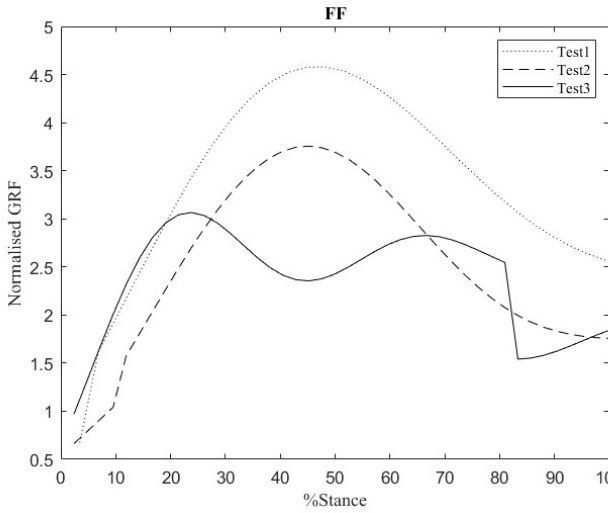
Participant 5

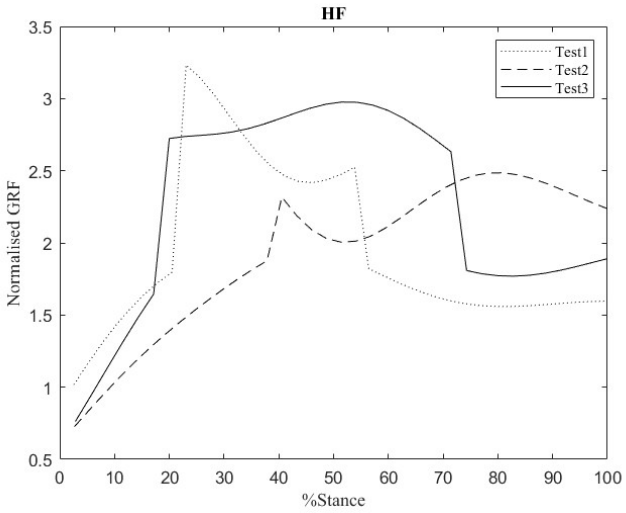


Participant 6

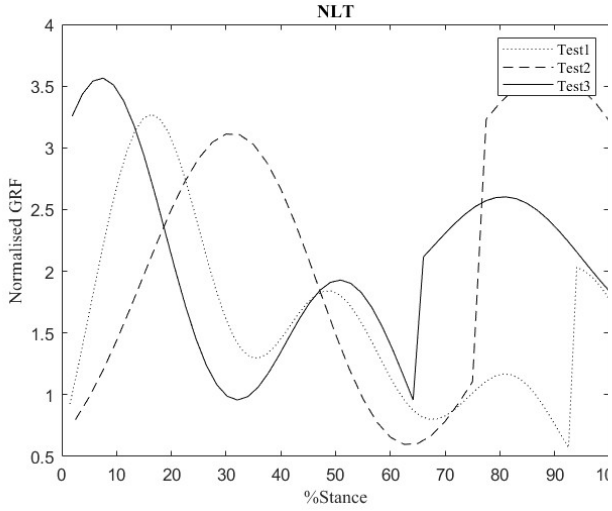


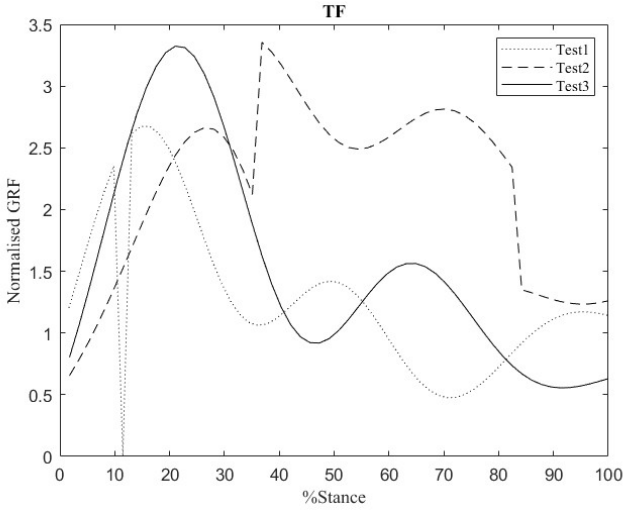


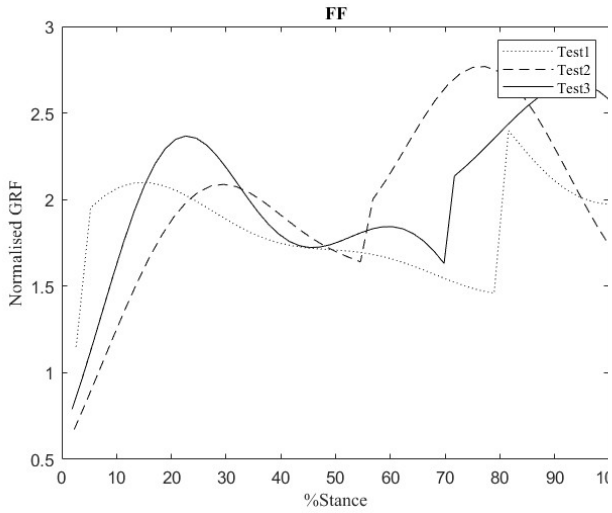


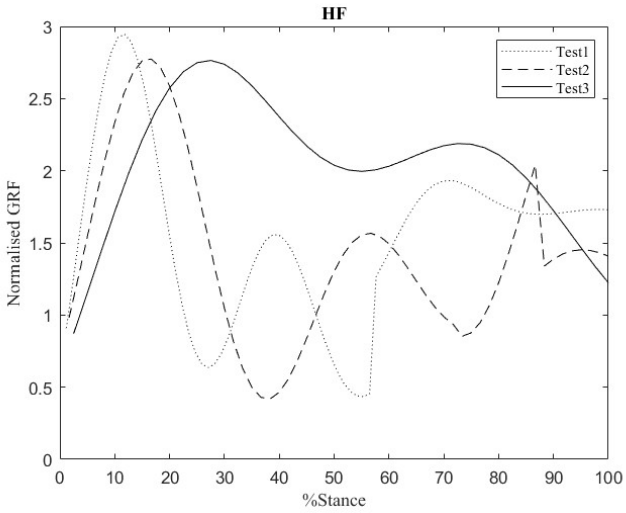


Participant 7

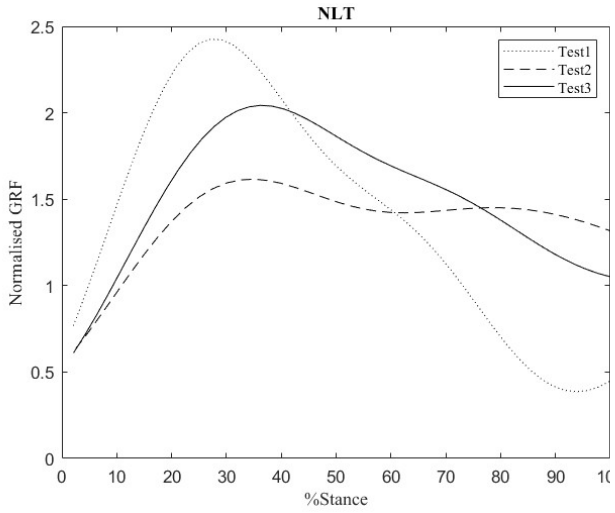


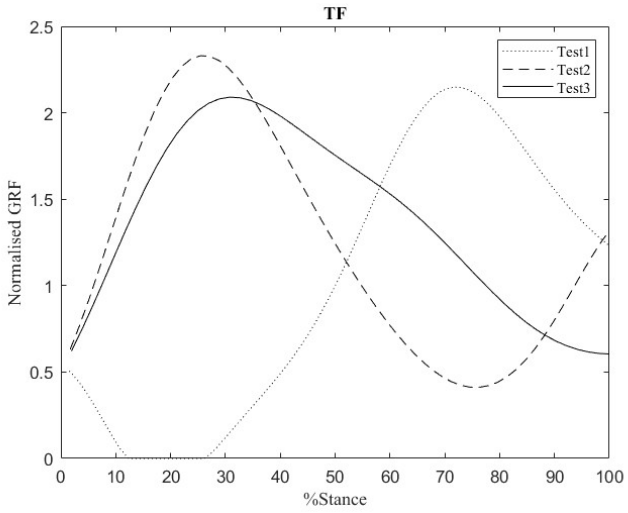


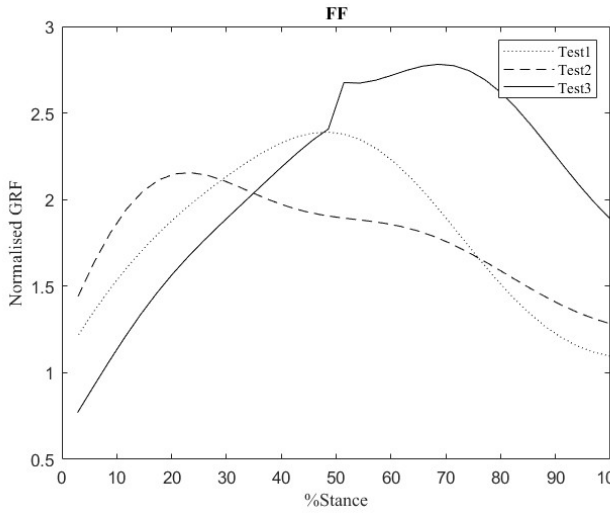


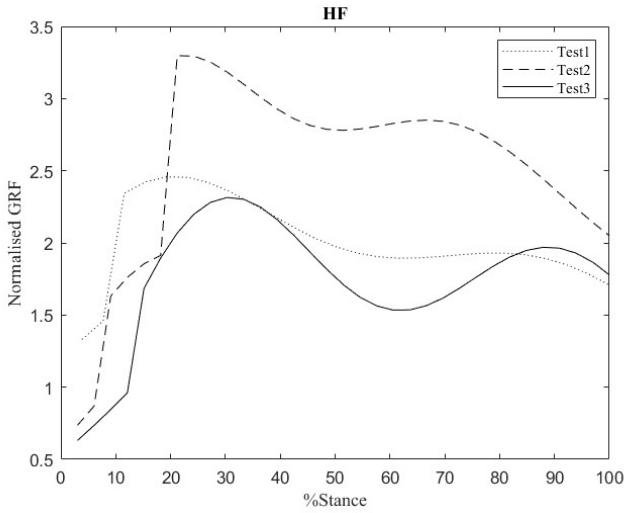


Participant 8

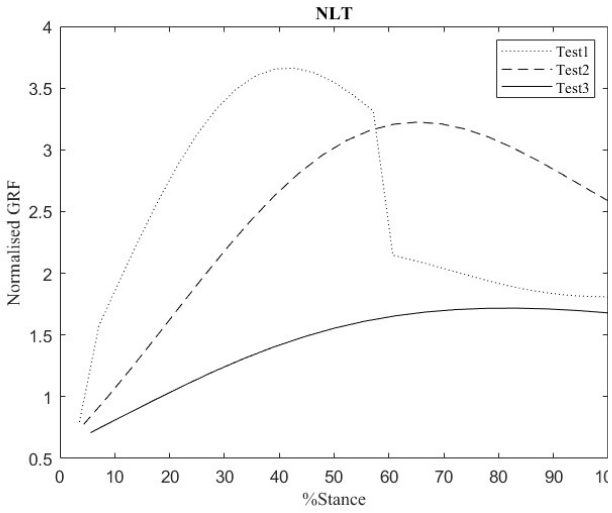


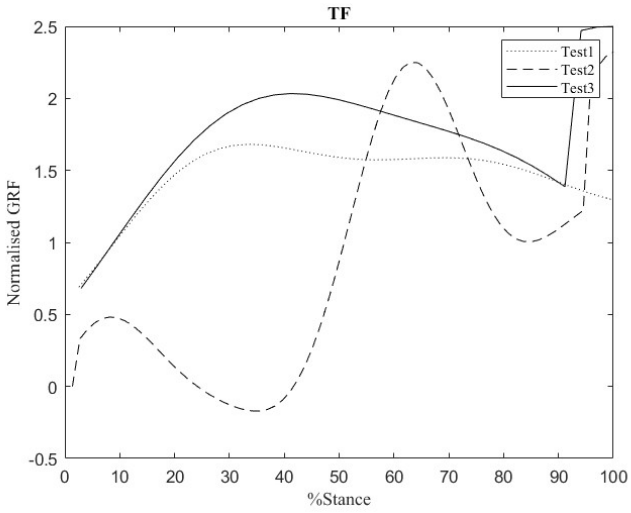


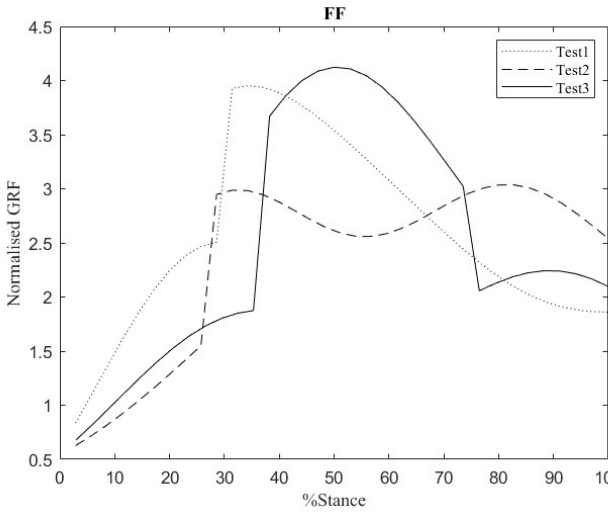


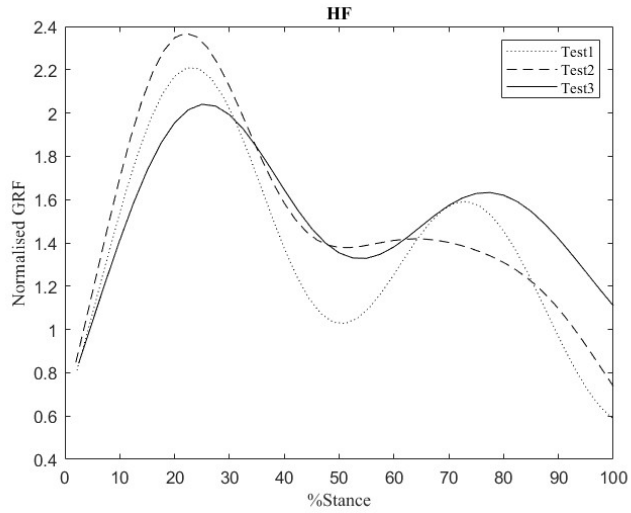


Participant 9

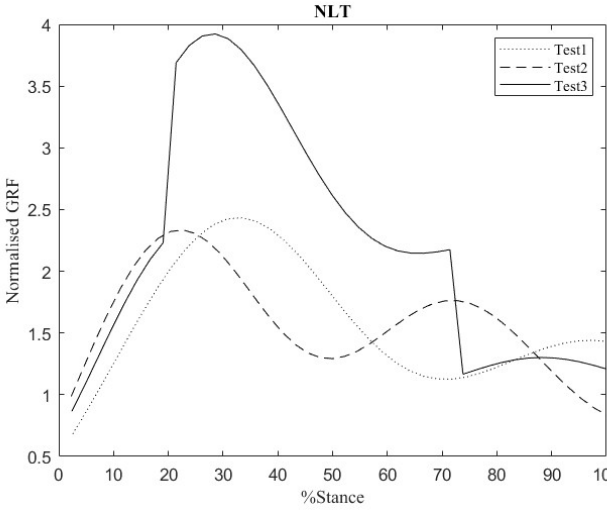


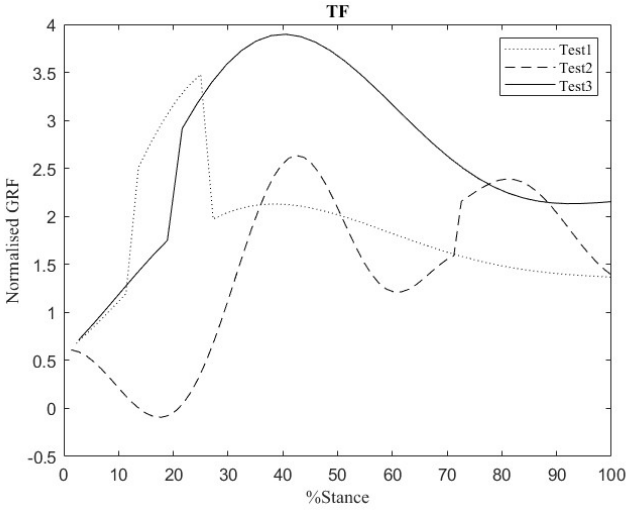


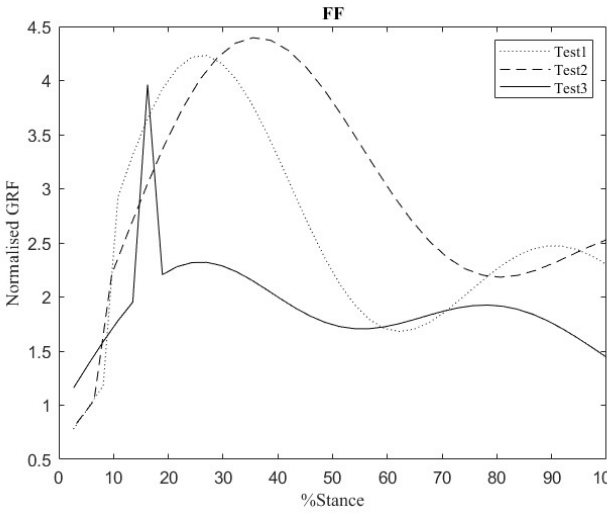


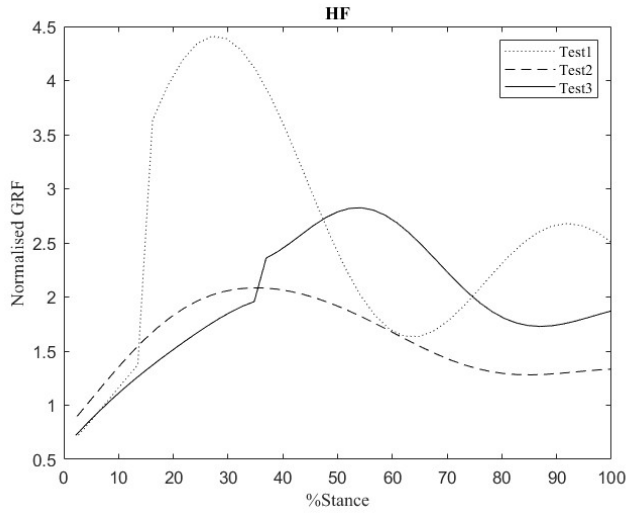


Participant 10









Appendix C – Ethics Clearance Certificate

UNIVERSITY OF THE WITWATERSRAND JOHANNESBURG

HUMAN RESEARCH ETHICS COMMITTEE (MEDICAL)

Office of the Deputy Vice-Chancellor (Research & Post Graduate Affairs)

TO: Ms T Mangera; Professor B Olivier; Mr R Chohan
School of Mechanical, Industrial & Aeronautical Engineering
University

E-mail: Taahira.Mangera@wits.ac.za

CC: Supervisor: Not applicable <>
and <HREC-Medical ResearchOffice@wits.ac.za>

FROM: Iain Burns
Human Research Ethics Committee (Medical)
Tel: 011 717 1252

E-mail: Iain.Burns@wits.ac.za

DATE: 2020/11/09

REF: *R14/49*

PROTOCOL NO: **M200925** *(This is your ethics application study reference number. Please quote this reference number in all correspondence relating to this study)*

PROJECT TITLE: *Modelling badminton movement for injury prevention and performance enhancement*

Please find attached the Clearance Certificate for the above project. I hope it goes well and that an article in a recognized publication comes out of it. This will reflect well on your professional standing and contribute to the Government funding of the University.

MSWorks2002\Iain0007\Clearscan.wps

UNIVERSITY OF THE WITWATERSRAND, JOHANNESBURG

R14/49 Ms T Mangera; Professor B Olivier; Mr R Chohan

HUMAN RESEARCH ETHICS COMMITTEE (MEDICAL)
CLEARANCE CERTIFICATE NO. M200925

NAME: (Principal Investigator)	Ms T Mangera; Professor B Olivier; Mr R Chohan
DEPARTMENT:	School of Mechanical, Industrial & Aeronautical Engineering University
PROJECT TITLE:	Modelling badminton movement for injury prevention and performance enhancement
DATE CONSIDERED:	2020/10/02
DECISION:	Approved unconditionally
CONDITIONS:	
SUPERVISOR:	Not applicable
APPROVED BY:	Dr CB Penny, Chairperson, HREC (Medical)
DATE OF APPROVAL:	2020/11/09

This clearance certificate is valid for 5 years from the date of approval. Extension may be applied for.

DECLARATION OF INVESTIGATORS

To be completed in duplicate and **ONE COPY** returned to the Research Office Secretary on the 3rd Floor, Phillip Tobias Building, Parktown, University of the Witwatersrand, Johannesburg.

I/we fully understand the conditions under which I am/we are authorized to carry out the above-mentioned research and I/we undertake to ensure compliance with these conditions. Should any departure be contemplated, from the research protocol as approved, I/we undertake to submit details to the Committee. **I agree to submit a yearly progress report.** When a funder requires annual re-certification, the application date will be one year after the date when the study was initially reviewed. In this case, the study was initially reviewed in **September** and will therefore reports and re-certification will be due early in the month of **September** each year. Unreported changes to the application may invalidate the clearance given by the HREC (Medical).

Principal Investigator Signature _____ Date _____